The interactome of Rift Valley fever phlebovirus nucleocapsid- towards the identification of new intervention strategies.

Timothy James Mottram, BSc

Submitted in the partial fulfilment for the degree of Doctor of Philosophy in Molecular Virology

MRC-University of Glasgow, Centre for Virus Research

Institute of Infection, Immunity and Inflammation

College of Medical, Veterinary and Life Sciences

University of Glasgow

September 2018

Abstract

Rift Valley fever phlebovirus (RVFV) is an ongoing threat to both humans and animals across the continent of Africa. RVFV is a member of the *Phlebovirus* genus and *Phenuviridae* family, within the *Bunyavirales* order. Members of the *Phlebovirus* genus are characterised by a negative sense tripartite RNA genome. The large (L) segment encodes the RNA-dependent RNA polymerase (L), the medium (M) segment encodes the two glycoproteins Gn and Gc, and the small segment (S) encodes the nucleocapsid (N) protein and the non-structural protein NSs. The N protein performs a number of important functions, including encapsidation of the viral genome allowing viral RNA replication and transcription. Research into N protein-protein interactions has been limited. The work presented in this thesis characterises previously unidentified functional residues of RVFV N protein and describes new insights into virus-host protein-protein interactions. Two previously uncharacterized N protein residues, F11 and F149, when substituted for alanine, performed all its known functions; Encapsidation of the viral genome, N-N multimerisation and L protein interaction. However, utilising a minigenome assay still showed these mutants lack replication capacity. This indicates that currently unknown interactions with these residues are disrupted. Furthermore, a proteomics study on N protein immunoprecipitated from lung epithelial A549 cell infections was performed to identify RVFV N interaction partners, revealing 23 potential candidates. A subsequent siRNA knockdown of candidates identified ß-catenin, Polyadenylate binding protein 1 and 4, Annexin 1 and 2, and Scaffold attachment factor B as important for functional viral replication. Previous research indicated ß-catenin, the effector molecule of the WNT pathway, was involved with RVFV replication. Utilising a TOPFlash reporter assay, it was determined that the WNT pathway, of which ß-catenin is the effector molecule, was inhibited by RVFV infection. The generation of a CRISPR-Cas9 ß-catenin knockout cell line provided a useful tool for further study into N protein-protein and RVFV-ß-catenin interactions. The knockout of ß-catenin significantly reduced RVFV replication, similarly to siRNA-mediated knock down. Additionally, it was observed through the use of confocal microscopy that upon infection with RVFV, ß-catenin relocalised from the plasma membrane to a diffuse pattern across the cytoplasm. Furthermore, during the course of this study, it was investigated whether RVFV N protein can

affect mosquito antiviral pathway(s), similarly to yellow fever virus (genus *flavivirus*) capsid protein. Using alphavirus Semliki Forest virus (SFV) as a model, allowing work to be carried out in a CL-2 lab setting, it was found that N protein does not possess such properties. However, Zika virus (genus *flavivirus*) capsid protein (ZIKV C) showed significant proviral properties, however, this effect did not occur via disruption of the siRNA pathway, the most efficient mosquito antiviral mechanism, as evidenced by ZIKV C having no effect within our siRNA assay. To summarise, the data in this thesis reveals new interactions between RVFV nucleocapsid protein and mammalian host proteins that are important for RVFV replication. It provides a basis for future research on RVFV (or phleboviruses, in general) nucleocapsid research. The disruption of RVFV N-host protein interactions or direct disruption of N function could lead to new therapeutic strategies against this important emerging virus.

Table of Contents

List of Tables

List of Figures

Abbreviations

Amp - Ampicilin
ANXA1 - Annexin A1
ANXA2 - Annexin A2
APC - Adenomatous polyposis coli
BSL - Biosafety level
BUNV - Bunyamwera Virus
CCHFV - Crimean-Congo Haemorhaggic Fever virus
CDC - Centre for Disease Control
CK1 - Casein kinase 1
CL-3 - Containment Level 3
co-IP - Co-immunoprecipitation
cRNA - Complementary antigenomic RNA
CSFV - Classical swine fever virus
CTNB1 - ß-catenin
DAF - Decay-accelerating factor
Dcr2 - Dicer 2
DC-SIGN - Dendritic Cell-Specific Intercellular adhesion molecule 3-Grabbing Non-integrin
delNSs - Non-structural deletion
DENV - Dengue Virus
DPBS - Dulbecco's Phosphate-Buffered Saline
DSP - (dithiobis(succinimidyl propionate))
dsRNA - double stranded RNA
DUGV - Dugbe virus
Dv1 - Dishevelled
EE - Early Endosome
eIF4E - Eukaryotic translation initiation factor 4E
EM - Electron Microscopy
ER - Endoplasmic Reticiulum
exo-siRNA - Exogeneous-short interfering RNA
FBXO3 - F-Box Protein 3
FBS - Fetal Bovine Serum
Fluc - Firefly Luciferase
Fz - Frizzled
GAG - Glycosaminoglycan
GFP - Green Fluorescent Protein
gRNA - Guide RNA
GSK3 - Glycogen synthase kinase-3
HBV - Hepatitis B virus
HBx - Hepatitis B viral protein
HCMV - Human cytomegalovirus
HCV - Hepatitis C virus
HDAC - Histone deacetylases
hRen - Humanized Renilla Luciferase
HRTV - Heartland virus
HTNV - Hantaan virus
Hδr - Hepatitis δ ribozyme
ICTV - International Committee on Taxonomy of Viruses
IFN-ß - Interferon- ß
IFV - Infectious Bronchitis Virus
IRES - Internal ribosome entry site
JUNV - Junin virus
Kan - Kanamycin
KSHV - Karposi's sarcoma-associated herpesvirus
LACV - La Crosse encephalitis virus
LE - Late Endosome
LFQ - Label-Free Quantification
LRP5 - Low-density lipoprotein receptor-related protein 5
LSV - Lone Star phlebovirus
^{m7}G - 7-Methylguanosine
MOI - Multiplicity of infection
NMP - Nuclear matrix protein
NSm - Non-structural protein m
NSs - Non-structural protein s
Opti-MEM - Opti-Minimum Essential Media
ORF - Open Reading Frame
PABP1 - Polyadenylate Binding Protein 1
PABP4 - Polyadenylate Binding protein 4
PAGE - Polyacrylamide Gel Electrophoresis
PCR - Polymerase Chain Reaction
PFU - Plaque forming units
PKR -Protein kinase R
PLB - Passive lysis buffer
PTV - Punta Toro phlebovirus
RdRp - RNA-dependent RNA polymerase
RISC - RNA-induced silencing complex
Rluc -Renilla luciferase
RNAi - RNA interference
RNP - Ribonucleoprotein
RPM - Revolutions per minute
RVFV - Rift Valley fever phlebovirus
S/MAR DNA - Scaffold/Matrix attachment region
SAFB - Scaffold attachment factor B

SFNV - Sandfly fever Naples virus
SFRP - Secreted frizzled related proteins
SFSV - Sandly fever Sicilian virus
SFTSV - Severe fever with thrombocytopenia syndrome virus
SFV - Semliki-forest virus
siHyg - short interfering RNA targeting Hygromycin B
SINV - Sindbis virus
siRNA - Short interfering RNA
SNP - Single nucleotide polymorphism
TCF/LEF - T-cell factor/lymphoid enhancer factor
TF - TopFlash
TFIIH - Transcription factor II H
TLE - Transducin-like-Enhancer
TOSV - Toscana phlebovirus
TSWV - Tomato spotted wilt virus
UTR - Untranslated region
UUKV - Uukuniemi phlebovirus
VLP - Virus-like particle
vPK - Viral protein kinase
VSRs - Viral suppressors of RNA silencing
WNV - West Nile virus
WT - Wildtype
XPD - Xeroderma pigmentosum group D
YFV - Yellow Fever virus
ZIKV - Zika Virus

Publications

Thesis data in preparation for publication

Mottram TJ, Dietrich I, Brennan B, Varjak M, Kohl A. (2018) Rift Valley fever phlebovirus nucleoprotein proteomic analysis identifies important WNT pathway interactions (In Preparation).

Data published during thesis.

Mottram TJ, Li P, Dietrich I, Shi X, Brennan B, Varjak M, Kohl A (2017). Mutational analysis of Rift Valley fever phlebovirus nucleocapsid protein indicates novel conserved, functional amino acids. Plos Negl Trop Dis 11(12): e0006155.

Varjak M, Donald CL, Mottram TJ, Sreenu VB, Merits A, Maringer K, Schnettler E, Kohl A (2017) Characterization of the Zika virus induced small RNA response in *Aedes aegypti* cells. PloS Negl Trop Dis 11(10): e0006010.

Data not included in this thesis.

Schnettler E, Sreenu VB, Mottram T and McFarlane M (2016). Wolbachia restricts insect-specific flavivirus infection in Aedes aegypti cells. J Gen Virol. 97(11): 3024-3029.

Acknowledgments

I would like to thank Professor Alain Kohl for his support throughout my PhD and everyone in the Kohl lab and members of the Henry Wellcome building level 4, James, Claire, Margus, Mel, Big Steph, Wee Steph, Christie, Jordan, Jamie, Isabelle and Ben. Particular thanks to Isabelle for supporting me during my first year and showing me the ropes of meticulous science. Thank you to Margus for allowing me to bounce ideas off him, for teaching me lab techniques and for helping me shape my PhD into something I am proud of accomplishing. Not only are you an inspiration as a scientist, with your expansive knowledge and sheer determination to succeed, but you are also a good friend. Ben and Margus, I don't envy you for having to read repeated iterations of my thesis, but I certainly thank you for it, it has been a great help!

I'm grateful to Jordan for keeping me moderately sane during the highs and lows of a PhD, I will certainly miss the unbelievable discussions we have had through the years, though I expect they won't be stopping any time soon. We have been through the fire and flames and came out the other side (relatively) unscathed. I couldn't have done it with anyone else. Jamie, you have also has been a sturdy rock with which to vent ones thoughts which was greatly appreciated. Your astounding ability to extract and distribute information around the lab is something I'll always remember. I expect you both to join me down south as soon as you are able!

And of course, thank you to my family, Alison and Jeremy. Both my mum and dad have supported me throughout my life, encouraging me when I've needed it and letting me go my own way in equal measure. While the competition between my dad and I will be fierce to the end, I hope I've done you both proud. Thank you to Granny Jennifer and your relentless interest in my activities, I expect to see a graduation photo on your desk! And lastly, I'd like to thank Anya, you provide me with the ultimate motivation to achieve the best I can, throughout all walks of life.

Authors Declaration

I declare that, except where explicitly stated that work was provided by others, that the following thesis is a result of my own work and has not been submitted for any other degree at the University of Glasgow or any other institution. Some work, including figures, has been or will be published in appropriate academic journals as indicated below.

Date 31/08/2018

Signature

Printed name

Timothy James Mottram

Chapter 1 Introduction

1.1 *Bunyavirales* molecular biology

1.1.1 *Bunyavirales* order classification

The *Bunyavirales* order is a large order of RNA viruses. The International Committee on Taxonomy of Viruses (ICTV) updated the relevant taxonomy of the formally known as *Bunyaviridae* family in 2017. The *Bunyavirales* order includes 9 distinct families; *Feraviridae, Fimoviridae, Hantaviridae, Jonviridae, Nairoviridae, Peribunyaviridae, Phasmaviridae, Phenuviridae* and *Tospoviridae*. The members of the *Bunyavirales* order all share some common characteristics; virions are spherical or pleomorphic and between 80-120 nm in diameter. Virions are enveloped and display glycoproteins on the surface of the envelope. The viral genome consists of three negative or ambisense single stranded RNA segments and all stages of virus replication occur in the cytoplasm (https://talk.ictvonline.org/taxonomy/).

The families within the *Bunyavirales* order are further categorised into 13 genera; *Hantaviridae* has one classified genus *Orthohantavirus, Peribunyaviridae* has two: *Herbevirus* and *Orthobunyavirus*. *Phenuviridae* has a further four genus; *Goukovirus, Phasivirus*, *Phlebovirus* and *Tenuivirus*. These distinct genera were identified through Bayesian modelling of sequence data and contain a number of important human and animal pathogens.

The *Bunyavirales* order consists primarily of arthropod borne viruses (arboviruses); that is, viruses transmitted through the bite of an arthropod vector including mosquitos, ticks, thrips and biting midges. With the exception of the *Hantaviridae*, which are transmitted through aerosolization of virus particles within rodent urine, saliva or faeces (Watson et al., 2014). *Hantaviridae* are also distinguished by the incidental nature of vertebrate infections that are almost always a dead-end host, resulting in the end of the virus infection chain. Not all members of the *Bunyavirales* order infect vertebrates, Tenuiviruses of the family *Phenuiviridae* and the *Tospoviridae* family are transmitted by thrips and are pathogenic to plants.

The transmission cycle of most bunyaviruses is maintained in nature through the invertebrate host, which can include *Phlebotominae* (commonly referred to as sandflies), mosquitoes, ticks, biting midge or thrips. Rift Valley fever phlebovirus of the *Phenuviridae* family is transmitted primarily by mosquitos and follows an enzootic cycle between ruminants, wild vertebrates and humans (Figure 1-1). Bunyaviruses multiply within the host after oral feeding or injection by the vector, though some members of the *Orthobunyaviridae* and *Phenuviridae* families are also transmitted transovarially by their vectors (Watts et al., 1973, Endris et al., 1983). Tick-borne arboviruses such as those found in the *Phlebovirus* genus can be transferred through transstadial transmission to the next development stage of the tick life cycle (Zhuang et al., 2018). The broad range of hosts, vectors and transmission cycles highlight the diversity of the *Bunyavirales* order and the importance of unveiling molecular mechanisms of each of its members.

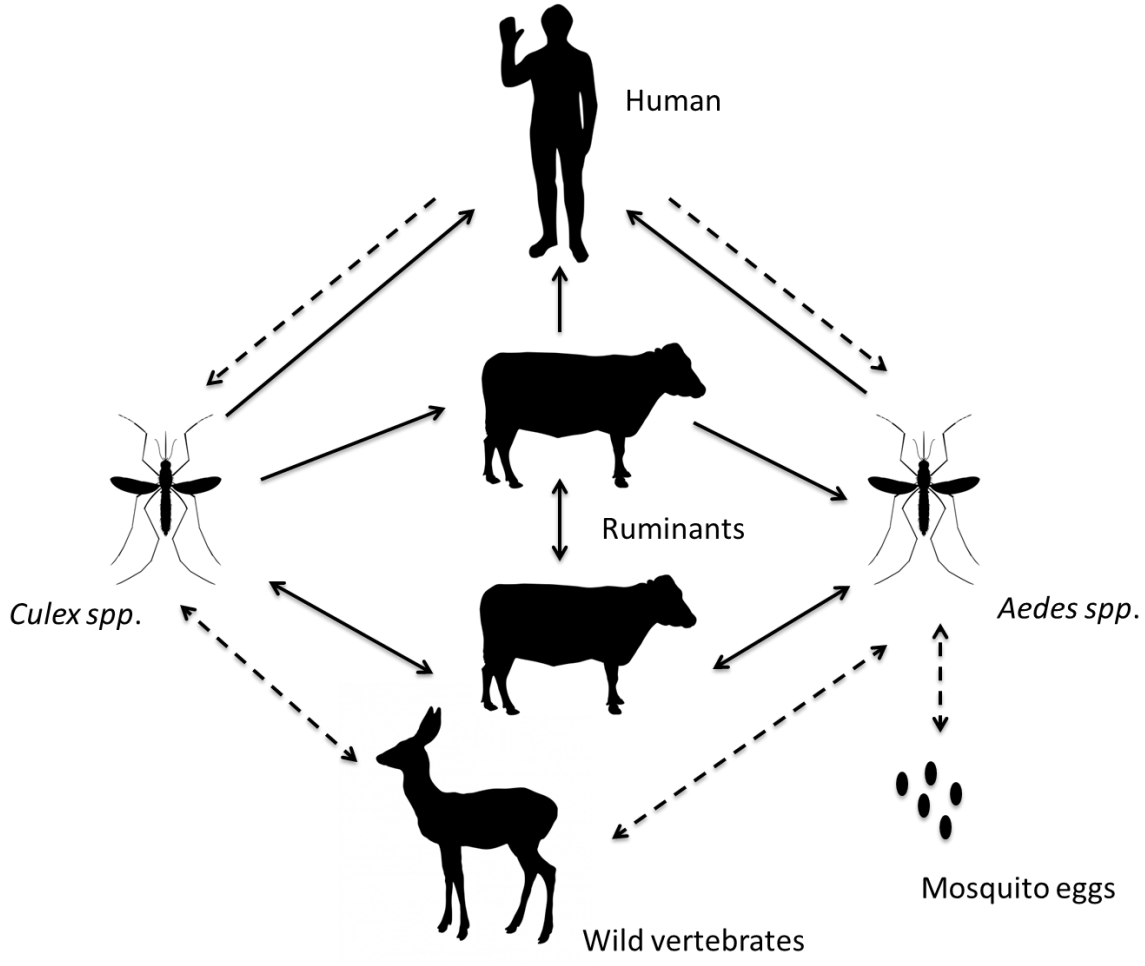

Figure 1-1. Mosquito-transmitted bunyavirus transmission cycle

The transmission cycle of Rift Valley fever phlebovirus (RVFV). Solid arrows represent confirmed routes of transmission through experimental data and dotted lines represent suspected routes of transmission. Adapted from (Lumley et al., 2017).

1.1.2 Classification and geographical distribution of Phenuiviridae.

The *Phenuiviridae* family is comprised of 4 genera: *Goukovirus*, *Phasivirus*, *Tenuivirus* and *Phlebovirus*. The *Goukovirus* genus prototype is Gouleako goukovirus, was thought to have prevalence in pigs throughout South Korea (Chung et al., 2014), however is now considered to be insect specific (Junglen et al., 2015). The *Phasivirus* prototype is Badu phasivirus, a recently discovered insect specific virus (Hobson-Peters et al., 2016). Viruses of the *Tenuivirus* genus are plant specific, characterised by the Rice stripe tenuivirus. The *Phlebovirus* genus is the largest and most widely studied genus of the *Phenuiviridae* family. The genus contains 10 virus species that are broadly divided into two specific groups based primarily on their genomic and vector similarities (Figure 1-2). The Phlebotomus group of viruses are transmitted by phlebotomines or mosquitoes however the Uukuniemi-like group are transmitted by ticks. Another important observation between the two groups is the lack of non-structural gene NSm in the Uukuniemi-like group, though there is no evidence of this distinction impacting vector specificity.

The Phlebotomine group consists of a number of important pathogens, including the prototype *Phlebovirus*, Rift Valley fever phlebovirus (RVFV, as described previously), Punta Toro phlebovirus (PTV), Sandfly fever Naples phlebovirus (SFNV) and Sandfly fever Sicilian virus (SFSV). The Uukuniemi-like group is based on Uukuniemi phlebovirus (UUKV) but also includes SFTS phlebovirus (SFTSV; previously known as severe fever with thrombocytopenia syndrome virus).These groups now include strains such as Toscana (TOSV), Heartland (HRTV) and Lone Star phleboviruses (LSV) that were previously assigned as species. The recent reorganisation of taxonomy has streamlined phylogeny allowing easier categorisation of emerging *Phenuiviridae*, particular as a growing number of novel *Phenuiviridae* have been identified. Phleboviruses have a global distribution determined by their specific vectors. TOSV is distributed across the Mediterranean basin, with seroprevalence in countries including Italy, France, Spain, Portugal and Cyprus in correspondence with its mosquito vector (Cusi et al., 2010). The distribution of vectors is evolving with climate change and globalization which is likely to result in further spread of phleboviruses into new ecological niches (Cusi et al., 2010, Gould et al., 2017).

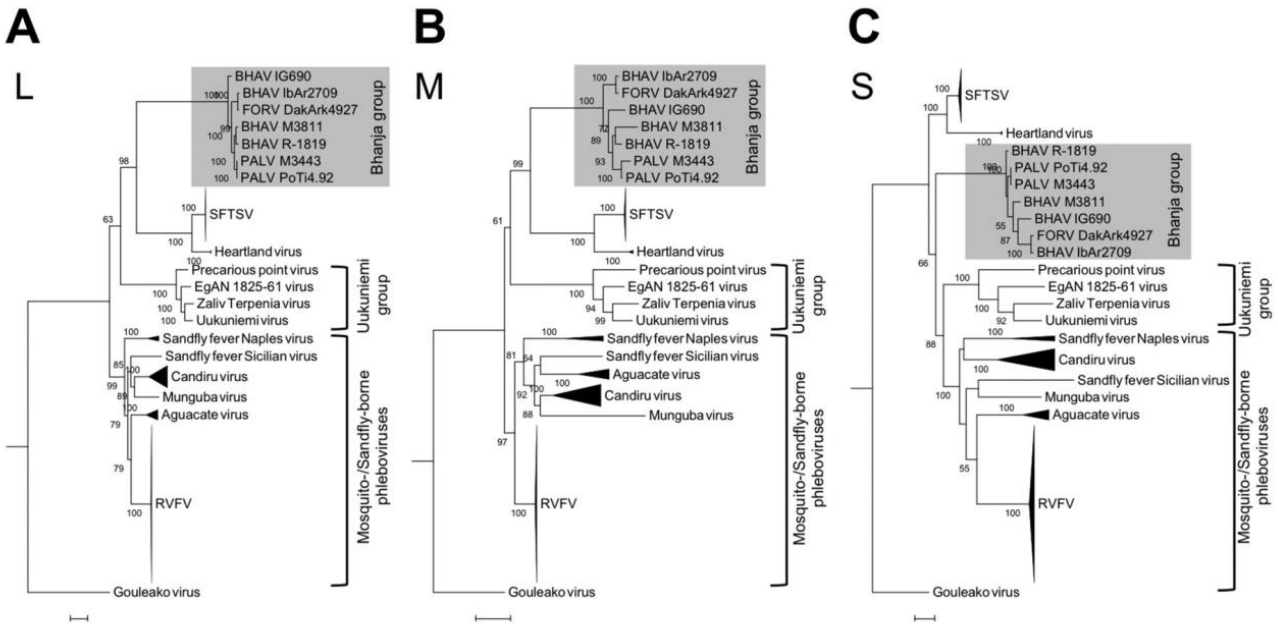

Figure 1-2. Phylogenetic analysis of phleboviruses.

Phylogenetic relationships between phleboviruses with highlighted vector groups analysed by nucleotide sequence modelling. (A) L segment RNA, (B) M segment RNA and (C) S segment RNA were analysed. Figure taken from (Matsuno et al., 2013).

1.1.3 Genome structure

The *Bunyavirales* is an order of viruses that are characterised by negative sense or ambisense single stranded RNA genome consisting of three unique segments. These segments are identified and named as large (L), medium (M) and small (S) based on their relative size (in base pairs). The size of each segment varies widely between different genera and strains of the *Bunyavirales* as highlighted in Figure 1-3. Genome structure of *Bunyavirales* members.Each segment is flanked by viral untranslated regions (UTR), the nt of each UTR are complementary, resulting in a characteristic pan-handle structure essential for the formation of viral ribonucleoproteins (RNP) (Lowen and Elliott, 2005, Gauliard et al., 2006).

The viral genomic segments encode four structural proteins: the negative sense L RNA segment encodes the RNA-dependent RNA polymerase (L). The negative sense, M RNA segment encodes the polyprotein precursor that is cleaved to produce the two glycoproteins, Gn and Gc. The S segment encodes the nucleocapsid (N) protein. Many of the *Bunyavirales* also encode for non-structural proteins as important virulence factors (Figure 1-3). The *Phenuiviridae* and *Tospoviridae* families uniquely employ an ambisense strategy on the viral S segment, encoding for the non-structural protein S (NSs). *Bunyavirales* members encode another non-structural protein NSm. *Tospoviridae* family uniquely utilises an ambisense M segment to encode NSm.

As bunyaviruses primarily have a negative sense single stranded RNA genome, upon infection each segment is used to transcribe a positive sense mRNA allowing the translation of viral proteins. In addition, each segment is copied in to an antigenomic RNA which is used as a template for the replication to generate nascent negative sense RNA genomes. However, the ambisense coding strategy employed in the S segment of some families also allows the generation of separate subgenomic RNAs. The generation of N subgenomic RNA occurs from the transcription of the negative sense genomic RNA however the NSs subgenomic RNA is transcribed from the antigenomic RNA (Figure 1-4)(Bouloy and Weber, 2010) This coding strategy was thought to function to temporally regulate the expression of N and NSs during infection, as the negative sense genomic RNA can be directly transcribed into mRNA, N protein expression occurs earlier in infection. The positive sense genomic RNA however has a further step

of transcription to negative sense anti-genome before generation of mRNA transcripts. The function of NSs as an interferon antagonist would indicate the need to be expressed early for successful infection and overcoming the host immune response. As such, RVFV packages positive sense NSs transcripts into virions that allow early expression of NSs in infection (Brennan et al., 2014). With RVFV, the transcriptional efficiency and promotor strength has also been shown to be higher for the negative sense N sequence than for the positive sense NSs sequence (Brennan et al., 2014). Bunyavirus morphology is characterised by three pan-handle RNP segments encased in an envelope studded with the glycoproteins Gn and Gc (Figure 1-4). Bunyavirus structure and morphology is further described in 1.1.5.

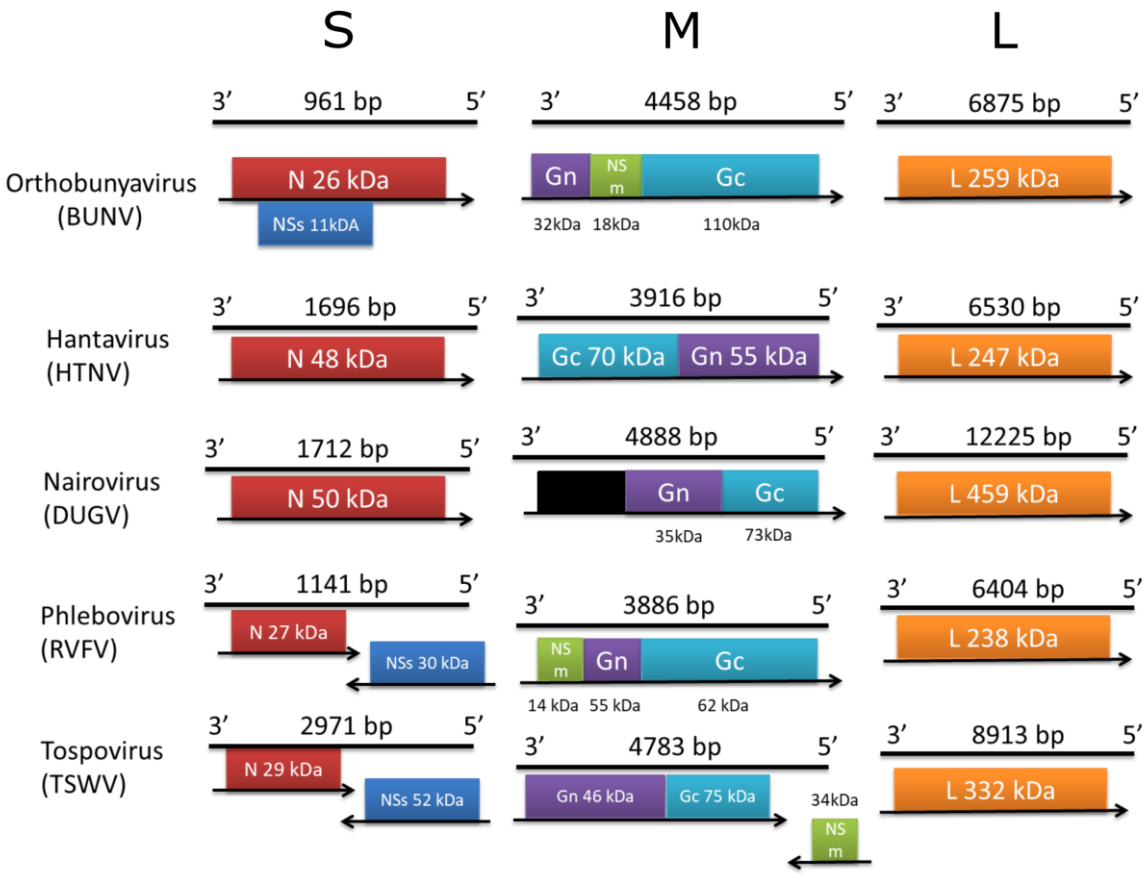

Figure 1-3. Genome structure of *Bunyavirales* members.

A schematic depicting the genome structure of members of the *Bunyavirales* order, including BUNV, HTNV, DUGV, RVFV and TSWV representing *Peribunyaviridae*, *Hantaviridae*, *Nairoviridae*, *Phenuviridae* and *Tospoviridae* respectively. All segments are presented in a 3' to 5' orientation as is convention for negative strand viruses, with arrows depicting the direction of transcription. Genome lengths are depicted above each viral segment and molecular weight of viral proteins is shown.

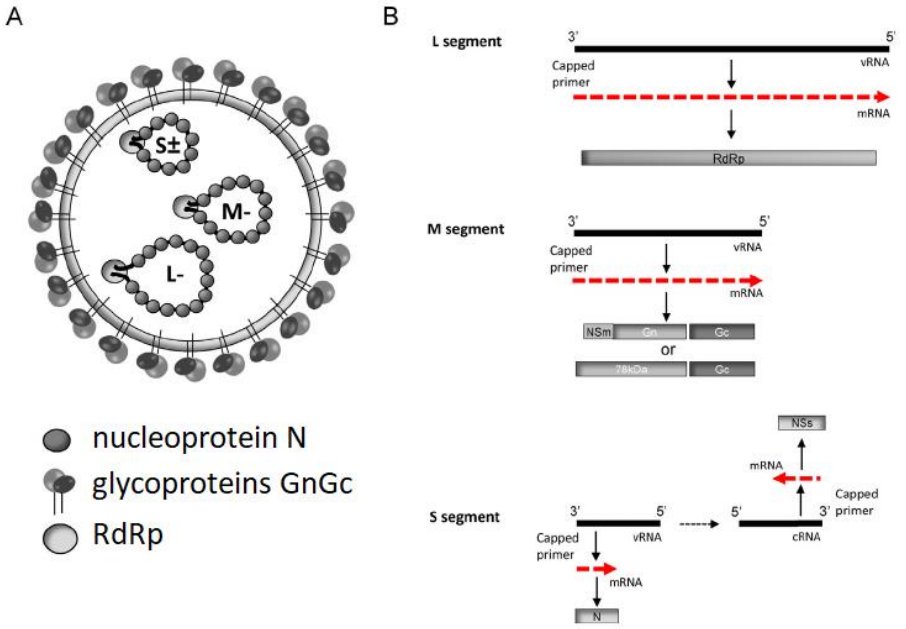

Figure 1-4. Viral structure and genome coding strategy of RVFV

Schematic representation of the organisation of the RVFV viral particle and its ambisense genome coding strategy. (A) A representation of the viral particle with the glycoproteins studding the viral envelope and the formation of "pan-handle" RNP complexes. (B) The negative sense genome is transcribed into a positive sense antigenome which is used as a template for genome replication, or it can be transcribed into mRNA for translation of the L or M precursors. The ambisense genome transcribes the N mRNA in the negative sense as above, however mRNA production of the NSs gene requires the generation of an intermediate antigenome RNA before transcription of NSs mRNA. Red dotted arrows represent mRNA.

1.1.4 Bunyavirus gene products: expression and function

1.1.4.1 RNA-Dependent RNA polymerase

The RNA-dependent RNA polymerase, commonly referred to as RdRp or L protein is encoded by the large segment of the genome. The molecular weight (m.w.) of L varies according to genus, and is found to be between 240 – 460 kDa. The L protein of the *Bunyavirales* order and *Arenaviridae* family contain a unique conserved region found between the premotif A and polymerase module A that can only be found in negative-stranded RNA viruses (Müller et al., 1994). The polymerase contains 6 polymerase modules labelled from PreA to A-E common between all RNA-dependent RNA polymerases. The L protein has also been identified to contain cap-snatching domains, a function exclusive to single stranded negative sense viruses (Reguera et al., 2010). La Crosse virus (LACV) These domains function to recognise capped cellular mRNAs and cleave 10-14 nucleotides downstream to prime viral mRNA transcription. This mechanism has been identified in *Orthobunyaviridae, Arenaviridae and Phenuiviridae* (Reguera et al., 2016, Brennan et al., 2011a, Shi and Elliott, 2009).

1.1.4.2 Nucleocapsid

The nucleocapsid (N) protein is the most abundant viral protein detected during bunyaviral infection. The size of N monomers varies between different members of the *Bunyavirales* order. A key function of N is multimerisation, where N binds to adjacent monomers to form multimeric structures (Ferron et al., 2011). The number of monomers required to form a functional multimeric structure again varies between *Bunyavirales* members (Table 1-1). N protein has two key structural elements that aid in the formation of multimeric structures. Primarily, it has a flexible N-terminal arm that can rotate through differing degrees in order to bind adjacent N proteins (Raymond et al., 2012). The binding of the N-terminal arm occurs in a hydrophobic globular binding pocket near the C-terminus of N. By observation of the crystal structure, it was shown that in the absence of bound RNA, the N-terminal arm binds into its own globular binding pocket resulting in a low-energy closed conformation, thus hinting that this process is strongly linked to the second primary function of N, the encapsidation of the viral genomic segments (Raymond et al., 2010).

The formation of N protein into multimeric structures allows the binding of the RNA genome into a positively charged RNA binding cleft (Figure 1-5). The binding cleft has a varied capacity depending on the size of the nucleocapsid, with RVFV N having the capacity to bind 6 nucleotides per monomer, thus 36 per hexamer (Raymond et al., 2012, Ferron et al., 2011). This encapsidation process is essential for the formation of RNP complexes, allowing the recruitment of L and the further transcription and replication of the genome. While the mechanism of this is relatively understudied, it has been shown in the related phlebovirus TOSV that the binding of RNA to TOSV N results in an inter-subunit rotation allowing the formation of a helical shape characteristic of many negative-strand viruses (Olal et al., 2014). In addition, the encapsidation process also functions to protect the viral genome from harsh cytoplasmic conditions including RNA degradation through RNase enzymes. N protein also plays an important role in packaging of genome into virions by interacting with the cytoplasmic tails of RVFV glycoproteins (Overby et al., 2007). As replication takes place in the cytoplasm during infection, both L protein and N protein are typically observed with a diffuse localisation throughout the cytoplasm.

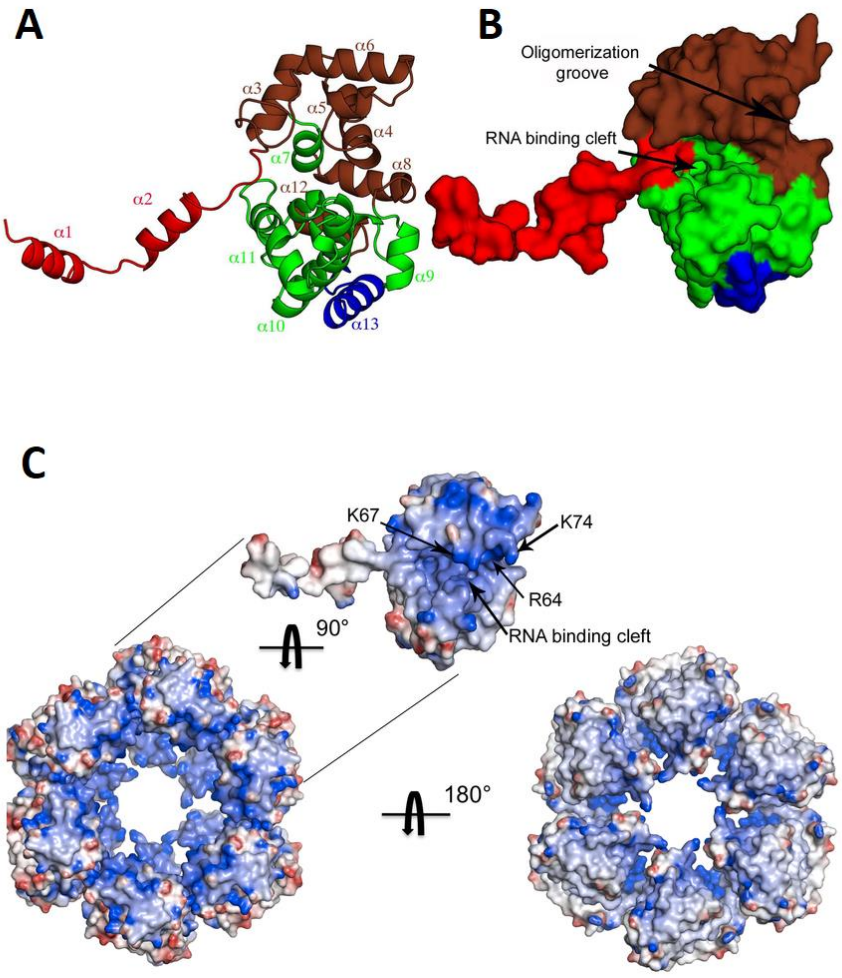

Figure 1-5. RVFV N protein monomeric and multimeric structure and electrostatic potential.

(A) A ribbon structure of RVFV N protein with highlighted subdomains; N-terminal arm in red, globular domains in brown and green and C-terminus in blue. (B) A surface structure of RVFV N protein with highlighted oligomerisation groove and RNA binding cleft. (C) The positively charged residues of N are evident on the internal ring of the multimeric structure. Taken from (Ferron et al., 2011).

Virus	Nucleocapsid size	Multimeric units
RVFV	27 kDa	6 units
RV	56 kDa	11 units
VSV	47 kDa	10 units
RSV	43 kDa	10 units
IVA	56 kDa	9 units
BUNV	26 kDa	4 units
HTNV	50 kDa	3 units

Table 1-1 N protein size and unit variation between –ve sense RNA viruses.

1.1.4.3 Glycoproteins

Bunyavirales order members encode for a single polyprotein on the M genomic RNA segment. This transcript encodes a polyprotein that is post translationally cleaved into two glycoproteins, Gn and Gc. In the case of RVFV, there is an additional cleavage event resulting in the production of a small non-structural protein termed (NSm) that is translated through alternative start codon usage of 5 AUG sites within the transcript. This alternative codon usage, potentially through a leaky scanning mechanism, results in the translation of two further non-structural proteins, NSm' and P78 (Figure 1-6)(Kreher et al., 2014). Gn and Gc are integral for virus attachment to the cell membrane and viral entry (De Boer et al., 2012b). They are type-I membrane glycoproteins that form functional heterodimers. Gn has been identified to contain a Golgi localisation signal and Gc an endoplasmic reticulum retention signal thus Gn-Gc heterodimers are formed in the ER before subsequent relocalisation to the Golgi apparatus (Andersson and Pettersson, 1998). The targeting signals found on Gn vary widely between different *Bunyavirales* members (Carnec et al., 2014). As bunyaviruses do not encode a matrix protein, the interaction between the C-terminal cytoplasmic tail of Gn and the nucleocapsid allows the assembly of RNP complexes into the virion and allows the budding of mature virions from the lumen of the Golgi (Piper et al., 2011, Hepojoki et al., 2010).

Glycoprotein Gc is composed mainly of ß-sheets and thus has been proposed to be a class II viral fusion protein (Garry and Garry, 2004), similar to those encoded by the *Flaviviridae* and *Arenaviridae*. Thus, Gc acts as the fusion molecule between the viral envelope and the host cell membrane. For the *Phenuiviridae*, the primary receptor for Gn has been identified as the

interceullar adhesion molecule-3-grabbing non-integrin (DC-SIGN) (Hofmann et al., 2013, Phoenix et al., 2016b). With RVFV, N-glycans on the surface of Gn have been shown to bind DC-SIGN. There is also evidence showing the C-type lectin (77% homology) L-SIGN can also be used as a receptor for entry of these viruses (Léger et al., 2016).

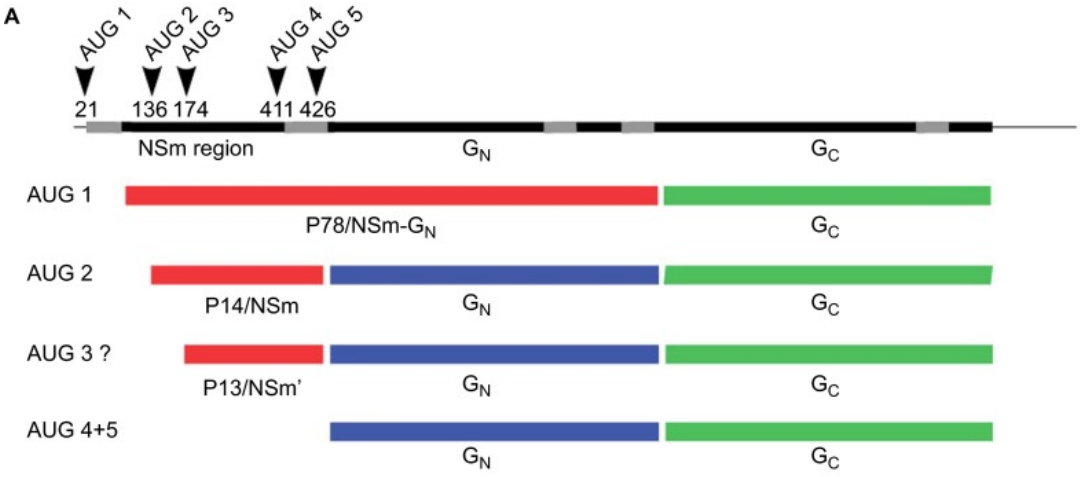

Figure 1-6 RVFV M segment polyprotein post processing and cleavage.

The polypeptide 78kD-Gc and NSm-Gn-Gc are transcribed from the 1st AUG and 2nd AUG respectively. There are two signal peptidase cleavage sites. The first cleavage site at 477-482 allows the cleavage of NSm-Gn-Gc into NSm and Gn. The second cleavage site resides at position 2088-2093 and functions to cleave the 78kD-Gc (Phoenix et al., 2016a). This site also cleaves NSm-Gn-Gc into NSm-Gn and Gc. Adapted from (Kreher et al., 2014).

1.1.4.4 Non-structural NSs proteins

The S segment of some bunyaviruses, including RVFV, encodes for a non-structural protein (NSs) in the positive sense orientation (Figure 1-3), whereas other bunyaviruses encode NSs from within the N ORF. In RVFV, the NSs protein is 265 aa long and 31 kDa in size. The primary function of vertebrate infecting bunyavirus NSs is believed to be the antagonism of the interferon system (Eifan et al., 2013). This function is conserved across bunyaviruses despite little sequence homology as evidenced by the sand-fly fever group of phleboviruses, where NSs amino acid sequence homology ranges between 7.5 and 28.6%, despite carrying out broadly similar functions (Xu et al., 2007). NSs is non-essential for replication, however non-functional NSs-deletant viruses (delNSs) often show an attenuated phenotype and reduced viral growth kinetics (Bird et al., 2008). RVFV NSs has been identified to inhibit the JAK/STAT signalling pathway; dysregulating the inflammatory response (Benferhat et al., 2012). However, most research focuses on NSs protein's inhibitory effect on general host transcription (Billecocq et al., 2004). Additionally, RVFV NSs specifically targets IFN-ß for transcriptional inhibition through the formation of a multiprotein repression complex that binds to the IFN-ß promoter (Figure 1-7) (Le May et al., 2008). NSs protein localises and accumulates in the nucleus through use of two PXXP motifs (Proline.any.any.Proline) present within the encoded amino acid sequence at positions 29 to 32 and 82 to 85. These motifs are absent in the RVFV clone 13 NSs and requires nuclear localisation to carry out its inhibitory functions (Billecocq et al., 2004). In RVFV specifically, it was previously considered that the highly acidic 17aa C-terminus of NSs functions, along with a ΩX*a*V (Aromatic.any.acidic.valine) motif to form distinct filamentous structures (Yadani et al., 1999, Cyr et al., 2015), however a crystallisation study of NSs with N and C terminal deletions still formed filamentous structures (Barski et al., 2017); this discrepancy is considered to be an artefact of single terminal deletions resulting in non-native self-interactions and destabilization of the filaments, an effect lost in N,C double mutants. These filamentous structures are an important virulence factor. The formation of filamentous structures requires a direct interaction between the terminal region of the NSs protein and p44 subunit of general transcription factor IIH (TFIIH) (Le May et al., 2004). By sequestering p44, the TFIIH complex components p62 and Xeroderma pigmentosum group D (XPD) subunits were degraded. RVFV NSs

protein binds p62 through the use of aa ΩX*a*V motif (Cyr et al., 2015) and F-box ubiquitin ligase (FBXO3) resulting in ubiquination of p62 and subsequent degradation and suppression of the IFN response (Kalveram et al., 2011, Kainulainen et al., 2014).

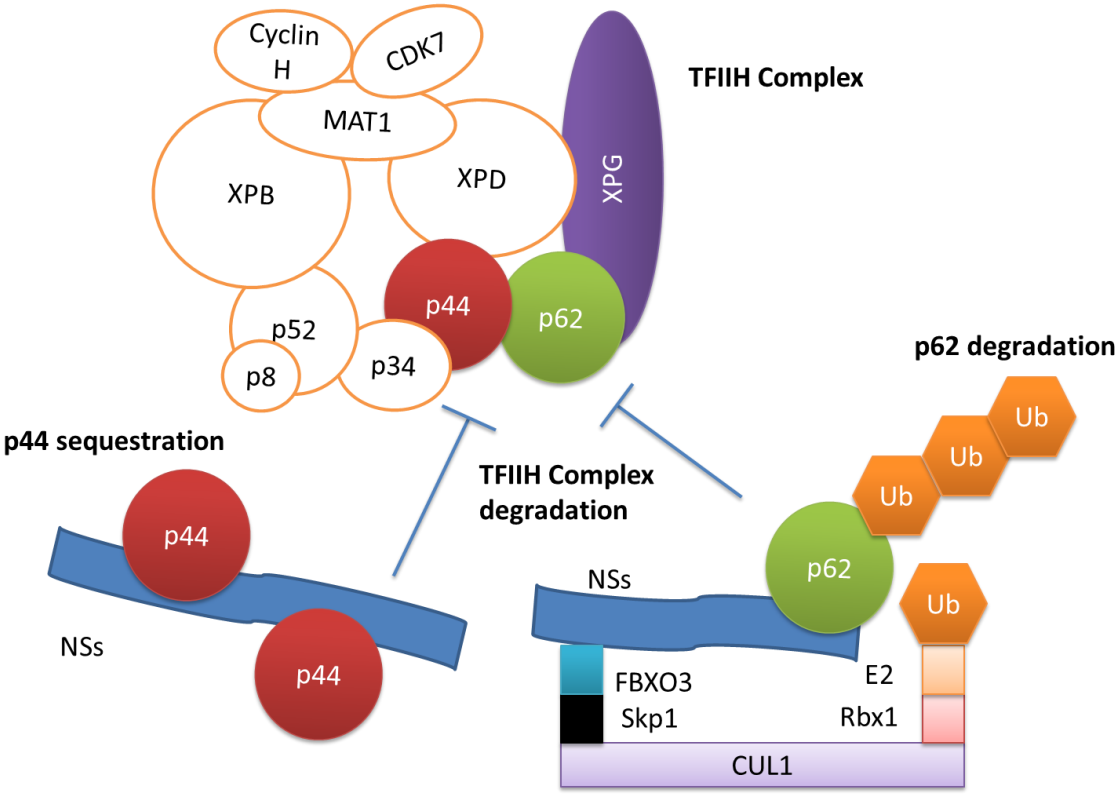

Figure 1-7. Schematic detailing the mechanism of NSs-mediated TFIIH suppression.

The TFIIH complex is inhibited either through the sequestration of p44 by the NSs protein or through NSs interaction with FBXO3 and subsequent ubiquitination and proteosomal degradation of p62. Adapted from (Ly and Ikegami, 2016).

1.1.4.5 Non-structural proteins NSm, Nsm' and P78

During the replication of RVFV, the leaky scanning and differential cleavage of the M segment polyprotein results in the expression of three non-structural proteins NSm, a 14-kDa cytosolic protein and P78 (NSm') and a 78 kDa glycoprotein (P78). Translation from the first AUG and further differential cleavage results in production of the NSm-Gn fusion protein known as P78 (Figure 1-6). The translation from AUG2 results in the expression of NSm and the translation from AUG3? results in NSm'. The translation from AUG4 and AUG5 express just the glycoproteins Gn and Gc. Both NSm and P78 are non-essential for viral replication, maturation and infection in cell culture (Won et al., 2006, Gerrard et al., 2007). NSm localises to the mitochondrial membrane and prevents early cellular apoptosis through inhibition of caspase 8, potentially caspase 9, and caspase 3 (Terasaki et al., 2013, Won et al., 2007). In addition, NSm is important for regulating reactive oxygen species (ROS) potentially through the activation of p38 MAPK (Narayanan et al., 2011). P78 however localises to the Golgi complex (Wasmoen et al., 1988) and forms heterodimers with Gc, resulting in packaging within the virus particle. However, despite expression within mammalian cells, packaging of P78 has only been observed in mosquito cell culture (Weingartl et al., 2014). NSm and NSm' are important for replication in the vector host and P78 has been identified as an important for virus dissemination within mosquitos (Kading et al., 2014, Kreher et al., 2014).

1.1.5 Virion structure

The virion structure of bunyaviruses are composed of four structural proteins. The nucleocapsid protein and the RNA-dependent RNA polymerase, which form the functional units of the ribonucleoprotein complex when bound the three RNA genomic segment and the glycoproteins Gn and Gc which are studded on the surface of the lipid envelope. The RNP complexes have a distinct shape within the cytoplasm and virion, displaying a circular panhandle structure important for replication in the infected cell (Obijeski et al., 1976). The average replication time for a genomic segment was estimated to be 40 min (Wichgers Schreur and Kortekaas, 2016). These RNPs are packaged into the virion in a non-selective process, resulting in many virions lacking genome segments. As expected with non-selective packaging, the intracellular genome segments average a S:M:L

ratio of 1:1:1 yet individual cells had major variation in genome segment ratio (Wichgers Schreur and Kortekaas, 2016). It is also evident that while the majority of packaged segments are genomic there are a proportion of antigenomic segments packaged in RVFV virions (Brennan et al., 2014).

Virion morphology and size varies between different members of the *Bunyavirales*. The virion diameter has been observed for a number of bunyaviruses including Bunyamwera orthobunyavirus (BUNV) at 108 ± 8 nm (Bowden et al., 2013), UUKV at 95-125 nm (Overby et al., 2008) and RVFV at 102 ± 3 nm (Bowden et al., 2013, Freiberg et al., 2008). The lipid envelope surrounding RVFV RNP complexes is studded with 350-375 glycoprotein spikes which measure 10 to 18 nm in length and approximately 5 nm in diameter (Ellis et al., 1988). RVFV and UUKV have both been found to have an icosahedral lattice of glycoproteins where T=12 (Freiberg et al., 2008, Overby et al., 2008). BUNV however was found to be pleomorphic (Bowden et al., 2013) and Tula orthohantavirus can form both spherical and elongated virions (Huiskonen et al., 2010) thus highlighting the diversity of morphologies seen within bunyaviruses virions.

1.1.6 Replication cycle

1.1.6.1 Viral Entry

Bunyaviruses have a similar entry mechanism to other enveloped viruses, utilising the virally-encoded glycoproteins Gn and Gc (1.1.4.3) in a heterodimeric conformation to bind to receptors on the host cell surface. Different bunyaviruses make use of varying receptors and cellular factors to gain entry to a multitude of different cell types from different host species. Arthropod-borne bunyavirus entry classically begins with the bite of an infected arthropod into the dermis of its vertebrate host. At the bite site, bunyaviruses first encounter dendritic cells and dermal macrophages (Albornoz et al., 2016), a process common to arboviruses that provides new cellular targets for infection (Pingen et al., 2016). To gain access to the intracellular environment, RVFV and other *Phleboviruses* utilise the glycosaminoglycan (GAG) heparin sulfate to dock to the membrane of the cell using electrostatic interactions (Figure 1-8 part 1) (De Boer et al., 2012a, Riblett et al., 2016). This was evidenced by

competitively inhibiting GAGs reduced *Phlebovirus* infection (Pietrantoni et al., 2015). As mentioned previously (1.1.4.3) RVFV and other members of the *Phlebovirus* genus utilise the C-type lectin DC-SIGN for infection and entry of dendritic cells. By overexpressing DC-SIGN on the surface of cells that do not effectively support bunyavirus infection, one can significantly improve infection with RVFV, UUKV and TOSV (Lozach et al., 2011). In addition to DC-SIGN, RVFV, TOSV and UUKV have been shown to exploit a second C-type lectin L-SIGN as a receptor (Léger et al., 2016). Hantavirus receptor-mediated entry is vastly different from other bunyaviruses due to the nature of Hantavirus aerosol transmission. Hantaviruses first cellular contact is with lung epithelium and Hantaviruses utilise intergrins $ß_1$, $ß_2$ (CD18) found on endothelial neutrophils, and $ß_3$ found on platelets and endothelial cells, to gain entry to the intracellular space (Raftery et al., 2014, Gavrilovskaya et al., 1998). Additionally, receptors decay-accelerating factor (DAF)/CD55 and the receptor for the global domain of complement C1q (gC1qR)/p32 are also important for Hantavirus entry (Krautkrämer and Zeier, 2008, Choi et al., 2008).

Once bound to the receptor, bunyaviruses must be endocytosed to gain entry to the intracellular environment. It was determined using a UUKV model system that receptors are recruited to virus particles to form a receptor-rich microdomain on the plasma membrane at the site of virus entry (Lozach et al., 2011). DC-SIGN was identified as an important endocytic receptor as well as attachment factor in UUKV infection, in contrast L-SIGN was not used during endocytosis indicating its role as purely an attachment factor (Léger et al., 2016). Bunyaviruses have been shown to utilise different endocytic methods to gain cellular entry. Orthobunyaviruses and nairoviruses primarily use clathrin-mediated endocytosis to infect cells, however the mechanism of *Phlebovirus* entry still remains unclear. UUKV entry has been associated with clathrin-coated pits and vesicles however clathrin silencing had no effect on the ability of UUKV to infect cells in culture (Lozach et al., 2011, Lozach et al., 2010). RVFV has been suggested in numerous studies to use a variety of different cellular entry methods, including clathrin, caveolin-dependent and micropinocytosis (Figure 1-8 part 2) (Harmon et al., 2012, De Boer et al., 2012b, Filone et al., 2010) thus bunyavirus entry may be cell, tissue or virus strain specific.

Upon uptake, bunyavirus particles are transported via vesicles through the endocytic machinery before subsequent fusion and penetration into the cytosol. Bunyaviruses transit through early endosomes (EE) to late endosomes (LE), encountering a pH ranging from ~6.5 in EEs to ~5.5-5 in LE. Endosomal acidification is thought to be the trigger for bunyavirus activation and penetration (Figure 1-8 part 3) (Harmon et al., 2012, De Boer et al., 2012b, Shtanko et al., 2014). The blocking of trafficking and maturation of EEs blocks infection of many bunyaviruses including UUKV and CCHFV (Shtanko et al., 2014, Hollidge et al., 2012, Lozach et al., 2010). RVFV and UUKV are late penetrating viruses, meaning that they penetrate between 20-40 min after internalisation which corresponds with the maturation of the late endosome (Lozach et al., 2010, De Boer et al., 2012b). In addition, bunyaviruses require an intact microtubule network for successful infection, allowing the trafficking of the LE towards the nucleus (Simon et al., 2009, Lozach et al., 2010).

Endocytosed viruses must fuse with the endosomal vesicle membrane to release their genome into the cytosol (Figure 1-8 part 4). This fusion event, as mentioned previously (1.1.4.3), is primarily mediated by the envelope glycoproteins Gn and Gc. In RVFV and UUKV infection, changes in glycoprotein conformation and resulting fusion event is triggered by low pH acidic conditions (Overby et al., 2007, De Boer et al., 2012b). Thus, upon conformational change, glycoproteins harpoon the endosomal lipid bilayer resulting in hemifusion and fusion pore formation allowing the viral RNA to be delivered into the cytoplasm (Albornoz et al., 2016).

1.1.6.2 Transcription and translation

Following entry of the viral genomic RNPs into the cytosol, transcription from genomic RNA occurs (Figure 1-8 part 5). This process involves the viral L protein utilising its cap-snatching mechanism of cleaving the 10-18 nucleotide long 7-methylguanosine (^{m7}G) cap from host cell pre-mRNA (Shatkin, 1976, Topisirovic et al., 2011). The host cell pre-mRNA caps are transferred to the 5' end of the viral transcript by L protein activity allowing recognition of viral mRNA by host cell ribosomes (Patterson et al., 1984, Garcin et al., 1995). The complementary regions of the viral genomic segments UTR regions are important for the formation of panhandle RNP structures; however they are also involved in the

binding of L to the RNP and crucial in determining promoter strength, therefore are important for regulating viral RNA synthesis (Kohl et al., 2004, Mir and Panganiban, 2004). The S, M and L mRNAs are bound by free ribosomes in the cytoplasm for translation, while M transcription is initiated in the cytoplasm, it is hypothesised that Gn subsequently recruits M complexes to membrane bound ribosomes at the ER (Wichgers Schreur and Kortekaas, 2016).

Bunyaviral mRNAs do not contain a poly(A) tail nor any U-rich sequences. Transcription termination signals are variable between segments but are generally located upstream of the 3' end of the genomic mRNA. Some termination signals have been identified such as a purine-rich region for M segment mRNA of RVFV and a C-rich motif for the S segment mRNA of SNV (Collett, 1986, Hutchinson et al., 1996). There have been two nucleotide motifs, 3'-GUCGAC-5' and 3'-UGUCG-5' identified in BUNV S segment mRNA that are critical to signalling termination (Barr et al., 2006). The intergenic region of *Phlebovirus* S segments termination signals vary between species. RVFV has been shown to contain a 5'-GCUGC-3' motif which plays a role in transcription termination (Lara et al., 2011, Ikegami et al., 2007, Albariño et al., 2007). UUKV however terminates the N signal at the end of the 3' NSs gene, whereas the NSs gene terminates within the N gene in the opposite orientation (Simons and Pettersson, 1991). SFTSV was found to contain overlapping termination signals in both N and NSs genes and termination occurred upstream of a 5'-GCCAGCC-3' motif (Brennan et al., 2017).

Bunyaviruses have been shown to have a unique coupled transcription-translation mechanism. As there are multiple transcription termination sites within the genomic sequence, the mRNA can hybridize to the genome at these sites resulting in premature termination. However, translocating ribosomes trailing the viral polymerase can prevent these hybridization events until the termination sequence is reached in the UTR (Barr, 2007).

1.1.6.3 Genome replication

Replication of the viral genome requires the generation of complementary antigenomic RNAs (cRNA) which are then used as a template to generate genomic RNA (gRNA) which can be further used as a transcription template or

packaged into virions (Figure 1-8 part 6). The mechanism that governs the switch between mRNA transcription and full length replication is unclear. There may be a link to the level of N to allow encapsidation of the cRNA and gRNA during replication, particularly as the cRNA is always found encapsidated (Elliott, 2014). Additionally, cRNAs and gRNAs can be identified by their lack of cap structure. During infection with RVFV, the transcription factor TFIIH interacting with NSs (1.1.4.4) may help balance transcription and replication during infection by limiting primers for transcription and thus favouring primer-independent replication (Le May et al., 2004). Interestingly, the M RNA is the most abundant viral RNA present within the infected cell during replication, followed by the L RNA and then S RNA (Barr et al., 2003), despite transcription and replication only requiring L and N proteins. Encapsidation of the genome by N protein is essential for genome replication, possibly through keeping the genome in a linear form, thereby allowing full genome synthesis (Guu et al., 2012). In hantaviruses, it has been proposed that a polymerase slippage mechanism, where the polymerase realigns on the RNA, removing an overhanging guanosine triphosphate group leaving a 5' uridine monophosphate allowing elongation to continue to generate a full length sequence (Garcin et al., 1995). Additionally, during replication it is key for bunyaviruses sequence integrity to be preserved. The L protein has been shown to be capable of repairing insertions and deletions during RNA replication (Walter and Barr, 2010).

1.1.6.4 Viral budding and release

The generation of infectious bunyavirus particles within the natural life cycle requires the packaging of all the genome segments into a single virion (Wichgers Schreur and Kortekaas, 2016), however it is possible to generate 2 segmented viruses expressing all the structural proteins through manipulation of the viral genome (Brennan et al., 2011b). Packaging has been shown to be a non-selective process which can result in the generation of virions missing one or multiple genome segments rendering the particles inert (Wichgers Schreur and Kortekaas, 2016). The intermolecular interactions between UTRs and genome segments may be important in the packaging process (Terasaki et al., 2011) though evidence of packaging in 2 segmented viruses lacking these regions indicate these intermolecular interactions are not essential (Brennan et al., 2011b).

Virus assembly takes place in the Golgi apparatus (Figure 1-8 part 7), as evidenced by the targeting signal of Gn, identified to be a 48 amino acid region spanning a transmembrane domain and the second hydrophobic domain in the cytoplasmic tail (Andersson and Pettersson, 1998, Gerrard and Nichol, 2002). The mechanism behind the retention of Gn in the Golgi is unknown, but may follow one of two models; the oligomerisation of Gn into structures too large to be secreted or the short transmembrane domains of Gn result in segregation from sterol- or sphingolipid rich transport vesicles (Gerrard and Nichol, 2002). The Golgi is also the site of viral factories, tubular structures and an actin matrix that functions to provide a stable scaffold for viral replication and budding (Fontana et al., 2008). Additionally, RNPs have been shown to target glycoprotein-rich regions of the Golgi through the interaction with Gn and Gc before budding (Overby et al., 2007, Rusu et al., 2012). Virions are transported from the Golgi apparatus to the plasma membrane via vesicles via exocytic release (Figure 1-8 part 8 and 9) (Shi et al., 2010).

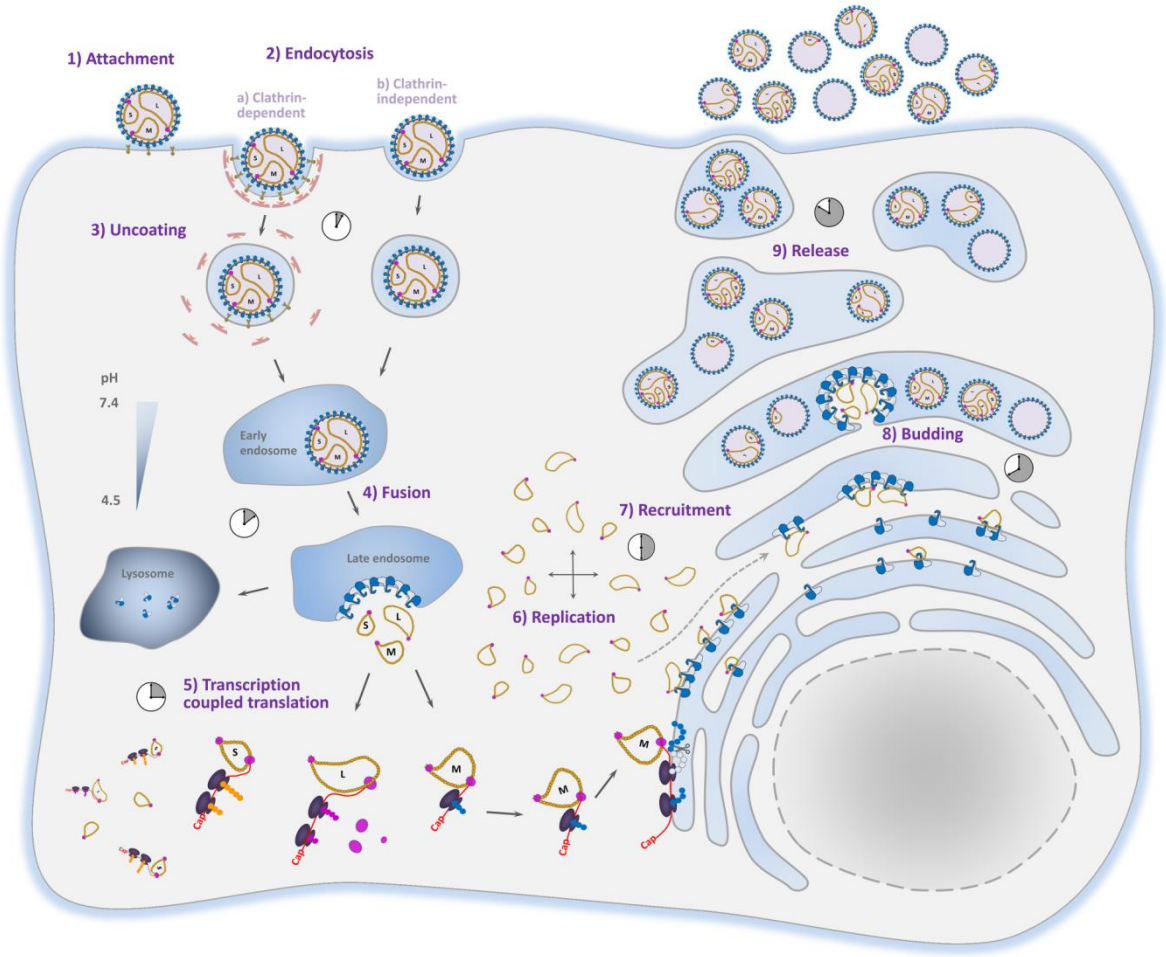

Figure 1-8. Schematic of RVFV life cycle.

(1) Attachment occurs with the interaction of cell surface receptors and RVFV Gn and Gc. (2) Entry occurs via clathrin-dependent or independent endocytosis. (3) The acidification of early endosomes results in the dissociation of clathrin and the uncoating of the virus particle. (4) Fusion occurs in the late endosome allowing release of the viral RNPs into the cytosol. (5,6) The RNPs are used as templates for transcription and replication. The S and L segments bind free ribosomes for translation in the cytoplasm, the M segment is translated by membrane bound ribosomes at the endoplasmic reticulum (ER). The formation of additional RNPs results in replication of the genomic segments. (7) The association of GnGc complex and RNPs recruits viral components to the Golgi. (8) RNPs accumulate at the Golgi and are non-specifically packaged into virions by budding from the Golgi lumen. (9) Mature virus particles are exocytosed from the cell. Taken from (Wichgers Schreur and Kortekaas, 2016).

1.2 *Phlebovirus genus* family

1.2.1 *Phlebovirus* infection and disease

Phleboviruses cause a multitude of different diseases in both humans and animals, of varying severity. Many of the phlebotomine group of viruses generally cause mild symptoms in humans. SFSV and SFNV infections for example are self-limiting and characterised by fever myalgia and headache (Cusi et al., 2010). TOSV also can cause febrile erythema or influenza like symptoms (Portolani et al., 2002). However can be a major cause of aseptic meningitis, particularly in the summer months when mosquito populations are most prevalent (Valassina et al., 2000).

Infection with the Uukuniemi-like group of viruses also has a wide variation in disease outcomes in animals and man. UUKV-infected individuals show no clinical signs of disease however the closely related Heartland phlebovirus is highly pathogenic resulting in a widely disseminated infection with multiple organ failure (Fill et al., 2017). Since its emergence, SFTSV has become a significant issue across China, Japan and South Korea. SFTSV causes fever, thromobytopenia, gastrointestinal symptoms and leukocytopenia amongst other symptoms (Liu et al., 2014). Infection with SFTSV leads to SFTS-like disease which has a mortality rate between 12-30% (Silvas and Aguilar, 2017).

1.2.2 RVFV disease

RVFV was first isolated in the Rift Valley, Kenya in 1930 after an outbreak displaying signs of enzootic hepatitis resulting in death of adult ruminants and pregnant ruminants abortion storms (Daubney et al., 1931). RVFV is primarily transmitted by *Aedes albopictus* and *Culex pipiens* mosquitos however the virus is replication competent in a large number of mosquito species including *Anopheles* species such as *An. pharonesis*, *An. stephensi* and *Cx. antennatus* among others (Nepomichene et al., 2018, Turell et al., 1996). Despite these mosquitos being susceptible, there is lack of evidence showing viral release in saliva and thus the role of these species in transmission is unknown. Since its identification, RVFV's geographical distribution has spread significantly to include most of the African continent and more recently spread to the Arabian

Peninsula in 2000-2001 (Madani et al., 2003). The gradual spread of RVFV may be related to the distribution of RVFV vector species that has been undergoing range expansion (Kraemer et al., 2015). There have been several severe outbreaks associated with RVFV including South Africa in 1950, Egypt in 1977 (Gear, 1979) and Saudi Arabia in 2000 (Madani et al., 2003). The Egyptian outbreak had a reported 200,000 human cases and 598 deaths with a estimated impact of $115 million. The outbreak in Egypt signified the first time RVFV had crossed the Sahara desert, an important geographical barrier. In 1979, RVFV was isolated from Madagascar, crossing the Mozambique channel, thus indicating the breakdown of another geographical barrier in the spread of the virus (Morvan et al., 1991). The outbreak in Saudi Arabia and Yemen showed RVFV's ability to spread across the Red Sea ((Cdc), 2000a, (Cdc), 2000b).The most recent significant outbreak in Kenya 2007 had an estimated 75,000 human cases however only 684 were reported and there were 158 deaths indicating a large discrepancy between the reporting of RVFV and predicted cases, likely due to lack of healthcare infrastructure and the classical febrile symptoms of RVFV being similar to other reportable diseases. The yearly rate of infection is unknown, however the average of reported cases across Africa between 2006-2012 was 459, with 101 case fatalities, though this excludes estimated cases within outbreaks (Nanyingi et al., 2015).

RVFV strains can be categorised into 7 main lineages based on molecular genotyping. This molecular epidemiology highlights the spread of RVFV throughout the African continent (Figure 1-9); particularly there are long distance translocations of RVFV species indicating human influence on the spread of RVFV between distant regions as evidenced by phylogenetic analysis of isolates. This is particularly apparent with the phylogenetic similarity between the Egyptian isolates of 1977-1979 and the Madagascar isolate 1979 (Pepin et al., 2010).

RVFV is primarily transmitted through mosquito bite; however there is evidence of infection from raw milk, contaminated bodily fluids and animal blood, thus abattoir workers are at higher risk of infection (Nyakarahuka et al., 2018, Labeaud et al., 2011). There has been no reported cases of horizontal transmission between humans, however, horizontal transmission has been shown

to occur spontaneously though rarely results in disease (Busquets et al., 2010). A case study in 2008 indicated that RVFV can be vertically transmitted (Adam and Karsany, 2008). RVFV infection in humans has an incubation period of between 2-6 days and most commonly manifests as a febrile illness with diarrhoea and malaise recovering within two days to one week after symptoms occur, however in approximately 1% of cases (largely dependent on strain and outbreak) infection can result in severe symptoms such as hepatitis, retinitis and haemorrhagic fever (Ikegami and Makino, 2011, Laughlin et al., 1979). Through the use of a mouse model, it was shown that pathogenesis begins early in the liver through the apoptosis of hepatocytes. Mice that survive hepatitis later develop meningoencephalitis. The virus exhibits a wide tissue and cell type tropism.

RVFV infection in ruminants has a more severe clinical outcome. RVFV primarily infects ruminants, including cattle, sheep, goats and camels. The virus has a varying seroprevalence of between 2-16% across endemic areas (Cêtre-Sossah et al., 2012, Nyakarahuka et al., 2018, Georges et al., 2018). RVFV has a 30% mortality rate in adult ruminants (Bird et al., 2009) and between 90-100% mortality in newborn lambs. The virus also causes a high abortion rate in pregnant ruminants (Coetzer, 1982). Thus, the impact of RVFV on rural communities can be devastating causing significant socio-economic problems (Chengula et al., 2013, Sindato et al., 2011). While there is evidence of low-level circulation of RVFV within wildlife, shown through virus detection and clinical signs of infection (Capobianco Dondona et al., 2016), there is no experimental evidence for a mammalian reservoir host (Rostal et al., 2017).

Research on RVFV has focused on a number of key strains. Pathogenic strains ZH501 and ZH548 were isolated from human cases during the Egyptian outbreak of RVF in 1977; the largest human outbreak of RVFV that resulted in acute febrile, ocular, encephalitic and fatal haemorrhagic disease (Gear, 1979). ZH501 was isolated from a fatal case of haemorrhagic fever, whereas ZH548 was isolated from a febrile self-limiting case. As RVFV is a significant human pathogen with no fully licensed vaccines or antiviral treatments, the virus requires handling in a high containment biosafety level 3 (CL-3) laboratory. Additionally, pathogenic RVFV has been recognised as a potential bioterrorism

agent and thus falls under additional legislation (Mandell and Flick, 2010). The strain used throughout this study was MP12, a vaccine strain derived from the serial plaque passage of ZH548 strain 12 times in the presence of the mutagen 5-fluorouracil (Caplen et al., 1985). The resulting MP12 strain encodes 25 mutations (11 aa substitutions) across the genome. Of these mutations, the attenuation of MP12 is by 7 amino acid changes in the M segment and 3 amino acid changes in the L segment (Lokugamage et al., 2012), the S segment encodes for N with only synonymous mutations and a moderately functional NSs protein with 1 non-synonymous mutation (Billecocq et al., 2008, Ikegami et al., 2015). The MP12 vaccine is conditionally licensed in the United States for veterinary use (Ikegami, 2017). Vaccination of livestock is the most effective way to reduce the economic impact of RVFV infection and while there are a number of vaccines, including the live attenuated MP12 and Smithburn vaccines, many of them come with inherent risks and the lack of ability to differentiate between infected and vaccinated animals (Smithburn, 1949, Botros et al., 2006). There are currently no policies in place supporting routine vaccination of livestock in any endemic countries for RVFV and thus the vaccine is used reactively to outbreaks, reducing the vaccines overall effectiveness (Bird and Nichol, 2012). The efficacy of individual vaccines varies greatly between human, adult ruminant and newborn ruminant application, as well as between different experimental models used such as mice and non-human primates. The formalin-inactivated RVFV vaccine had an efficacy of 67% in adult sheep however challenge induced abortion in 2 of 2 pregnant ewes (Harrington et al., 1980). The MP12 vaccine in comparison resulted in no abnormal effects when given to 3 pregnant ewes in one study (Morrill et al., 1987) however a separate study found that four month old calves vaccinated with MP12 resulted in necrotic lesions in the liver (Wilson et al., 2014). Further evaluation of efficacy and safety of these vaccines may allow for increased confidence for policymakers to implement scheduled vaccination programs in endemic areas reducing the overall economic burden of the disease.

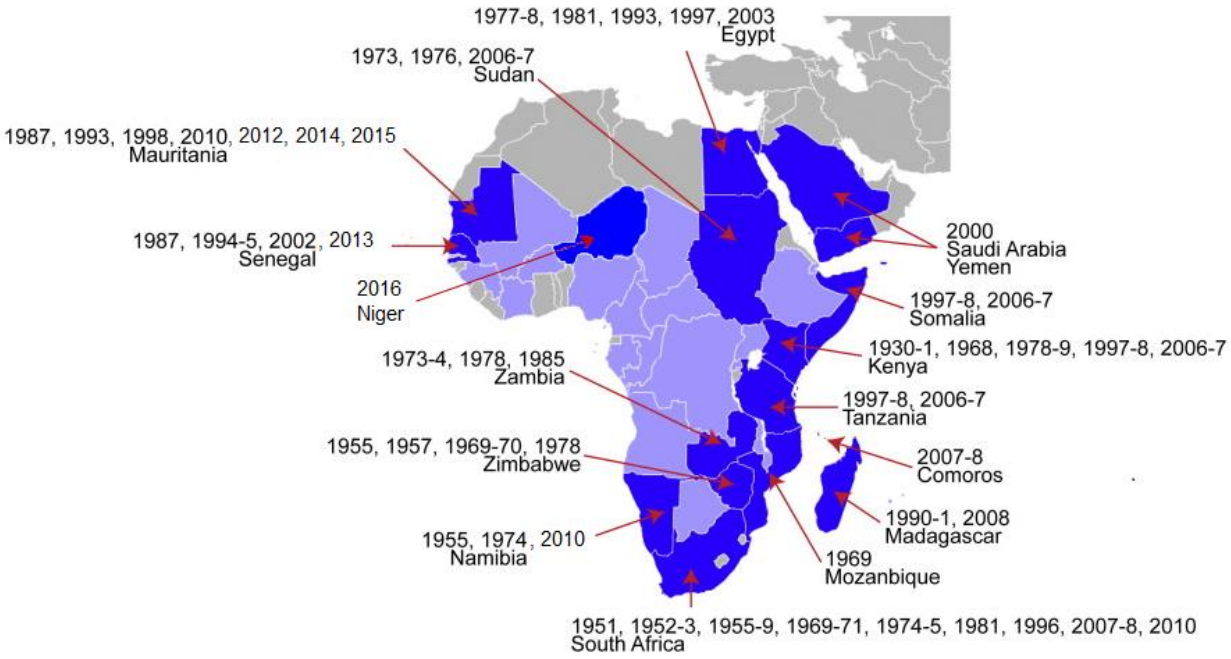

Figure 1-9. Distribution of RVFV as of 2018.

The dark blue areas indicate significant outbreaks, the lighter blue areas indicate serological evidence or virus isolation. Years of outbreaks are shown and updated from the CDC. Adapted from (Ikegami, 2012).

1.2.3 RVFV reverse genetics

The first reverse genetics system for bunyaviruses was developed in 1996 (Bridgen and Elliott, 1996) based upon a system described for rabies virus (Schnell et al., 1994). The bunyavirus rescue system involves the expression of "helper" plasmids encoding the viral structural proteins N and L, which assist in the formation of viral RNPs, in addition cDNA copies of each of the three viral segments in the antigenomic sense have a bacteriophage T7 RNA polymerase promoter before the 5'UTR of the viral antigenomic RNA; and simplified later (Lowen et al., 2004). After the 3' UTR sits a hepatitis δ virus ribozyme (Hδr) and the T7 terminator. The Hδr functions to allow the self-cleavage of the antigenomic RNA transcript generating the correct viral transcript size and sequence. The three plasmids, containing cDNA copies of either the S, M or L antigenomic RNA segments are transfected into cells expressing the T7 RNA polymerase such as BSR-T7/5 or Huh-T7-Lunets (Buchholz et al., 1999, Kaul et al., 2007). Upon transfection, the antigenomes are transcribed by the T7 RNA polymerase generating positive-sense or antigenomic RNA transcripts. These RNA transcripts can then be translated to produce the virally encoded proteins. The viral proteins (specifically N & L) form RNP complexes which can initiate the replication of the antigenomic RNA into genomic RNA, which can be further packaged into virions and released from the cell. The additional helper plasmids encoding N and L cDNA under the T7 promoter allow more efficient formation of RNPs thereby increasing the success of viral rescue.

The 5'-triphosphorylated transcripts produced by the T7 polymerase induce high levels of IFN through RIG-I (Hornung et al., 2006) and thus, may interfere with the successful rescue of RVFV, in particular attenuated viruses lacking IFN-antagonism. However, analysis of a Pol-I/II based rescue system showed a similar efficiency regardless of interferon antagonism (Habjan et al., 2008). Further research showed BSR-T7/5 cells have a compromised RIG-I pathway and thus is not stimulated by T7-derived RNA transcripts (Habjan et al., 2008).

The T7-based system is versatile, allowing reverse genetics and phenotypic experiments that been used in a number of RVFV studies. Reverse genetic systems of RVFV have been used to generate a two-segmented RVFV virus (Brennan et al., 2011b) and the rescue of RVFV containing a V5 tagged L protein

(Brennan et al., 2011a). It was also used in mutagenesis studies investigating the RVFV glycoprotein Gn (Phoenix et al., 2016a). The T7 system is also widely used across the bunyaviruses, such as investigating cellular roles for BUNV NSs (Weber et al., 2002) and demonstrating the flexibility of the BUNV genome through rescue of an ambisense S segment virus (Van Knippenberg and Elliott, 2015).

In order to breakdown the study of bunyaviruses into their component processes, minigenome systems have also been developed. The minigenome system allows studies of such viruses including BSL-3 and BSL-4 pathogens to be carried out at lower safety levels. The system is similar to the reverse genetics system previously described. Briefly, cDNA expression plasmid encoding RVFV N and L proteins are transfected into T7 RNA polymerase-expressing cells along with a reporter plasmid that expresses a reporter gene in the negative sense (replacing the virally encoded ORF), flanked by viral genomic UTRs. The expression of N and L form functional RNP complexes recognising the UTRs flanking the reporter gene, thus by binding the viral UTRs the RNPs are transcribed and replicated, resulting in the production of the reporter protein (usually luciferase or GFP). This system allows an assessment of the functionality of the N and L proteins as well as their ability to recognise the cognate UTR of the virus in question. There have been many studies that have utilised this system such as studying the effects of protein phosphatase-1 on RVFV replication (Baer et al., 2016), the assessment of MP12 N and L proteins to replicate different virus species (GOLV & AMTV) M segment minigenomes (Ly et al., 2017) and to evaluate the importance of the non-coding regions of the viral segments and their involvement in regulating RNA synthesis (Gauliard et al., 2006).

The minigenome system can be adapted further through the addition of a plasmid expressing the gene M segment viral glycoprotein polyprotein precursor. This allows viral assembly, maturation, packaging and egress to occur, generating virus-like particles (VLPs). These VLPs are capable of delivering packaged RNPs into recipient cells for a single-cycle of replication, as there is no genomic template for further transcription of the viral glycoproteins within the recipient. Pre-transfection of recipient cells with N and L can allow measurement of luciferase reporter genes transferred from the donor cells via VLPs. The morphology of the VLPs in UUKV are identical to authentic virions

(Overby et al., 2008). VLP systems have been used for assessing inhibitors of RVFV replication (Piper and Gerrard, 2010), for identifying the packaging signals within the coding and non-coding regions of RVFV genomic segments (Murakami et al., 2012).

Utilising these molecular tools it was possible to explore the molecular interactions governing RVFV nucleocapsid during viral replication and thus informing on unknown functions. Understanding these interactions will allow future study focused on novel intervention strategies for this emerging viral threat.

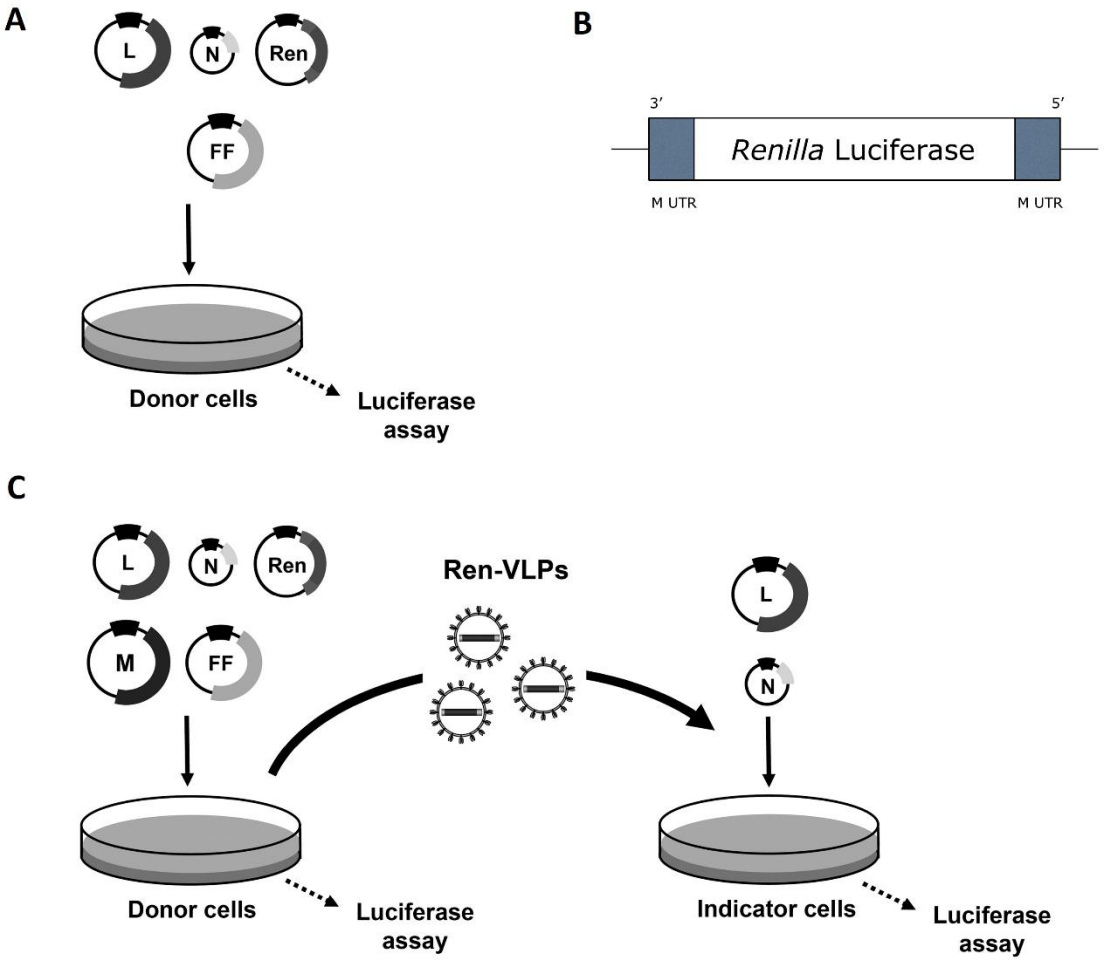

Figure 1-10. Schematic of RVFV reporter systems.

A schematic of minigenome and VLP reporter systems for RVFV. (A) Minigenome assay system with the transfection of four plasmids and subsequent reading of *Renilla* luciferase (*Rluc*) and *Firefly* luciferase (*Fluc*). (B) A schematic of the reporter Ren plasmid use in minigenome and VLP assays, contains the *Rluc* ORF flanked by RVFV M segment UTRs in the genome-sense orientation. (C) Virus-like particle (VLP) assay similar to the minigenome assay however with the addition of M plasmid expressing viral glycoproteins Gn and Gc. Thus, VLPs can form and be used to transduce indicator cells pre-transfected with RVFV N and L plasmids before measurement of *Rluc*. Adapted from (Habjan et al., 2009).

Chapter 2 Aims

Previous research on RVFV has primarily focused on the non-structural protein NSs with regards to the interaction of viral proteins with host cell proteins. Information on the function of RVFV N proteins, not including the formation of RNPs, is largely unknown.

The aim of this project was to gain insights into the N protein of RVFV in order to understand the basic processes undertaken during the virus life cycle.

These aims included:

(i) To perform a mutagenesis study on RVFV N to assess any potential functional residues.

(ii) Perform a proteomics study of RVFV N protein to identify host protein interactors and validate interactions through experimentation.

(iii) Assess importance of interactors through siRNA experiments using minigenome and reporter virus systems.

(iv) Further investigate the WNT pathways effect on RVFV replication.

(v) Assess RVFVs impact on the WNT pathway, and vice versa.

(vi) Determine RVFV N protein effect on mosquito antiviral RNA interference pathways.

Chapter 3 Materials

3.1 Cell Culture

3.1.1 Eukaryotic Cell Lines

- A549: derived from adenocarcinomic human alveolar basal epithelial cells (86012804, Public Health England). The cells were maintained in DMEM supplemented with 10% (v/v) Heat-inactivated fetal bovine serum (FBS) (Gibco). A549 ß-catenin knockout cells are a CRISPR knockout single cell clone generated using a CRISPRcas9 lentivirus construct (A gift from Isabelle Dietrich, Oxford University, UK) in the course of this project. A549 ß-catenin knockout control cells are a CRISPRcas9 lentivirus cell line with non-functional guide RNA. Knockout and control cells are supplemented with puromycin (100 µg/ml) for selection.

- Aag2: derived from *Ae. aegypti* (Received from P. Eggleston, Keele University, UK) and were grown in L-15+Glutamax (Life Technologies) supplemented with 10% Tryptose Phosphate Broth (Life Technologies), 10% Heat-inactivated FBS (Gibco) and 100 units/mL of penicillin and 100 µg/mL of streptomycin. AF5 cells are a single cell clone derived from the Aag2 cells (Varjak et al., 2017b) with a confirmed functional RNAi pathway. The cell line AF319, is a derivative of AF5 cells however they have the key RNAi effector protein Dicer 2 (Dcr2) knocked out which blocks the cleavage of dsRNA into siRNAs(Varjak et al., 2017b).

- BHK-21: a baby hamster kidney derived cell line (Macpherson and Stoker, 1962). Maintained in Glasgow modified Eagle's medium (GMEM) (Gibco) with 10% (v/v) Heat-inactivated FBS, 10% (v/v) Tryptose Phosphate Broth and 100 units/mL of penicillin and 100 µg/mL of streptomycin.

- BSR-T7/5: A BHK-21 derived clone constitutively expressing bacteriophage T7 RNA polymerase (Buchholz et al., 1999). Provided by Dr Karl-Klaus Conzelmann (Ludwig-Maximilians-Universität München). Cells were maintained in Glasgow modified Eagle's medium (GMEM) (Gibco) with 10% (v/v) Heat-inactivated FBS, 10% (v/v) Tryptose Phosphate Broth and 100

units/mL of penicillin and 100 µg/mL of streptomycin supplemented with 1mg/ml G418 (Promega) to maintain selection pressure for cells expressing T7 RNA polymerase.

- BSR-T7/5 (clone 21): A derivative single cell clone of BSR-T7/5 showing increased expression of T7 RNA polymerase (Mottram et al., 2017).

- HEK-293FT: Human embryonic kidney derived cell line. Maintained in DMEM with 10% (v/v) Heat-inactivated FBS, supplemented with 0.1 mM non-essential amino acids and 100 units/mL of penicillin and 100 µg/mL of streptomycin.

- Huh7-Lunet-T7: Derivative of Huh-7 cells, generated from liver carcinoma cells (Nakabayashi et al., 1982), constitutively expressing the bacteriophage T7 RNA polymerase (Kaul et al., 2007). Provided by Dr Ralf Bartenschlager (Universitätsklinikum Heidelberg). Maintained in DMEM with 10% (v/v) FBS and 0.1 mM non-essential amino acids supplemented with Zeocin (100 µg/ml) (Thermo Fisher Scientific) to maintain selection.

- Vero E6: African green monkey kidney cells provided by Prof Richard M. Elliott. Maintained in DMEM, supplemented with 10% (v/v) FBS.

3.1.2 Competent Bacteria

Plasmid amplified for stocks and through general cloning techniques were generated through the use of DH5α competent cells genotype; F^- Φ80*lac*ZΔM15 Δ(*lac*ZYA-*arg*F) U169 *rec*A1 *end*A1 *hsd*R17 (rk^-, mk^+) *pho*A *sup*E44 λ^- *thi*$^-$ 1 *gyr*A96 *rel*A1 (Thermo Fisher Scientific). Plasmids generated through In-Fusion cloning kit (Clontech) were amplified in supplied Stellar Competent cells genotype; F–, endA1, supE44, thi-1, recA1, relA1, gyrA96, phoA, Φ80d lacZΔ M15, Δ (lacZYA - argF) U169, Δ (mrr - hsdRMS - mcrBC), ΔmcrA, λ–. Bacteria were grown at 37˚C on either Luria-Bertani (LB) broth or LB agar plates under the selection of either ampicillin (100 µg/ml) or kanamycin (100 µg/ml).

3.1.3 Virus Strains

Recombinant RVFV strain MP12 (Caplen et al., 1985) used in this project was derived from plasmids supplied by Prof Richard M. Elliott. Working stocks of RVFV rMP12 and RVFV rMP12delNSs:eGFP were generated by passaging the virus in BHK-21 cells (4.1.8). RVFV rMP12delNSs:*hren* was also previously described and provided by Prof Richard M. Elliott.

pCMV-SFV6-*RLuc*-2SG plasmid was generated in Prof Andres Merits laboratory (University of Tartu, Estonia), it was used to rescue SFV6(3H)-RLuc-2SG virus (Tamberg et al., 2007, Saul et al., 2015) (Rodriguez-Andres et al., 2012). This plasmid served as a backbone to generate new viruses during this project and virus was rescued using a previously described protocol in BHK-21 cells (4.1.8).

BUNV, rBUNVdelNSs2 and BUNVNanoLuc (provided by Prof Richard M. Elliott) were used in this study to assess the impact of ß-catenin on bunyavirus replication. Working stocks were generated by passaging the virus in BHK-21 cells (4.1.8).

3.2 Molecular Biology

3.2.1 Oligonucleotides

A list of oligonucleotides used throughout this project is provided in the supplementary material (9.1).

3.2.2 Plasmids

Plasmid	Description	Reference
pTM1 RVFV L3V5	pTM1 plasmid backbone containing a T7 promoter to drive transcription followed by an Internal Ribosome Entry Site (IRES) driving translation. Plasmid encodes the modified RVFV MP12 RNA-dependent-RNA polymerase (L) sequence containing an inserted V5 sequence towards the 3' terminus.	Provided by Benjamin Brennan (Brennan et al., 2011a).
pTM1 RVFV MP12 N **pTM1 RVFV MP12 L**	pTM1 plasmid encoding RVFV MP12 nucleocapsid (N) protein or L protein.	Provided by Richard Elliott.
pTVT7 M-Hren-M	pTV plasmid expression of negative sense Humanized *Renilla* (*hRen*) under T7 promoter flanked by RVFV M segment UTRs	Provided by Benjamin Brennan.
pTM1 FF Luc	pTM1 plasmid encoding Firefly luciferase.	Provided by Isabelle Dietrich.
pTM1 UUKV N **pTM1 UUKV L**	pTM1 plasmid encoding UUKV N protein or L protein.	Provided by Richard Elliott / Veronica Rezelj.
pTM1 UUKV N RVFV motif	pTM1 plasmid encoding UUKV N protein with a tick-borne phenuviridae specific motif replaced with the motif found in RVFV.	Generated during this project.
pTM1 RVFV MP12 N Mutant Gly32Ala **pTM1 RVFV MP12 N Mutant Asp34Ala** **pTM1 RVFV MP12 N Mutant Trp125Ala** **pTM1 RVFV MP12 N Mutant Ser148Ala** **pTM1 RVFV MP12 N Mutant Phe149Ala** **pTM1 RVFV MP12 N Mutant Asp181Ala** **pTM1 RVFV MP12 N Mutant Pro182Ala** **pTM1 RVFV MP12 N Mutant Arg185Ala** **pTM1 RVFV MP12 N Mutant Phe11Ala**	pTM1 plasmid encoding RVFV MP12 N protein with an alanine or glycine substitution point mutation.	Generated during this project (5.2.1).

pTM1 RVFV MP12 N Mutant Phe11Gly		
pTM1 HB29 N	pTM1 plasmid encoding SFTSV N protein or L protein (Strain Hubei 29; HB29).	Provided by Benjamin Brennan
pTM1 TOSV N	pTM1 plasmid encoding TOSV N protein or L protein.	Provided by Benjamin Brennan
pCMV RVFV N	pTM1 plasmid encoding RVFV N under CMV promoter	Generated during this project.
pTVT7 RVFV MP12 S Segment **pTVT7 RVFV MP12 M Segment** **pTVT7 RVFV MP12 L Segment**	Full length RVFV MP12 antigenomic Small (S), Medium (M) and Large (L) segments cloned into the pTVT7 backbone driven by a bacteriophage T7 promoter and flanked at the 3' by a hepatitis Δ ribozyme facilitating self-clevage.	Provided by Benjamin Brennan
pTVT7 RVFV S Segment N Mutant 2-14 **pTVT7 RVFV S Segment N Mutant 2-31** **pTVT7 RVFV S Segment N Mutant F11A** **pTVT7 RVFV S Segment N Mutant Y30A** **pTVT7 RVFV S Segment N Mutant Asp34Ala** **pTVT7 RVFV S Segment N Mutant Phe149Ala** **pTVT7 RVFV S Segment N Mutant Arg185Ala**	Full length RVFV MP12 antigenomic S segment in the pTVT7 backbone with specific point mutations to the N sequence.	Generated during this project.
p14 RVFV MP12	p14 backbone encoding His-6 tagged RVFV N protein	Provided by Ping Li.
p14 RVFV MP12 N Mutant 2-14AA **p14 RVFV MP12 N Mutant 2-30AA** **p14 RVFV MP12 N Mutant Phe11Ala** **p14 RVFV MP12 N Mutant Phe11Gly** **p14 RVFV MP12 N Mutant Y30A** **p14 RVFV MP12 N Mutant Gly32Ala** **p14 RVFV MP12 N Mutant Asp34Ala**	p14 backbone encoding His-6 tagged mutant RVFV N protein	Generated during this project (5.2.1).

p14 RVFV MP12 N Mutant Trp125Ala **p14 RVFV MP12 N Mutant Ser148Ala** **p14 RVFV MP12 N Mutant Phe149Ala** **p14 RVFV MP12 N Mutant Asp181Ala** **p14 RVFV MP12 N Mutant Arg185Ala**		
pCMV-SFV(Rluc-H)6-2SG	Full length viral SFV6 genome containing *Rluc* ORF and two subgenomic promoters used as a backbone for cloning.	Constructed by Prof Andres Merits (University of Tartu, Estonia).
pCMV-SFV(Rluc-H)6-p19	Full length viral SFV6 genome containing *Rluc* ORF and Tombusvirus p19 ORF under the subgenomic promoter.	Generated during this project (7.2).
pCMV-SFV(Rluc-H)6-BUNVN	Full length viral SFV6 genome containing *Rluc* ORF and the BUNV N ORF under the subgenomic promoter.	Generated during this project (7.2).
pCMV-SFV(Rluc-H)6-RVFVN	Full length viral SFV6 genome containing *Rluc* ORF and the RVFV N ORF under the subgenomic promoter.	Generated during this project (7.2).
pCMV-SFV(Rluc-H)6-ZIKVC	Full length viral SFV6 genome containing *Rluc* ORF and ZIKV C ORF under the subgenomic promoter.	Generated during this project (7.2).
pCMV-SFV(Rluc-H)6-eGFP	Full length viral SFV6 genome containing *Rluc* ORF and the eGFP ORF under the subgenomic promoter.	Generated during this project (7.2).
pCCI-SP6-Zika	pCCI-SP6 plasmid containing full length Zika genome used as a template to generate Zika C DNA during cloning.	Constructed by Prof Andres Merits (University of Tartu, Estonia)(Mutso et al., 2017).
SFV4(3H)-*Rluc*-p19	SFV4 full length viral DNA containing the *Rluc* ORF and Tombusvirus p19 ORF under specific sub-genomic promoters, used as a template during cloning.	Previously generated in the Kohl lab (Attarzadeh-Yazdi et al., 2009).
LentiCRISPR v2	CRISPRcas9 lentiviral vector	Provided as a gift from Feng Zhang (Addgene plasmid # 52961).
Human Beta-catenin GFP	Expression of mammalian ß-catenin GFP under a CMV promoter	Human Beta-catenin GFP was a gift from Alpha Yap (Addgene plasmid # 71367).

M50 Super 8x TOPFlash	Beta-catenin reporter containing TCF/LEF promoter sites upstream of a firefly luciferase reporter.	M50 Super 8x TOPFlash was a gift from Randall Moon (Addgene plasmid # 12456).

3.2.3 Enzymes

3.2.3.1 Modifying enzymes

Benzonase was used for digestion of transfected template plasmid in VLP assays was purchased from Merck Millipore. For PCR, GoTaq G2 Flexi DNA polymerase (Promega) or KOD Hot start DNA polymerase (Merck Millipore) were used.

3.2.3.2 Restriction enzymes

Restriction enzymes used for checking successful insertion of gene products during cloning were purchased from New England Biolabs.

3.2.4 Antibodies

Primary		Dilution		
Antibody	**Primary Target**	**WB**	**IP**	**IF**
Rabbit anti-RVFV MP12 N (Provided by Richard M. Elliott).	RVFV MP12 N	1:5000	1:500	1:250
Rabbit anti-BUNV N (Provided by Richard M. Elliott).	BUNV N			1:250
Rabbit anti-ß-Actin (Abcam, #ab8227).	ß-Actin	1:2000		
Rabbit anti-ß-Catenin (R&D Systems).	ß-Catenin	1:1000		
Mouse anti-ß-Catenin (Cell Signalling #2677).	ß-Catenin	1:1000		1:250
Mouse anti-Annexin-A1 (R&D Systems #MAB3770).	Annexin-A1			1:100
Mouse anti-Annexin-A2 (R&D Systems #MAB3928).	Annexin-A2			1:100

Secondary		Dilution		
Antibody	**Target**	**WB**	**IP**	**IF**
Anti-rabbit Alexa Fluor 405 (Invitrogen #A-35551).	Rabbit IgG			1:500
Anti-rabbit Alexa Fluor 488 (Invitrogen #35552).	Rabbit IgG			1:500
Anti-mouse Alexa Fluor 568 (Invitrogen #A-11019).	Mouse IgG			1:500
Anti-rabbit IgG HRP-linked (Abcam #ab205718).	Rabbit IgG	1:2000		
Anti-mouse IgG HRP-linked (Thermo Fisher Scientific #31430).	Mouse IgG	1:2000		
Anti-rabbit Veriblot (Abcam #ab131366).	IgG	1:2000		
Anti-rabbit IgG (H and L) DyLight 680 (Thermo Fisher Scientific #35568).	Rabbit IgG	1:10000		
Anti-mouse IgG (H and L) DyLight 800 4x PEG (Thermo Fisher Scientific #SA5-35521).	Mouse IgG	1:5000		

3.3 Reagents

3.3.1 Cell Culture

- Glasgow Minimal Essential Medium (GMEM), Dulbecco Modified Eagle Medium (DMEM), 2x Temin's Modified Eagle Medium (MEM) and Tryptose Phosphate Broth (TPB) were purchased from Gibco.

- Versene (E&O Laboratories).

- Trypsin solution: Versene (E&O Laboratories) supplemented with 10x trypsin.

- Heat-inactivated fetal bovine serum (FBS) (Gibco)

- Dulbecco's phosphate buffered saline (DPBS) 10x purchased from Sigma.

- 0.6% Avicel overlay: Avicel 1.2% (w/v) in H_2O diluted 1:1 with 2x MEM supplemented with 4% FBS.

- Formaldehyde fixing solution: 8% (v/v) formaldeyde (Sigma) in PBS.

- TransIT-LT1 transfection reagent purchased from MirusBio.

- Lipofectamine 2000 and Lipofectamine RNAMax purchased from Thermo Fisher Scientific.

- Dharmacon purchased from GE Healthcare.

- Opti-Minimum Essential Medium (Opti-MEM) purchased from Thermo Fisher Scientific.

- Antibiotic G418 sulfate (G418) purchased from Promega and used at 100 mg/ml.

- Zeocin purchased from Invivogen and used at 100 mg/ml.

3.3.2 Bacterial Culture

- Ampicillin sodium salt (Amp) purchased from Fisher.

- Kanamycin sulfate (Kan) purchased from Sigma.

- LB agar (Miller) purchased from E&O Laboratories.

- LB broth purchased from E&O Laboratories.

3.3.3 DNA/RNA Analysis

- Plasmid isolation from bacterial culture was carried out using either a Maxiprep kit (Thermo Fisher Scientific) or Miniprep kit (Bioline).

- Cloning was performed using In-Fusing cloning tools purchased from Clontech.

- Agarose gel used in DNA gels: 1% (w/v) UltraPure agarose (Invitrogen) in TAE buffer (Thermo Fisher Scientific).

- Agarose gel used in RNA gels: 1% (w/v) NuSieve GTG agarose (Lonza) in TBE buffer (Novex).

- TAE buffer was purchased from Thermo Fisher Scientific.

- TBE buffer was purchased from Thermo Fisher Scientific.

- GeneRuler 1kb Plus ladder and 6x DNA Loading Dye used in DNA gels purchased from Thermo Fisher Scientific.

- 100bp ladder used in RNA gels purchased from Thermo Fisher Scientific.

- Purification and extraction of DNA from agarose gels was performed using a gel extraction kit purchased from GE Healthcare.

- Ethidium bromide used in DNA visualisation was purchased from Promega.

- Gel Red used in RNA visualisation was purchased from Biotium.

- Human Wnt3a recombinant protein was purchased from R&D Systems.

3.3.4 Western Blotting

- SeeBlue Plus2 protein ladder was purchased from Thermo Fisher Scientific.

- Bolt LDS 4x, Bolt Sample reducing agent 10x, Bolt 4-12% Bis Tris and Bolt MES buffer were purchased from Thermo Fisher Scientific.

- Amersham Protran 0.45 nitrocellulose membrane was purchased from GE Healthcare.

- Semi-dry blotting buffer: 48 mM Tris, 39 mM glycine, 20% (v/v) methanol

- Blocking buffer: 2% (w/v) skimmed milk powder (Marvel) in PBS/0.1% (v/v) Tween-20.

- Wash buffer: PBS/0.1% (v/v) Tween-20.

- Pierce ECL western blotting substrate was purchased from Thermo Fisher Scientific.

3.3.5 Immunofluoresence

- Permeabilisation solution: 0.5% (v/v) Triton X-100 in PBS.

- Prolong Diamond Antifade Mountant (Thermo Fisher Scientific).

- KPL TrueBlue Peroxidase substrate for focus forming assay was purchased from Seracare.

- DRAQ7™ DNA dye (Abcam).

- Microscope (LSM 710, Zeiss).

3.3.6 Immunoprecipitation

- Lysis/Wash buffer – 20 mM Tris pH 7.5, 150 mM NaCl, 5 mM $MgCl_2$, 0.5% Triton X-100, Halt™ Protease inhibitor cocktail (Thermo Fisher Scientific).

- Lysis buffer Proteomics – 50 mM Tris pH 7.5, 200 mM NaCl, 1 mM EDTA, 10% glycerol, 1ul/ml Benzonase (Merck Millipore), protease inhibitor cocktail (Thermo Fisher Scientific) 1% Np-40.

- Wash buffer Proteomics – 50 mM Tris pH 7.5, 200 mM NaCl, 1 mM EDTA, 1% Np-40 (Sigma).

- Pierce™ Protein A magnetic beads were purchased from Thermo Fisher Scientific.

3.3.7 Protein Purification

- Wash buffer: 40 mM Imidazole, 0.3M NaCl, 50 mM Tris pH 8.0, 10% glycerol.

- Elution buffer: 200 mM Imidazole, 0.3 NaCl, 10 mM Tris pH 8.0, 10% glycerol.

- Protein storage buffer: 10mM Tris pH 8.0, 150mM NaCl, 10% glycerol.

- Vivaspin 6 centrifugal concentrators were purchased from Sigma.

- HisPur Ni-NTA resin was purchased from Thermo Fisher Scientific

3.3.8 Luciferase Assay

- Dual Luciferase kit (Promega).

- Steady Glo Luciferase kit (Promega).

- Firefly Luciferase kit (Promega).

3.4 Software

- CLC Genomics or Geneious software packages were used for sequence analysis and primer design.

- ZEN software (Zeiss) was used for analysis of immunofluorescence images.

- Irfanview (Irfan Skiljan, 2017) and ImageStudio (LI-COR, 2017) were used for image processing.

- Graphpad Prism version 6 (GraphPad Software, 2017) was used for graphic design and statistical analysis.

- Inkscape was used for figure production.

- Molecular graphics and analyses were performed with the UCSF Chimera package. Chimera is developed by the Resource for Biocomputing, Visualization, and Informatics at the University of California, San Francisco (supported by NIGMS P41-GM103311).

Chapter 4 Methods

4.1 Cell Culture

4.1.1 Maintenance of eukaryotic cell lines

Mammalian cells were maintained in either T25, T75, T150 or T225 vented flasks at 37 °C with 5% CO_2 and were split either 1:5 or 1:10 after confluency. To maintain, cells were washed with 5 ml PBS versene before adding trypsin and incubating for 5 minutes at 37 °C. Subsequently, cells were transferred into a falcon tube and centrifuged at 1000 x g for 5 minutes. Following centrifugation, cells were resuspended in fresh cell culture media. Mosquito cells were maintained in T25 non-vented flasks at 28 °C with no CO_2; once confluent, the cells were scraped and were split 1:5.

4.1.2 Transfection of eukaryotic cell lines

At approximately 24 hours post seeding (or 70-80% confluency) cells were transfected using either Lipofectamine 2000 (Thermo Fisher Scientific), LT1 (Mirus Bio), RNAiMax (Thermo Fisher Scientific) or Dharmafect (GE Healthcare). Volumes of Opti-MEM and transfection reagent varies dependent on plate size, reagent used and was occasionally varied further based on quantity of transfected DNA (According to manufacturer's instructions).

Lipofectamine 2000 & LT1			
Cell culture plate	Media volume per well/flask (ml)	Transfection reagent volume per well/flask (µl)	Total Opti-MEM volume per well/flask (µl)
T25	4	5	500
6-well plate	2	4	400
12-well plate	1	2	200
24-well plate	1	1	100

Dharmafect & RNAimax			
Cell culture plate	Media volume per well (ml)	Transfection reagent volume per well (µl)	Total Opti-MEM volume per well (µl)
24-well plate	1	2	100

Half of the total Opti-MEM volume was supplemented with the total volume of transfection reagent and mixed gently; the second half was mixed separately with the required DNA, siRNA and/or dsRNA in a microcentrifuge tube. The Opti-

MEM transfection reagent mix was combined with the DNA or siRNA and incubated for 20 minutes at room temperature before being applied directly onto the well containing fresh cell culture media.

4.1.3 Minigenome assays

BSR-T7/5, BSR-T7/5 CL21 or Huh7-T7-Lunet cells were seeded in a 24-well plate at approximately 1 $x10^5$ cells per well. At 24 hours post seeding, cells were transfected with 25 ng pTM1-FF-Luc (a firefly luciferase expressing plasmid under the T7 promotor, used as an internal control to normalise variations in transfection efficiency and total cell count), 0.5 µg of the *Renilla* based reporter plasmid pTVT7-GM:hRen, 0.2 µg pTM1-L and 1 µg pTM1-N (RVFV MP12 based), empty pTM1 or one of the N protein mutant clones using either Lipofectamine 2000 or LT1 transfection reagent. The total amount of DNA added per well was kept constant by the addition of empty pTM1. At 24 hours post-transfection, cell culture supernatant was removed and cells were lysed with 100 µl passive lysis buffer (PLB; Promega). Firefly and *Renilla* luciferase activity was measure using the Dual Luciferase Reporter Assay system (Promega), as per the manufacturer's instructions.

4.1.4 Virus-like particle assay

BSR-T7/5 CL21 cells were seeded in a 12-well plate at approximately 2 $x10^5$ cells per well. At 24 hours post seeding, cells were transfected in a similar manner to the minigenome assay with RVFV MP12 based plasmids; 25 ng pTM1-FF-Luc, 0.5 µg pTVT7-GM:hRen, 0.25 µg pTM1-L and 0.5 µg pTM1-N, empty pTM1 or one of the N protein mutant clones. Additionally, DNA mixtures were supplemented with 0.5 µg pTM1-M encoding the Open Reading Frame (ORF) for the RVFV viral glycoproteins Gn and Gc. After 48 hours, the supernatant was removed and treated with 2 µl Benzonase nuclease (Merck Millipore) for 4 h at 37 °C to eliminate any plasmid DNA not encapsidated into viral particles. Of the treated supernatant, 160 µl was subsequently added to a 12-well plate of BSR-T7/5 CL21 cells pre-transfected 24 h prior with 0.5 µg pTM1-N and 0.5 µg pTM1-L. At 24 h post VLP infection, cells were lysed in 200 µl PLB. Firefly and *Renilla* luciferase activity was measured as above.

4.1.5 TOPFlash reporter assay

Huh7-Lunet-T7, A549 or HEK-293FT cells were seeded in a 24 well plate at approximately 6 x10^4 cells per well. After 24 hours, cells were transfected with 290 ng M50 Super 8x TOPFlash per well. At 24 hours post transfection, cells were infected with rMP12, rMP12delNSs, rBUNV or rBUNVdelNSs at MOI 1. Samples were taken at the timepoints indicated, cells were lysed with 100 µl 2x passive lysis buffer (Promega) and luciferase signal was measured.

4.1.6 CRISPR-Cas9 knockouts

A stock of ß-catenin knockout A549 cells were generated using the lentiCRISPRv2 system Guide RNAs (gRNA1 GAAACAGCTCGTTGTACCGC, gRNA2 AGAACGCATGATAGCGTGTC) were cloned through restriction digest with *BsmBI* into lentiCRISPRv2 plasmid by Isabelle Dietrich, University of Oxford. HEK 293T cells were transduced with lentiCRISPRv2-gRNA plasmids, p8.91 and pVSV-G. After 48 hours, supernatant was harvested, filtered and supernatant applied to A549 cells allowing transduction of the generated lentiviruses. Lentivirus integrated cells were selected for by the addition of 1 µg/ml Puromycin. In the course of this thesis, these mixed cell cultures were cloned and purified by serially diluting into 6 well plates. After 7 days, formed single cell clones were transferred by scraping to a 24 well plate containing appropriate media. After 7 days, cultures were scraped and transferred into T25 flasks. At 4 days post seeding, the absence of ß-catenin was confirmed by Western blot (4.3.2). A culture containing integrated lentivirus but maintained presence of ß-catenin was used as a control.

4.1.7 siRNA knockdowns

4.1.7.1 Virus infection

A549 were plated at a density of 6 x10^4 cells per ml in a 24 well plate. After 24 hours, triplicate wells were transfected with 5 pmol Silencer Select siRNA (Life Technologies) targeting CTNB1, ANXA1, ANXA2, PABP1, PABP4, SAFB or DCD using 1 µl RNAimax transfection reagent (GE Healthcare). At 72 hours post-transfection, A549 cells were infected with rMP12delNSs:h*Ren* at MOI 0.01. After

24 h post infection, cells were lysed in 100 µl 2x passive lysis buffer (Promega). Rluc activity was measured according to manufacturer's instructions (4.3.4.1).

4.1.7.2 Minigenome Assay

Huh7-Lunet-T7s were plated at $1x10^5$ cells per ml in a 24 well plate. siRNA was transfected as previously described in 4.1.7.1. At 72 hours post-transfection of the siRNA, cells were transfected with 0.5 µg pTM1 N, 0.25 µg pTM1 L, 25 ng pTM1-FF-Luc, and 0.5 µg pTVT7-GM:hRen. After 24 h, cells were lysed in 100 µl passive lysis buffer. Dual luciferase was measured according to manufacturer's instructions (4.3.4.1).

4.1.8 Generation of virus stocks

Stocks of wild-type and recombinant RVFV, BUNV and SFV were generated by passaging the virus at a low multiplicity of infection (MOI) (0.01 plaque forming units [PFU]/cell) in either BHK-21 or Vero E6 cells. Cell media was removed and replaced with virus inoculum in 2% (v/v) FBS in PBS. After 1 h incubation at 37 °C, fresh media containing 2% (v/v) FBS was added. The propagation of SFV viruses was performed in BHK cells at 37 °C as above and harvested at 6 days p.i. Generation of RVFV and BUNV virus stocks were performed in Vero E6 cells at 33 °C with the same method as above.. Harvested supernatant was then clarified by centrifugation at 4,000 x g for 10 min, aliquoted and stored at -80 °C for further use. All experimentation with RVFV was conducted under containment level 3 conditions.

4.1.9 Virus infections

Cells were seeded in 24 well, 96 well plates or T225 flasks and allowed to reach approximately 70% confluence. Virus dilutions were made in 2% (v/v) FBS/PBS. Cell culture media was removed and replaced with 100 µl, 200 µl or 10 ml virus inoculum for a 96 well, 24 well or T225 flask respectively. Virus inoculum was adsorbed onto cells at 37°C for 1 h. Following virus adsorption, the flasks or plates were topped up with appropriate cell culture medium. Application of infectious material onto cells was considered time point 0 h p.i.

4.1.10 Plaque forming assay and focus forming assay

Plaque assays were performed on monolayers of confluent BHK-21 cells in 12 or 6 well plates. The cell media was removed and 10-fold serial dilutions of virus inoculum (in 2% (v/v) FBS/PBS) was added to the monolayer. Following 1 h incubation at 37 °C, an overlay of MEM supplemented with 2% (v/v) FBS and 0.6% (v/v) Avicel was added. The plates were incubated at 37 °C for 5 days after which they were fixed with formaldehyde solution for 1 h. After fixation, the formaldehyde fixing solution was removed and 0.1% (v/v) Toluene blue staining agent was added. The plates were incubated for 30 minutes at room temperature after which the staining agent was removed, the plates were washed with distilled water and then left to dry.

For determining RVFV MP12delNSs:*hRen* titre, a focus forming assay was performed. Serial dilutions of virus inoculum in PBS/2% (v/v) FBS were applied to confluent BHK-21 cell monolayer. After 1 h incubation at 37°C, cell monolayer was overlaid with MEM overlay supplemented with 2% FBS and 0.6% Avicel. The assay was incubated for 5 days, after which was fixed with formaldehyde buffer for 1 h. After fixation, permeabilisation solution was applied to the monolayer and before further incubation of rabbit anti-RVFV N antibody (1:500 in standard blocking buffer) for 2 h. The monolayers were washed three times with washing buffer and incubated with anti-rabbit HRP-linked antibody (1:5000 in standard blocking buffer) for 1 h. Subsequently, cells were washed with PBS and foci detected by adding TrueBlue peroxidase substrate at room temperature for 30 min. The plates were rinsed with distilled water and foci counted.

Virus titres were calculated using the equation:

$$\frac{PFU\ or\ FFU}{ml} = \frac{Number\ of\ plaques\ or\ foci}{Dilution\ x\ Volume(mL)}$$

4.1.11 Immunofluroescence

A549 or Huh7-T7-Lunet cells were seeded in glass-bottomed 24-well plates or 24 well plates with 15 mm coverslips at a density of 1 x10^5 cells per well. Transfections (4.1.2) or infections (4.1.9) were carried out on the seeded cells as previously described. At the respective time points, cell culture supernatant

was removed and the cells were fixed with formaldehyde solution. Cells were subsequently permeabilised using permeabilisation solution (0.5% (v/v) Triton X-100 in PBS) for 30 minutes. Following permeabilisation, cells were probed with primary antibody at the relevant concentration in 2% (v/v) FBS PBS and incubated overnight at 4 °C with gentle agitation. The following day, cells were washed three times with PBS 0.1% (v/v) Tween-20 before the addition of fluorescently-labelled secondary antibody in 2% (v/v) FBS PBS at the recommended concentration. The secondary antibody was incubated for 1 h at room temperature. Cells were subsequently washed twice with PBS 0.1% (v/v) Tween-20 before the addition of 1:100 DRAQ7™ DNA dye (BioStatus) in PBS. Samples were shaken for 10 minutes before washing once with distilled water and further mounting using hard set Prolong Diamond Antifade Mountant (Invitrogen).

4.2 Molecular Cloning

4.2.1 DNA Amplification

Polymerase chain reaction (PCR) was performed using KOD Hot Start polymerase for high fidelity reactions and GoTaq Flexi 2 polymerase for low fidelity reactions according to the manufacturer's instructions. PCR mixes and cycling conditions are as follows;

KOD Hot Start Polymerase

PCR Components

Amount	**PCR Component**
25 µl	2x KOD Master Mix
1 µl	10 mM Forward Primer
1 µl	10 mM Reverse Primer
50 ng	Template DNA
Up to 50 µl total	H_2O

Cycling Conditions

Initial Denaturation: 95°C 2 min

30 cycles:

Denaturation: 95°C 1 min

Annealing: Primer dependent 1 min

Extension: 72°C 1 min/kb

Final Extension: 72°C 5 min

Hold: 4˚C

GoTaq Flexi 2 polymerase

PCR Components

Amount	PCR Component
10 µl	5x GoTaq buffer
4 µl	25 mM $MgCl_2$
1 µl	10 mM dNTPs
1 µl	10 mM Forward Primer
1 µl	10 mM Reverse Primer
50 ng	Template DNA
0.25 µl	GoTaq Flexi 2 DNA polymerase
Up to 50 µl total	H_2O

Cycling Conditions

Initial Denaturation: 95˚C 2 min

30 cycles:

Denaturation: 95˚C 1 min

Annealing: Primer dependent 1 min

Extension: 72˚C 1 min/kb

Final Extension:72˚C 5 min

Hold: 4˚C

4.2.2 Site-directed mutagenesis

Site-directed mutagenesis was performed with complementary primers designed for inverse PCR, where the desired point mutations were flanked by complementary plasmid sequence. The PCR was performed using KOD Hotstart polymerase with PCR mixes and cycling conditions as stated:

PCR Components

Amount	**PCR Component**
25 µl	2x KOD Master Mix
1 µl	10 mM Forward Primer
1 µl	10 mM Reverse Primer
50 ng	Template DNA
Up to 50 µl total	H_2O

Cycling Conditions

Initial Denaturation: 95°C 2 min

30 cycles:

Denaturation: 95°C 20 seconds

Primer Annealing: 61°C 10 seconds

Extension: 70°C 2 min

Final Extension: 70°C 7 min

Hold: 4°C

Following PCR amplification, samples were treated with 2 units of DpnI enzyme for 2 hours at 37°C digesting methylated input template plasmid. Products were

purified via gel electrophoresis and gel extraction (detailed in 4.2.4) before In-fusion and bacterial transformation (detailed in 4.2.5).

4.2.3 In-Fusion cloning

Restriction free cloning was used as a primary method for gene insertion into specified vectors. The target vector was initially linearized using either restriction enzymes or through PCR. Primers were designed in a way to obtain 15 base pair long complementary sequences between the insert and the vector at both the 5' and 3' ends. PCR products were purified as below before use in an In-Fusion reaction using the In-Fusion HD Cloning Plus kit (Clontech). The reaction was set up using equal moles of insert and linearized vector, 2 µl 5x In-Fusion HD enzyme premix and a volume of ddH_2O up to 10 µl total. The reaction was incubated for 15 min at 50 °C and subsequently placed on ice. 5 µl of the reaction mixture was used to transform 50 µl Stellar Competent cells (Clontech) as described in 4.2.5.

4.2.4 Agarose gel electrophoresis

PCR products and digested DNA products were visualised on gels consisting of 1-2% (w/v) agarose, 0.04 µg/mL Ethidium bromide/Gel Red in either 1x TAE or 1x TBE buffer. Samples were mixed with 6x Gel loading dye and loaded on to the gel submerged in 1x TAE/TBE buffer. Additionally, Generuler 1kb+ DNA ladder was also loaded. Electrophoresis was performed at 100V to allow separation of desired fragments. If required, gel extraction was performed using the GE Healthcare gel extraction kit according to manufacturer's instructions.

4.2.5 Bacterial transformation

50 µl Stellar Competent cells, DH5α or Bl21 Rosetta cells were incubated with 1-5 µl plasmid on ice for 30 minutes before heat shock at 42 °C for 30 seconds. Cells were recovered on ice for 2 minutes before the addition of 500 µl S.O.C growth media. Transformed cells were subsequently placed at 37 °C and agitated at 180 revolutions per minute (RPM) for 1 hour. Cells were plated on LB agar plates containing antibiotic (100 µg/mL) and incubated at 37 °C overnight.

4.2.6 Plasmid isolation

Single colonies were selected from LB agar plates using a pipette tip and were placed in 5 mL or 150 mL LB Broth containing 100 µg/mL antibiotic and incubated overnight shaking 180 RPM at 37 °C. Plasmid was isolated from the small-scale culture using the Miniprep kit or from the large-scale culture using the Maxiprep kit (Qiagen) according to the manufacturer's instructions. To confirm successful cloning, plasmid was sent for Sanger sequencing (Source BioScience). Plasmid DNA concentration was quantified using a Nanodrop.

4.2.7 Cellular RNA extraction

Cell monolayers were harvested using 1x Trypsin in Versene before centrifugation at 2000 x G for 5 minutes. Cells were resuspended in 100 µl Versene before transfer into 1 mL Trizol LS reagent (Thermo Fisher Scientific). After which, 200 µl chloroform/mL Trizol was added and the sample vortexed for 15 seconds. The sample was centrifuged for 15 min at 12,000 x G at 4°C. The upper aqueous phase was transferred to a clean Eppendorf tube then 500 µl isopropanol and 0.5 µl RNAse free glycogen (10 mg/ml) was added. The sample was incubated at room temperature for 10 min before centrifugation for 10 min at 12,000 x G at 4°C. The supernatant was removed and the RNA pellet washed with 500 µl 70% (v/v) ethanol and centrifuged for 15 min at 14,000 x G twice. The ethanol wash was then removed and the RNA pellet air dried before being resuspensed in 20 µl nuclease free H_2O.

4.2.8 cDNA synthesis

Reverse transcription of cDNA from cellular RNA extraction was used for Real-time qPCR analysis. SuperScript® III First-Strand Synthesis System for RT-PCR kit was used to synthesise cDNA. Firstly, the following components were combined in a 0.2 ml tube:

Component	Amount
Total RNA	~1-5 µg
Random primers 50ng/µl	2 µl
10 mM dNTP mix	1 µl
ddH_2O	Up to 10 µl

The reaction was incubated at 65°C for 5 min then placed on ice for 1 min, after which the following components were added:

Component	Amount
5x RT buffer	4 µl
0.1 M DTT	1 µl
RNaseOUT™ (40 U/ µl)	1 µl
SuperScript® III RT (200 U/ µl)	1 µl

The sample was incubated for 5 min at 25°C, followed by 1 h at 50°C and then 15 min at 70°C to inactivate the enzyme. Synthesised cDNA was stored at -20°C.

4.3 Protein Analysis

4.3.1 Co-immunoprecipitation

4.3.1.1 Virus infection

For proteomic analysis, A549 cells were seeded in a T225 flask ($2.5x10^7$ cells) and infected with rMP12 at MOI 5 in 2% FBS/PBS for 1 h before topping up of culture media. At 16 h post infection media was removed, cells were washed with 5 ml PBS and 5 ml IP lysis buffer added. After 5 min, cells were resuspended and transferred to a 15 ml falcon tube. The cell lysate was kept on ice for 20 min before centrifugation at 16,000 x G for 20 min. Meanwhile, the magnetic bead antibody complex was prepared by first washing 100 µl of the Protein A or G magnetic beads per sample in 500 µl IP wash buffer and vortexing for 15 seconds. Washing was repeated twice before resuspension in 200 µl IP wash buffer containing Halt protease inhibitors and addition of anti-RVFV N or anti-β-catenin antibody (details given in 3.1.5). Magnetic bead-antibody complex was rotated for 1 h and incubated at 4°C. Subsequently, the antibody-bead complex was washed with 500 µl wash buffer and rotated for 5 min at 4°C, this process was repeated twice. The antibody-bead complex was resuspended in 100 µl IP wash buffer. The cell lysate and antibody-bead complex were combined and rotated for 2 h and incubated at 4°C. Following which, the sample was washed with 500 µl IP wash buffer and rotated for 5 min at 4°C, repeated three times. The sample was transferred to a fresh tube before the

immunoprecipitated protein was eluted from the beads through the addition of 100 µl loading buffer containing 1x Bolt LDS sample buffer and 1x Bolt Reducing agent (Thermo Scientific) and incubation at 90°C for 10 min. Samples were further analysed via mass-spectrometry (4.3.3) or Western blot (4.3.2).

4.3.1.2 Transfection

For N protein interaction analysis, BSR-T7/5 cells were seeded in 6 well plates ($1.2x10^6$ cells) and transfected with 500 ng pTM1 L3V5 (expressing a V5-epitope tagged RVFV polymerase protein) and 1 µg pTM1 N or pTM1 N mutant. At 24 h post transfection, media was removed and 1 ml IP lysis buffer added. For Co-IP of transfected cells, 30 µl Pierce Protein A magnetic beads were used bound with anti-V5 antibody and protocol continued as 4.3.1.1. The immunoprecipitated protein was eluted through the addition of 50 µl loading buffer and incubation at 90°C for 10 min. Samples were analysed by Western blot (4.3.2).

4.3.2 Western blotting analysis

Samples were loaded on to precast Bolt 4-12% Bis-Tris (Thermo Scientific) gels for polyacrylamide gel electrophoresis (PAGE) under denaturing conditions and ran using 1x MES SDS running buffer at 100 V for 80 min. Using a Trans-Blot SD semi-dry transfer cell (BioRad) proteins were transferred on to a nitrocellulose membrane of 0.45 µm pore size (GE Healthcare) by soaking in 1x semi-dry transfer buffer and subjected to a constant voltage of 15V for 45 min. Following transfer, the membrane was blocked for 1 h at room temperature using Western blot blocking buffer. After blocking, antibodies (as specified in 3.2.4) were diluted in blocking buffer and incubated with the membrane overnight at 4°C or 1 h at room temperature with mild rocking. The membrane was then washed three times with PBS-Tween washing buffer before the addition of secondary antibody diluted in blocking buffer for 45 min at room temperature. After incubation, the membrane was washed three times with PBS-Tween washing buffer and visualised using the Odyssey® CLx (LI-COR) or Pierce ECL Western blot substrate (Thermo Scientific) visualised on ChemiDoc MP Imaging system (BioRad).

4.3.3 Mass-spectrometry analysis

A549 cells were infected and co-immunoprecipitated as previously described (4.3.1.1). Mass-Spectrometry of eluted immunoprecipitation samples was carried out at the FingerPrints Proteomics facility (Dundee) with an Ultimate 3000 RSLCnano-system (Thermo Scientific) coupled to LTQ OrbiTrap Velos Pro (Thermo Scientific). In-Gel digestion was performed on samples to digest proteins into peptides for analysis via mass-spectrometry. This process was carried out at the Dundee facility by their standard protocol. The OrbiTrap Velos Pro was operating in data dependent acquisition mode using FT-MS and FT-MS/MS. Detailed configuration provided below;

FTMS Full AGC Target:1000000

Ion Trap MSn AGC Target:5000.00

Fill Time FTMS (ms): 500

Fill Time ITMS (ms): 100

Lock Mass: 445.120024

FT-MS:

Resolution: 60000

Mass Range (m/z):335-1800

Scan Type: Full

Polarity:Positive

Data Type:Profile

FT-MS/MS:

Resolution: 30000

Mass range: Normal

Data Type: Centroid

Activation Type: CID

Min. Signal Required: 5000

Isolation Width: 2.00

Normalized Coll. Energy: 35.0

Default Charge State: 2

Activation Q: 0.250

Activation Time: 10.00

Progenesis LC-MS software was used to compare sample spectra and protein identification was performed using Mascot. MaxQuant software version 1.5.2.8 was used downstream to obtain label free quantification intensity (LFQ) values used in label-free quantification. LFQ values are generated through MaxQuant by computing the sum of all identified protein intensities divided by the theoretical maximum number of peptides as calculated through *in-silico* digest. LFQ values undergo a process that reduces the need for "household" proteins that are unchanged during the experiment and maximises the information gained from signal ratios across samples through normalisation of intensity. The mass spectrometry proteomics data have been deposited to the ProteomeXchange Consortium via the PRIDE (Vizcaíno et al., 2016) partner repository with the dataset identifier PXD010423 (Deutsch et al., 2017, Perez-Riverol et al., 2016).

4.3.4 Luciferase assay

Luciferase assays were carried out using either the Dual-Luciferase Reporter (Promega), SteadyGlo (Promega), or Luciferase Reporter systems (Promega) following the manufacturer's instructions. Dual-Luciferase Reporter and Luciferase Reporter assays were measured using a GloMax 20/20 single tube luminometer (Promega), with a 10 second integration time for each reading. Luciferase assays performed under CL3 conditions used the SteadyGlo system and were measured without the use of injectors on a GloMax 20/20 system.

4.3.4.1 Transfection

Luciferase assays were carried out using Dual Luciferase (Promega), Steady Glo (Promega), Nano-Glo (Promgea) or *Renilla*-Glo (Promega) kits following the

manufacturer's instructions. *Renilla*, firefly and Nano luciferase was measured on a Glomax luciferase machine with an integration time of 10 seconds.

4.3.4.2 Gene modified SFV Infection

Aag2, AF5 or AF319 cells were seeded at 1.5 x10^5 cells per well in 24 well plates. After 24 h, cells were infected with either SFV6 (3H)-FFLuc, SFV6(3H)-RLuc-2SG-p19, SFV6(3H)-RLuc-2SG-ZIKA_C, SFV6(3H)-RLuc-2SG-RVFV_N, SFV6(3H)-RLuc-2SG-BUNV_N or SFV6(3H)-RLuc-2SG-eGFP at MOI 0.01 or 0.001. Cells were lysed at 24, 48 and 72 h post infection with 100 µl passive lysis buffer and *Rluc* measured.

4.3.4.3 siRNA/dsRNA Sensor Assay

Aag2, AF5 or AF319 cells were seeded at 1.5 x10^5 cells per well in 24 well plates. After 24 h, cells were infected with either SFV6(3H)-FFLuc, SFV6(3H)-RLuc-2SG-p19, SFV6(3H)-RLuc-2SG-ZIKA_C, SFV6(3H)-RLuc-2SG-RVFV_N, SFV6(3H)-RLuc-2SG-BUNV_N or SFV6(3H)-RLuc-2SG-eGFP at MOI 1. At 24 h post infection, cells were transfected with 100 ng pIZ-Fluc and co-transfected with dsRNA against FLuc, dsFLuc, LacZ or dsLacZ. Alternatively, co-transfected with siRNAs against FLuc, siFLuc or Hygromycin B resistance gene, siHyg. using 1 µl Dharmafect per well. After 24 h, cells were lysed with 100 µl passive lysis buffer and firefly luciferase signal was measured within the cell monolayers.

4.3.4.4 Cell Viability

Cells were seeded in 96 well plates to 70% confluency. After 24 h, cells were infected with rMP12, rMP12delNSs:eGFP, mock infected or treated with (1 µg/ml) puromycin (as a control). At 7 and 24 h post infection, cells were lysed for 10 min with 30 µl Cell Titre Glo buffer and substrate. Luciferase based cell viability assay was carried out using the Cell Titre-Glo luciferase kit (Promega) according to the manufacturer's instructions. Luminescence was measured on a GloMax luciferase machine with an integration time of 5 seconds.

4.3.5 Protein purification

4.3.5.1 Expression

BL21 Rosetta2 competent bacterial cells were transformed with 50 ng p14 RVFV N or mutant N expressing plasmid and plated out as previously described (4.2.5). A colony was selected and placed in 3 ml LB broth containing ampicillin (100 µg/ml). The culture was grown overnight at room temperature on a shaking incubator (180 rpm). The overnight cultures were transferred into a conical flask containing 200 ml fresh LB/ampicillin and grown at 37°C until the culture reached an A_{600} between 0.5-0.8. After which, the culture was cooled to room temperature and IPTG was added to a final concentration of 0.1 mM. The culture was placed on a shaker (150 rpm) for 18 h at room temperature. Subsequently, the cells were harvested by centrifugation at 3000 x G and stored at -20°C for up to a week.

4.3.5.2 Purification

The cell pellet was thawed, resuspended in 4 ml 1x lysis buffer per 50 ml pelleted culture B-PER Protein Extraction Reagent (Thermo Fisher Scientific) containing Halt EDTA-free protease inhibitor and DNase (50 µg/ml) and rotated at room temperature for 1 h. After which, 20 mM Imidazole, 0.3 M NaCl, 50 mM Tris pH 8.0 and 10% (v/v) glycerol final concentration was added. The cell lysate was centrifuged at 4000 x G for 30 min at 4°C. For a 50 ml culture, 300 µl Ni-NTA resin was equilibrated with 2 ml Protein Equilibration buffer through rotation at 4 °C for 5 min twice. The clarified supernatant was added to the equilibrated Ni-NTA resin in a 15 ml falcon tube and incubated at 4°C with gentle rotation for 30 mins. The supernatant was discarded and Ni-NTA resin resuspended in 2 ml protein purification wash buffer. The sample was rotated at 4°C for 5 minutes before centrifugation at 5000 x G for 1 minute and removal of supernatant. Washes were repeated at least 3 times. The purified protein was eluted using 500 µl protein purification elution buffer per 50 ml culture and with rotation at 4 °C for 15 mins. Finally, the sample was centrifuged at 5000 x G for 1 minute and supernatant transferred to a fresh tube. Purified protein was buffer exchanged to protein storage buffer using Vivaspin® 500 Centrifugal Concentrator (molecular weight cut-off MWCO 10,000Da) according to manufacturer's instructions. Protein samples were checked for purity using SDS-

PAGE (4.3.2) and stained with SyproOrange (Sigma) according to manufacturer's instructions.

4.3.6 RNA binding assay

Recombinant purified protein was examined for *in vitro* RNA-binding activity through dissociation of bound RNA from the sample. 2x RNA gel loading buffer was added to 5-10 µg of recombinant purified protein before visualisation on 2% NuSieve GTG agarose gel (Lonza) stained with GelRed (Biotium).

4.3.7 Multimerisation assay

Purified protein was buffer exchanged from protein storage buffer to 10% glycerol in PBS (v/v). Dithiobis(succinimidyl propionate)(DSP)(Thermo Fisher Scientific) was added to 5 µg of recombinant protein at 1 mM final concentration and incubated at 20°C for 30 min. The reaction was stopped through the addition of loading buffer containing 4x LDS sample buffer before analysis via SDS-Page (4.3.1.1)

Chapter 5 Mutagenesis of RVFV N protein to investigate N-N interactions

5.1 Introduction

N proteins within the *Bunyavirales* order are essential structural proteins for viral replication. Across the order, the protein largely performs the same important functions: the encapsidation of the viral genome, the formation of multimers, the association with the RdRp and the interaction with the glycoprotein Gn for packaging. The binding of the viral genomic RNAs by N is important for the formation of viral RNP complexes that subsequently associate with L allowing transcription and replication to occur, and in addition function to protect the viral genome from harsh conditions found within the intracellular environment (Hornak et al., 2016). Secondly, the formation of multimeric structures of N is essential for the formation of RNP complexes in infected cells. The N-terminal arm binds adjacent N monomer in a globular hydrophobic groove that results in ring-shaped oligomers and allows the formation of filamentous RNPs required to replicate the viral genome (Ferron et al., 2011, Alfadhli et al., 2001). The binding of RNA and the formation of multimeric rings allows the association and binding of the RdRp to the viral genomic RNAs to take place, and thus transcription and replication can occur (Leonard et al., 2005, Osborne and Elliott, 2000). Finally, the N-terminal of Gn has been shown to interact with N in the packaging process at the Golgi apparatus (Piper et al., 2011).

Additionally, there are a number of studies focusing on the other members of the *Bunyavirales* order that have not been investigated within the context of RVFV. *Orthohantavirus* N protein is thought to have RNA chaperone activity, involving the dissociation of RNA duplexes allowing the binding of L protein to the 5' end of the RNA for genome replication (Mir and Panganiban, 2006a, Mir and Panganiban, 2006b). Sin Nombre orthohantavirus N has also been shown to have cap-snatching activity through the binding and accumulation of mRNA caps in cytoplasmic processing bodies, the sequestered caps are then used as primers for the initiation of viral mRNA synthesis (Mir et al., 2008). Within the *Peribunyaviridae,* the order prototype virus Bunyamwera orthobunyavirus (BUNV) nucleocapsid has been shown to carry out largely the same functions as RVFV N (Panganiban and Mir, 2009, Eifan and Elliott, 2009). However, many members of

the *Bunyavirales* order have largely different N protein structures and thus may perform unrelated functions. For example, Crimean-Congo haemorrhagic fever orthonairovirus (CCHFV), a member of the *Orthonairovirus* genus within the *Nairoviridae* family, showed a structural alignment with other *Bunyavirales* N proteins that indicated CCHFV N was more closely related to the arenavirus Lassa virus than other members of *Bunyavirales* (Carter et al., 2012). Thus, other N functions may still be discovered.

Previous studies have revealed a number of important residues essential for the primary functions of RVFV N. The RNA binding cleft has been identified as two distinct components: a) 18 core conserved residues at the centre of the protein and b) residues within the N-terminal arm hinge region. The inner surface of the RNA binding groove is lined with conserved hydrophobic amino acids; conversely the rim has conserved positively charged residues. Thus the core can bind RNA at a high affinity via contact with the hydrophobic amino acids and by base stacking (Raymond et al., 2012). Structurally, the RNA binding cleft showed no RNA sequence specificity or changes in binding affinity (Raymond et al., 2012) despite previous aptamer studies showing a slight preference for specifically designed RNA aptamers (Ellenbecker et al., 2012). Crystallisation of RVFV N allowed the structure to be solved, which showed ring-shaped hexamers, a structure mediated by the N-terminal arm of N binding to an adjacent subunit in the hydrophobic groove (Ferron et al., 2011). Additionally, a variation in the packing of subunits within the hexameric ring in the two crystal structures analysed indicates N's ability to form varying subunit structures that would allow the formation of the serpentine-like RNP structures required for the encapsidation and replication of the viral genome (Ferron et al., 2011). The residues Y3, L7, I9, F11, V16, I21, Y24, V25, F28 and Y30 on the N-terminal arm of RVFV N are important residues for filling the hydrophobic groove (Table 5-1). Mutation of essential residues within the groove can prevent the formation of multimers and therefore stop the formation of viral RNPs (Le May et al., 2005).

The link between RNA binding and N oligomerisation has been tentatively investigated. Electron microscopy (EM) of only N protein showed small oligomers, conversely the EM sample containing both N and RNA showed the typical circular multimeric structures expected from N crystallography (Ferron et

al., 2011). Thus, it has been suggested that in the absence of RNA, the N-terminal arm of N subunits binds to its own oligomerisation groove, resulting in a closed “low-energy” conformation (Ferron et al., 2011). In the presence of RNA, it is predicted that the N-terminal arm opens and stabilises, allowing the further recruitment of N subunits and the formation of higher order structures (Ferron et al., 2011).

There have been several studies that identify important functions of named amino acid residues, summarised in Table 5-1. These residues were all found to be involved in multimerisation or RNA binding and as such, were used as a reference in selection of residues for a mutagenesis study.

The primary aim of this study was to inform on and characterise amino acids that are not associated with the multimerisation and RNA binding function of RVFV N yet are conserved within the *Phlebovirus* genus and thus are likely to be important and may reveal unknown functions.

Residue	Function	Reference
M1	Contacts Trp125 dimer interface	(Raymond et al., 2010)
Y3	Project from N terminal arm - interact with hydrophobic groove	(Ferron et al., 2011)
Y4	Observed loss of dimer formation (destabilisation of helix a1)	(Raymond et al., 2010)
Q5	Contacts Trp125 dimer interface	(Raymond et al., 2010)
L7	Project from N terminal arm - interact with hydrophobic groove	(Ferron et al., 2011)
I9	Contacts Trp125 dimer interface, Project from N terminal arm - interact with hydrophobic groove	(Raymond et al., 2010, Ferron et al., 2011)
F11	Observed loss of dimer formation (destabilisation of helix a1), Project from N terminal arm - interact with hydrophobic groove	(Raymond et al., 2010, Ferron et al., 2011)
A12	Intersubunit van der waals contacts	(Raymond et al., 2010)
V16	Project from N terminal arm - interact with hydrophobic groove	(Ferron et al., 2011)
I21	Project from N terminal arm - interact with hydrophobic groove	(Ferron et al., 2011)
Y24	Project from N terminal arm - interact with hydrophobic groove	(Ferron et al., 2011)
V25	Project from N terminal arm - interact with hydrophobic groove	(Ferron et al., 2011)
F28	Project from N terminal arm - interact with hydrophobic groove	(Ferron et al., 2011)
Y30	Project from N terminal arm - interact with hydrophobic groove, Hinge region stacks with 5'most base in RNA binding (base 1)	(Ferron et al., 2011)
F33	"Back pocket" of RNA binding slot interacts with base 2	(Raymond et al., 2012)
R64	Predicted RNA binding cleft, loss of RNA binding in triple mutant*	(Ferron et al., 2011)
G65	Interacts with base 5 in narrow pocket	(Raymond et al., 2012)
K67	Predicted RNA binding cleft, loss of RNA binding in triple mutant*	(Ferron et al., 2011)
K74	Predicted RNA binding cleft, loss of RNA binding in triple mutant*	(Ferron et al., 2011)
A109	Lines RNA binding slot interacts with base 3 and 4	(Raymond et al., 2012)
A110	Lines RNA binding slot interacts with base 3 and 4	(Raymond et al., 2012)
V120	Intersubunit van der Waals contacts	(Raymond et al., 2010)
V121	Intersubunit van der Waals contacts	(Raymond et al., 2010)
E124	Intersubunit van der Waals contacts	(Raymond et al., 2010)
W125	Contacts Met1, Gln5, Ile9 and Trp125 of second monomer. Critical for dimer formation	(Raymond et al., 2010)
L126	Interacts with base 5 in narrow pocket	(Raymond et al., 2012)
P127	Interacts with base 5 in narrow pocket	(Raymond et al., 2012)
T131	Intersubunit van der Waals contacts	(Raymond et al., 2010)
P147	Lines RNA binding slot interacts with base 3 and 4	(Raymond et al., 2012)
F176	Interacts with base 5 in narrow pocket	(Raymond et al., 2012)
R178	Forms salt bridge with Ala245	(Raymond et al., 2010)
I180	Lines RNA binding slot interacts with base 3 and 4	(Raymond et al., 2012)
P199	Lines RNA binding slot interacts with base 3 and 4	(Raymond et al., 2012)
A202	Lines RNA binding slot interacts with base 3 and 4	(Raymond et al., 2012)
A245	Forms salt bridge with Arg178	(Raymond et al., 2010)

Table 5-1. Summary of known RVFV N residue functions.

A table compiling the predicted and known functions of RVFV N protein residues from studies primarily focused on the RNA binding capabilities. Information compiled from (Ferron et al., 2011),(Raymond et al., 2012) and (Raymond et al., 2010)

5.2 Results

5.2.1 N Protein Conservation and Mutagenesis

To assess the conservation of the N protein sequence between members of the *Phlebovirus* genus, 14 Phlebovirus N sequences in GenBank (http://www.ncbi.nlm.nih.gov/genbank/) were aligned using a pairwise alignment in Geneious (Appendix 9.2) and conserved residues were identified (Figure 5-1). The conservation of N between RVFV and other species of *Phlebovirus* varies greatly, at 48% aa similarity between RVFV and TOSV and as little as 36% between RVFV and UUKV. The alignment of phleboviruses forms into two distinct groups, phleboviruses transmitted by an insect vector or transmitted by ticks. From this alignment five amino acids were selected for alanine substitution and downstream functional analysis. Alanine substitution was chosen due to its biochemical nature, as it retains the shape of the structure via the beta carbon; however it has no further side chain chemistry. This small selection of mutants was selected based upon sequence conservation between phleboviruses, targeting those residues that were most likely to have a significant conserved function. Additionally, residues were included that are presented on the surface of the N protein, and not close to previously known functional areas such as the RNA binding pocket therefore excluding some of the more highly conserved residues within the alignment. Thus a targeted approach was used; fewer mutants were selected due to time constraints and to allow for complete downstream experimental evaluation and confirmation of residue functions. Residue F11, a previously analysed residue found on the N-terminal arm of N, is highly conserved between the insect-borne phleboviruses, with the exception of Candiru virus (CDUV). In the UUKV-like tick-borne virus group however the phenylalanine is often substituted with an isoleucine. While the function of F11 had been previously identified, unpublished work from the Elliott laboratory indicating it is possible to rescue a functional N-terminal arm deletion mutant may have shed doubt on the residues structural functions. Residue Y30 of RVFV has been previously analysed and is conversed across both phlebovirus groups. Residues D34, F149 and N181 are conserved across the *Phlebovirus* genus and have no associated functions. Additionally, as mentioned previously, the prior unpublished work from the Elliott laboratory had indicated that it is possible to rescue a RVFV virus with an N-arm deletion, and thus would be a

valuable tool with which to generate an RVFV N tagged virus that does not affect the globular formation of N. This would also allow us to examine the impact of N-N interactions on N protein functions. To test this, two N-arm mutants, a deletion of amino acids 1-14 and 1-31, were also introduced to the panel of mutants (Figure 5-2).

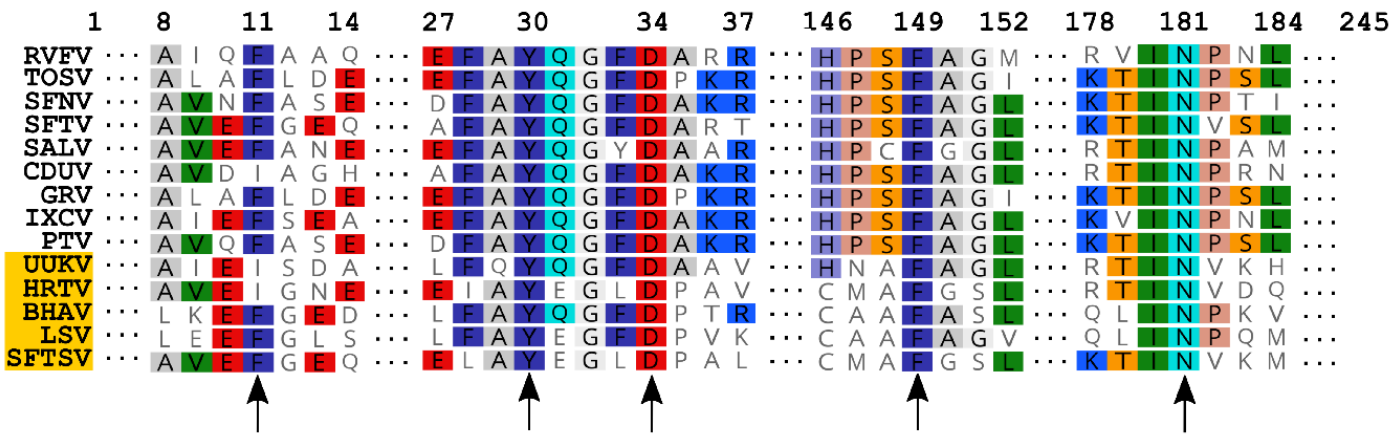

Figure 5-1. Alignment of *Phlebovirus* sequences and indicated point mutations.

Rift Valley fever phlebovirus (RVFV), Toscana phlebovirus (TOSV), sandfly fever Naples phlebovirus (SFNV), sandfly fever Turkey phlebovirus (SFTV), Salehabad phlebovirus (SALV), Candiru virus (CDUV), Granada phlebovirus (GRV), Heartland phlebovirus (HRTV), Ixcanal phlebovirus (IXCV), Punta Toro phlebovirus (PTV), SFTS phlebovirus (SFTSV), Uukuniemi phlebovirus (UUKV), Lone Star phlebovirus (LSV), Bhanja phlebovirus (BHAV) Genbank sequences were aligned, conserved regions identified and cross referenced with previous literature. Amino acid positioning is relative to the RVFV N sequence. The tick-borne phleboviruses are highlighted in yellow.

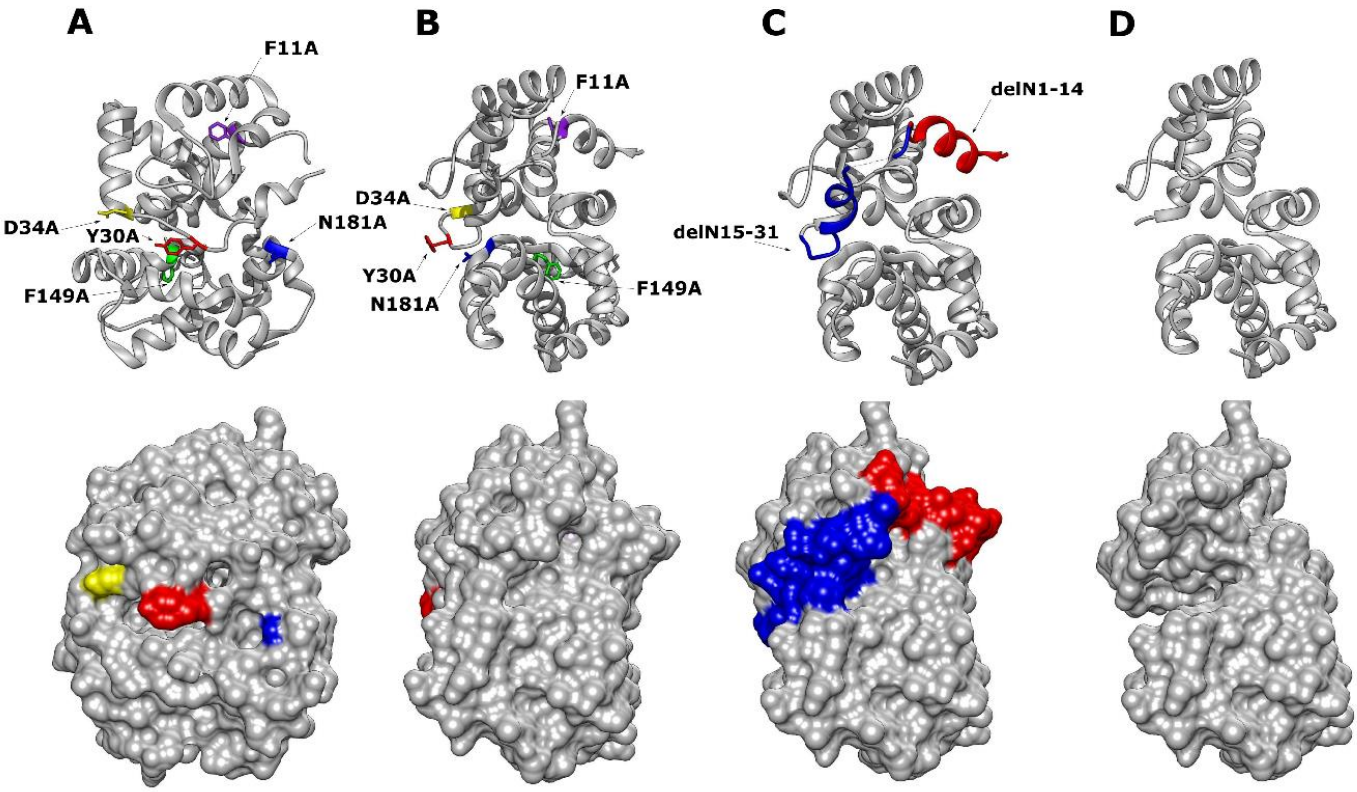

Figure 5-2. Chimera 3D Model of RVFV N protein monomer with highlighted mutant residues.

(A) RVFV N protein with highlighted mutations in ribbon view, F11A purple, Y30A red, D34A yellow, F149A green, N181A blue (top image)and corresponding surface view (bottom image). (B) Alternative orientation of RVFV N with 90° offset to (A). (C) RVFV N protein with highlighted N-terminal arm deletion mutations, 1-14 in red and 15-31 in blue. (D) Mutant RVFV N with the full delN1-31 mutation and corresponding surface view. Figure based on data generated in a previous study (PDB: 3LYF) (Raymond et al., 2010).

5.2.2 Effect of N mutants on reporter systems

To test the functionality of each RVFV N mutant we employed a minigenome system. As N is under differential expression from the S segment via an ambisense coding strategy, a plasmid containing only the N coding sequence was used to study N in isolation and avoid any deleterious effects that NSs may have on the functions of N or on the minigenome activity (Brennan et al., 2011a). The minigenome system involves the expression of the N protein ORF (pTM1-N) as opposed to plasmids that express full mRNA copies of the viral S segment such as pTVT7 RVFV MP12 S Segment. In addition to pTM1-N, the minigenome system requires the viral RdRp expressed in a pTM1-L plasmid, both under the expression of a T7 RNA polymerase promoter. Together, the N and L plasmids transfected into T7 RNA polymerase expressing cells bind to the mRNA generated from a third plasmid, a virus genome segment analogue with the viral coding sequence replaced with the *Rluc* ORF leaving the viral M segment UTRs intact (Figure 5-3). The viral N and L proteins form RNP complexes that recognise M segment UTRs and transcribe *Rluc* gene resulting in luminescent signal. The level of luminescence correlates to the efficiency of viral RNP formation through the measurement of transcriptional activity. The pTM1-N plasmids were used as a basis in this study to express mutant N proteins. As shown in Figure 5-4, both delN1-14 and delN1-31 N arm mutants have no activity in the minigenome system. Interestingly, the conserved mutants showed a wide variation in their minigenome activities. The mutants F11A and F149 had no transcription activity, whereas Y30A and N181A both showed significantly increased activity and D34A showed reduced activity, all relative to the wildtype (WT) N (Figure 5-4). A previous mutagenesis study of BUNV N showed that inconsistent protein expression levels can significantly impact minigenome system activity (Eifan and Elliott, 2009), and therefore a Western blot assay was performed on cell lysates from the minigenome assay to determine the expression levels of the N protein mutants. The expression of transiently expressed N protein mutants was consistent, however, mutant delN1-31 showed greatly reduced expression levels. Furthermore, through the generation and utilisation of BSR-T7/5 CL21, a single cell clone of BSR-T7 cells with increased expression of T7 RNA polymerase, delN1-31 expression was detected (Figure 5-5).

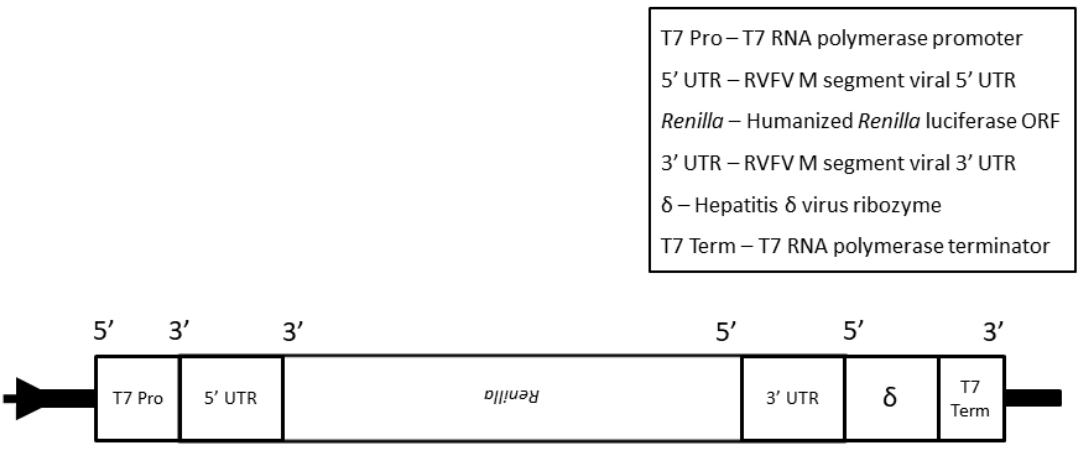

Figure 5-3. Schematic of pTVT7–GM:hRen

The pTVT7 backbone contains a T7 promoter followed by RVFV viral UTRs flanking both the 5’ and 3’ end of the *Renilla* luciferase ORF. The *Renilla* ORF is in the anti-sense orientation and thus does not produce mRNA transcripts from T7 polymerase activity. Furthermore there is a Hepatitis δ virus ribozyme to allow self-cleavage and generation of the correct 3’UTR end, allowing recognition by RVFV RNP complexes. Finally, the cassette contains a T7 terminator sequence.

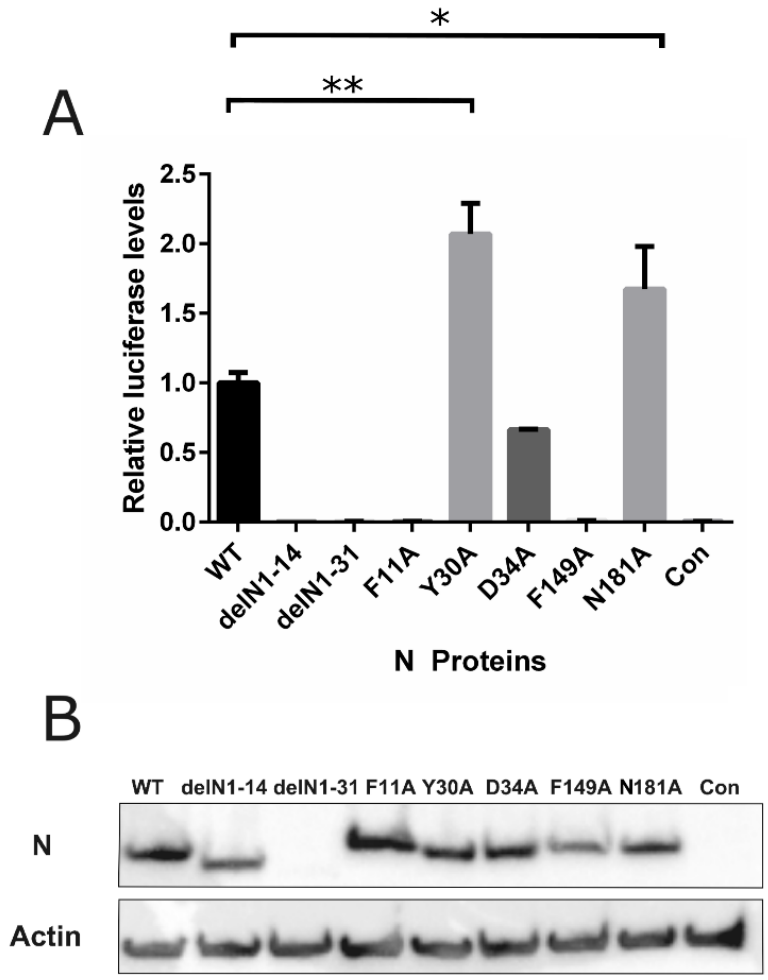

Figure 5-4. Minigenome activity of RVFV N mutants and western blot of expression levels.

BSR-T7/5 cells were transfected with pTM1-N (wildtype [WT] N, mutant N) or empty pTM1 plasmid as a negative control (Con), pTM1-L, pTVT7-GM:hRen and pTM1-FF-Luc as a transfection control. (A) Cells were lysed 24 hours post transfection to measure the minigenome activity with the presence of WT RVFV N or its mutant version. Experiments were performed in triplicate and values calculated by dividing *Rluc* activity by *Fluc* activity to normalise variable transfection efficiency. Mean values together with standard error are shown, *denotes $p<0.05$, ** for $p<0.001$ using Student's T-test. (B) Western blot analysis of cell lysates, probed with RVFV anti-N antibody (top panel) and anti-actin (bottom panel) as loading control.

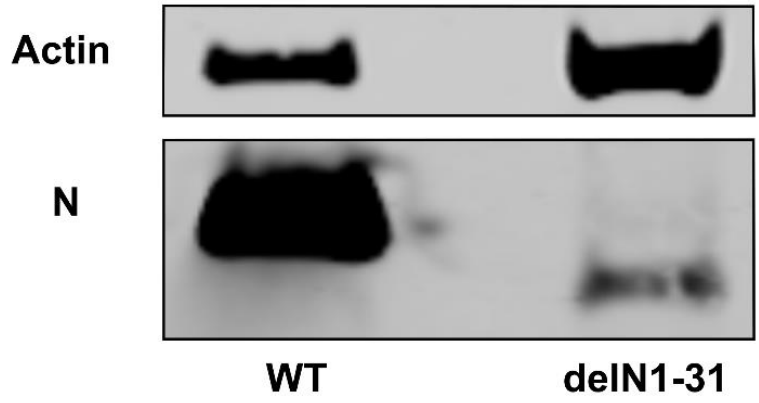

Figure 5-5. Relative expression levels of delN1-31 mutant.

BSRT7/5 CL21 cells were transfected with pTM1-N and delN1-31 mutant plasmids, followed by cells lysis 24 hpt. Western blot probing for anti-actin (top panel) and anti-RVFV N (bottom panel) antibodies. Four times more cell lysate from delN1-31 transfected cells was loaded for expression analysis.

Furthermore, *Fluc* transfection control values were evaluated for any significant changes in general cellular transcription/translation upon the transfection and expression of RVFV N or mutant N proteins. As shown in Figure 5-6, there was no significant difference due to the presence of the mutants or WT N.

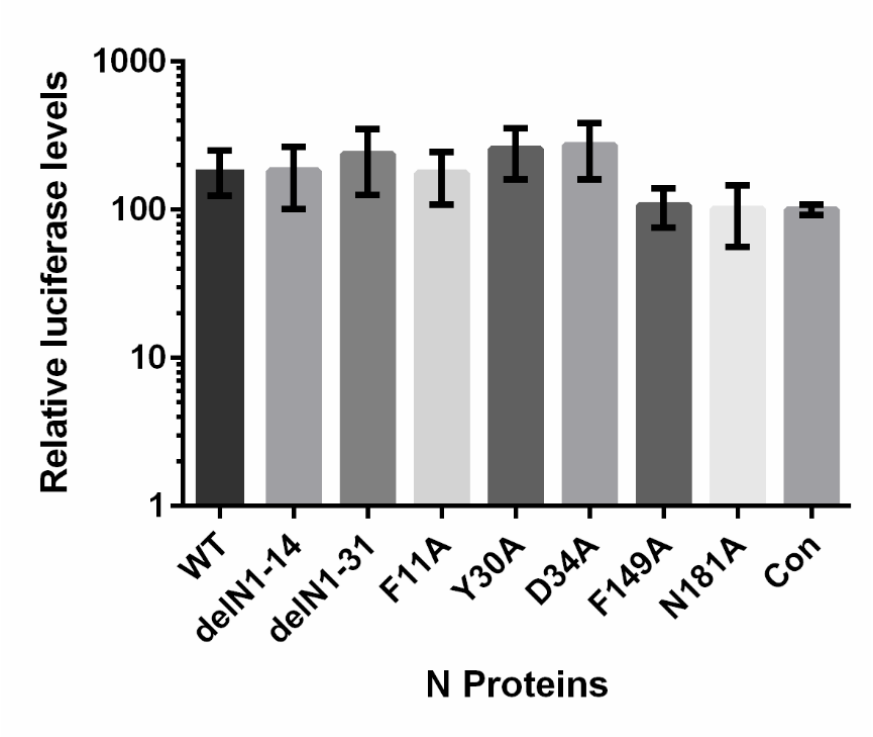

Figure 5-6. Effect of N protein on *Fluc* expression.

The Firefly luciferase (*Fluc*) values for the minigenome experiment described in Figure 5-4. Mean values together with standard error of triplicate experiments are shown, Student's T test showed no significant difference as compared to control plasmid.

One of RVFV N's described functions is the interaction with the N-terminal glycoprotein tail of Gn that mediates the packaging of viral RNPs into virions before budding at the Golgi apparatus. To assess the capacity for N mutants to form virus-like particles we employed an assay based upon packaging the minigenome system into VLPs with the addition of the plasmid expressing glycoproteins. BSR-T7/5 CL21 cells were transfected with RVFV M segment minigenome reporter pTVT7-GM:hRen, pTM1-N or mutant N, pTM1-L and additionally pTM1-M encoding the glycoprotein precursor of RVFV M segment. At 48 h post transfection, cell culture media of the donor cells containing the produced VLPs was clarified by centrifugation and nuclease treated to prevent the reporter plasmid carry over, thereby reducing background luciferase levels. The nuclease-treated supernatant was used to inoculate recipient BSR-T7/5 CL21 cells pre-transfected with pTM1-L and WT pTM1-N plasmids. The supplementary plasmids express stable RNP complexes that can, in the case of functional packaging, transcribe reporter template released into the cells from virus-like particles resulting in translation and *Rluc* expression. The VLP data corroborated data shown in the minigenome assay presented in Figure 5-7. The WT N and its mutants Y30A, D34A and N181A showed functional packaging of the reporter template into the VLPs.

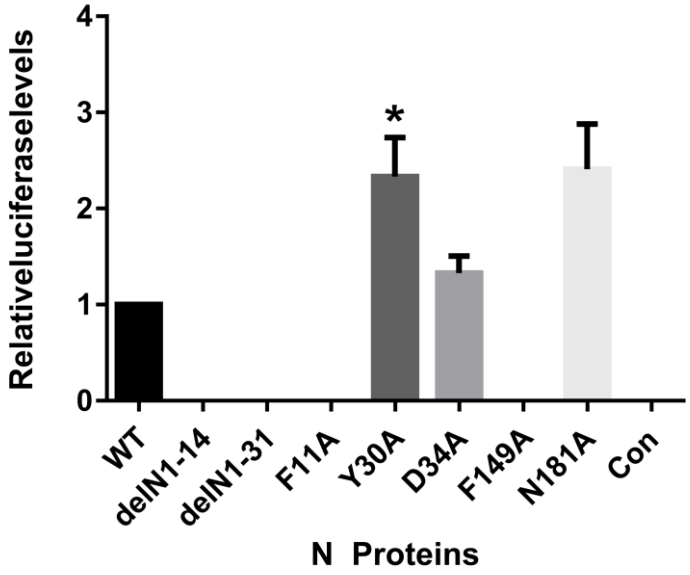

Figure 5-7. RVFV N mutant activity in a VLP assay

BSR-T7/5 CL21 cells were transfected with pTVT7-GM:hRen, pTM1-L, pTM1-M, pTM1-FF-Luc and WT or mutant pTM1-N. In case of control cells pTM1-N was replaced with pTM1. At 48 hours post transfection, the supernatant was harvested and treated with Benzonase. The treated supernatant was applied to recipient BSR-T7/5 CL21 cells pre-transfected with pTM1-L and WT pTM1 N. *Rluc* activity was measured 24 h post-infection. Experiments were performed in triplicate and repeated three times, mean values together with standard error are shown. Mean values together with standard error are shown, *denotes $p<0.05$ using Student's T-test.

5.2.3 N mutant proteins- assessment of functional properties

RVFV N has a number of key functions: encapsidation of viral RNA, multimerisation of N into functional higher order structures and the association and binding of the viral RdRp (Ferron et al., 2011, Raymond et al., 2010, Raymond et al., 2012), all of these functions are required for the successful formation of viral RNPs. Thus, it was important to assess each mutant for their ability to perform each of these functions. To assess the encapsidation and RNA binding capacity, we utilised the N protein's ability to non-specifically bind any cellular RNA (Raymond et al., 2010, Dong et al., 2013). During the protein purification process from *E. coli*, purified N binds non-specific bacterial RNA (Figure 5-8A). This RNA can be dissociated by using formamide-containing RNA loading buffer, which denatures N and thus, it releases bound RNA fragments (Figure 5-8B). The RNA binding activity was evident for the delN1-14, F11A, D34A, F149A and N181A mutants, however the full arm mutant delN1-31 and mutant Y30A had no detectable RNA bound. This was consistent with the measurement of 260nm/280nm ratios for all these purified protein samples.

RVFV N, sized 27kDa, has been shown to form higher order structures: tetramers, pentamers and hexamers. Therefore, it was important to assess if the mutant's capacity to multimerise was impaired, which could explain the results of the minigenome system. To capture the multimerisation states of N we employed a DSP chemical crosslinking assay on purified N protein from the bacterial expression system (Figure 5-8C). The arm mutant delN1-31 had impaired capacity to form higher order structures, however the other mutants all showed normal multimerisation properties.

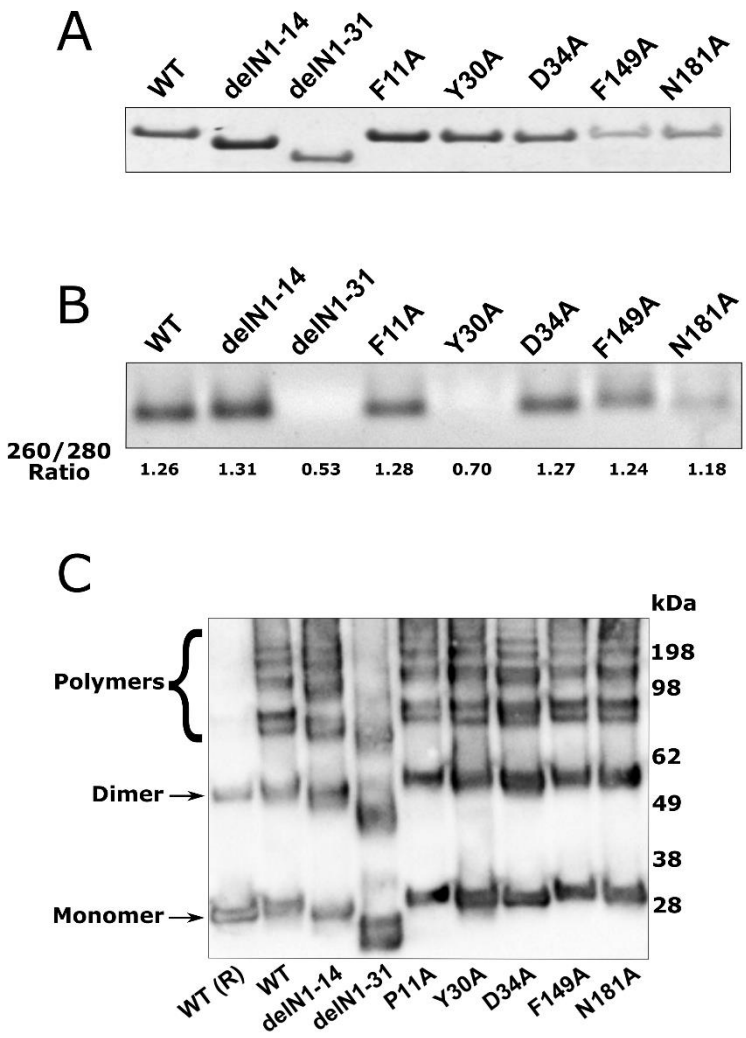

Figure 5-8. Purified RVFV N protein RNA binding capacity and multimerisation properties.

(A) InstantBlue staining was performed to confirm the purification of N protein or its mutants. (B) The *in vitro* RNA binding activity of WT and mutant N proteins was determined by dissociation of non-specifically bound bacterial RNA with a buffer containing formamide. Representative image of three repeats shown and 260nm/280nm ratios for this experiment indicated below the image. (C) DSP chemical cross-linking was used to determine the multimerisation capacity of purified mutant proteins, cross-linked samples were analysed by Western blot using anti-RVFV N antibodies. ß-mercaptoethanol was added to the control (WT(R)) to reduce the di-sulfide bonds after multimerisation; representative image of three independent experiments.

The interaction between N and the viral L protein is essential for the formation of replication-active RNP complexes. Through the use of a construct expressing a V5-tagged L protein (L3V5) (Brennan et al., 2011a) we performed a co-immunoprecipitation (co-IP) to assess the direct interaction between the polymerase and the N mutants (Figure 5-9). pTM1-L3V5 and pTM1-N (or its mutant variants) were co-transfected into BSR T7/5 CL21 cells 24 hours before subsequent immunoprecipitation. To reduce the effect of bound RNA influencing the interaction, the experiment was performed in the presence of RNase A. To note, due to the encapsidation ability of N, RNA pre-bound within the N binding cleft would not be removed under these conditions as it would be protected from cleavage by RNAse A. The co-IP with an anti-V5 antibody was followed by western blotting with anti-N and anti-V5 sera to identify the capacity for N to bind to the L protein. As expected, the mutants Y30A, D34A and N181A that had activity in the minigenome assay interacted with the L protein. Interestingly, mutants delN1-14, delN1-31, F11A and F149A also showed binding ability despite showing no functional RNP complexes. Thus, we suggested that any functional deficiencies observed are irrespective of the N-L interaction, however, L polymerase processivity could be affected.

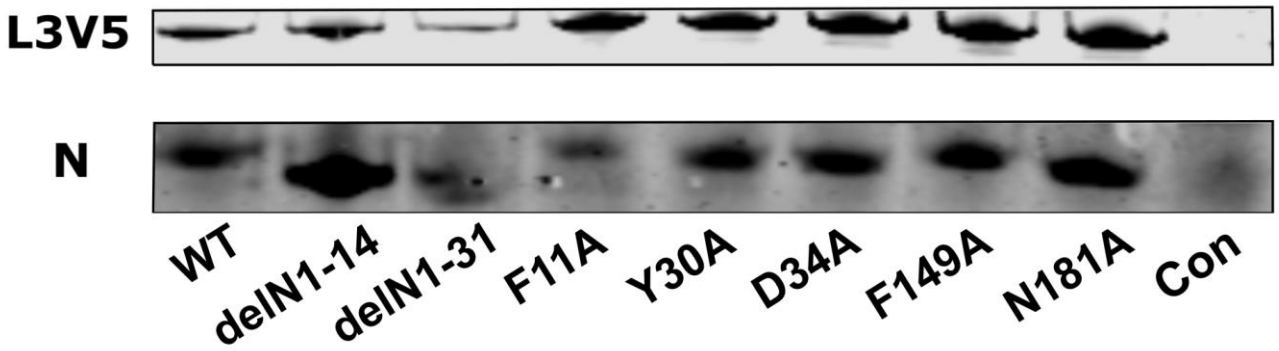

Figure 5-9. RVFV L3V5 polymerase interaction with WT and mutant N proteins.

BSR-T7/5 CL21 cells were transfected with pTM1-L3V5 and pTM1-N (or its mutant version). For a negative control, the pTM1-L3V5 plasmid was replaced with empty pTM1 (Con). At 24 h post transfection, the cells were lysed and lysate applied to magnetic beads bound with anti-V5 antibody. The bound proteins were dissociated from the beads and analysed by Western blot using anti-V5 and anti-RVFV N antibodies. Following the treatment with secondary antibodies the membranes were visualised using LI-COR. The image is representative of three independent repeats.

5.3 Discussion

This study aimed to inform on previously unknown conserved phlebovirus N residues in order to gain an understanding into the fundamental biology of RVFV and its replication cycle. The highly conserved nature of RVFV N within identified isolates, as evidenced by multiple sequence alignment (Appendix 9.2), indicates the propensity for conserved residues to confer essential functions. RVFV MP12, an attenuated strain of RVFV generated by serial passage under chemical mutagen, was used in this study. The RVFV MP12 N has no non-synonymous mutations compared with the pathogenic parental strain ZH548 and thus, the data on functional amino acids is applicable both for MP12 studies and natural RVFV isolates.

This study identified two residues, F11A and F149A, to have unknown essential functions in the formation of viral RNP complexes and/or transcription or replication of the viral genome. The F149A mutant in particular had no activity in the minigenome assay and had lost the ability to form VLPs, however performed all functions previously identified as essential for RVFV N protein. The surface exposed nature of F149A and location at a predicted protein binding cleft has lead us to hypothesise that this residue may be involved in the interaction with host cellular factors important for normal N processes. Further study of this mutant was out of the scope of this study, however an explorative experiment using immunoprecipitation followed by proteomics to identify interactors of F149A comparative to WT N may reveal impacted host processes that are important for RVFV N function. Furthermore, this avenue of study can be widened to assess host protein interactions with other members of the *Phlebovirus* genus. The mutant D34A showed slightly reduced activity in the minigenome system yet performed all known functions, thus may also be involved in host protein interactions, particularly considering its surface exposed nature.

The F11A mutant shows no activity in the minigenome system. A previous study has identified a F11G mutant to be involved in the loss of N-N dimer formation, through the use of a GST-fused N protein. They hypothesise that the disruption involves misfolding of the N-terminal region and disruption of the N-N interaction (Le May et al., 2005). Interestingly F11A showed full multimerisation

capability within our cross-linking system and additionally still associated with the viral L protein and encapsidated the genome. As the G residue can be more flexible than A, it could explain the discrepancy in results between F11G and F11A. Testing the F11G mutant within the DSP crosslinking assay, or through immunoprecipitation of a GST fused F11A mutant would provide confirmation regarding the nature of these two mutants. It is clear that the F11A mutant is essential for N protein function; it may impact a function other than N-N dimer formation. For example, the processivity of RNA synthesis could be affected, or binding of further host factors required. By assessing the generation of *Renilla* RNA transcripts it would be possible to assess whether the effect is on transcription or on translation.

Two mutants, Y30 and N181, were shown to have increased activity in our minigenome system (Figure 5-4). The N181A residue has no previously described function yet showed increased activity in the minigenome assay and formed functional VLP complexes. This indicates that N181A must retain the capacity to interact with Gn in the formation of VLPs. Interestingly; Y30 had previously been identified as an essential residue, involved in the multimerisation of N protein and base stacking of RNA within the RNA binding groove. Additionally Y30 is thought to be a key residue in the hinge region of the N-terminal arm, allowing flexibility and thus facilitating the binding of N into various multimeric structures (Raymond et al., 2012). The Y30A mutant in this study however appeared to have reduced RNA binding capacity yet still formed multimeric structures. A previous study indicated that the Y30A mutation did not disrupt N-N interactions and thus, it retained its multimerisation capability (Le May et al., 2005). Additionally, a mutagenesis study in UUKV, also of the *Phlebovirus* genus, identified Y30A as active within a minigenome reporter system (Katz et al., 2010b) though the study did not assess its RNA binding capacity. The reduced RNA binding capacity did not negatively affect the expression of the minigenome reporter *Rluc* or packaging into VLPs.

The nature of N proteins ability to non-specifically bind cellular RNAs has been proposed as a mechanism for preventing translation of cellular transcripts, however, the levels of Firefly luciferase from transfection control plasmid in the minigenome assay showed no significant change in the presence of N signifying

no general shutdown of translation (Figure 5-6). There may however be an inverse relationship between minigenome activity and RNA binding, this would require further confirmation. We hypothesise that the reduced RNA binding capacity may positively affect RNA replication by a looser binding of RNA into the binding pocket allowing increased processivity of the L protein in the transcription and replication of the genome, at the expense of genome protection. The testing of this hypothesis was outside the scope of this study.

The delN1-14 and delN1-31 arm mutants showed no activity in the minigenome assay. A study on UUKV N N-terminal mutants showed no activity on CAT signal based minigenome system (Katz et al., 2010a). This study supports the hypothesis that phleboviral N protein N-terminal arm is functionally essential. Interestingly, in our study the delN1-14 mutant retained the ability to form multimers and encapsidate RNA. Thus, these data suggest that the removal of the 1st helix of the n-terminal arm does not impair multimerisation and RNA binding, yet these functions are impaired with the removal of the 2nd helix. The delN1-31 arm mutant showed impaired multimerisation. While able to form dimers and tetramers, delN1-31 showed impaired formation of higher order structures indicating an importance for the 2nd helix in successful N-N binding in a functional conformation. We hypothesise that the removal of the 1st alpha helix reduces the stability of binding into N subunits oligomerisation groove, however the 2nd helix provides enough stability to identify the interaction in a cross-linking assay. Comparatively, a delN1-19 mutant in UUKV N showed approximately 25% N-N binding capacity (Katz et al., 2010a), thus indicating a reduced level of multimerisation, this supports our hypothesis for RVFV delN1-14. The loss of function may also be due to the impairment of the RNA-dependent RNA-polymerase L to track along the viral RNP, or the resulting N protein multimeric structures having an unfavourable orientation or configuration conducive to successful transcription or replication. The delN1-31 arm mutants lack of activity is likely due to its inability to from higher order multimeric structures and bind viral RNA. Interestingly, delN1-31 still showed interaction with the polymerase L (Figure 5-9), therefore it is highly likely that the interaction domain with L is not within the N-terminal arm, and L interaction does not require functional formation of the RNP complexes.

In conclusion, this study indicates the importance of identifying essential residues for understanding the fundamental processes of RVFV N protein while also informing on residues conserved across the phleboviruses and thus may have wider importance within the genus. The availability of mutational information is an important resource for further study, particularly for the investigation of RVFV N interaction with the host proteins and other essential functions, for example, the multimerisation capacity, the link between non-specific RNA binding and minigenome activity and L protein processivity. Through understanding of these processes, we may identify potential therapeutic targets against RVFV as there is currently no specific antiviral treatment available.

The functional similarity of phlebovirus N proteins, as evidenced by the mutagenesis of Y30A and the delN1-14 mutants similarity with UUKV, indicates that the mutagenesis data may be relevant for informing on functional residues of other phleboviruses. The residues identified can be used as a basis for determining interaction domains of newly identified phlebovirus N – host protein interactions. Additionally, this mutagenesis study can be used as a basis for influencing therapeutic or vaccine design. Further analysis of replication deficient RVFV N mutants and the rescue of mutant RVFV viruses may reveal significant attenuation that can be used in vaccine trials. A significant issue with vaccination of ruminants across the African continent is the inability to distinguish between seropositive and vaccinated animals. To continue this study, an attenuated N mutant RVFV strain maybe be distinguished from active RVFV infection by generation of monoclonal antibodies to specific mutant residues and thus may be a candidate for an effective veterinary vaccine. These findings may also influence structure-based drug design, designed to disrupt interactions such as binding the interaction domains of the N-terminal arm via P11 or more accessible residues such as F149. This study will provide a significant basis with which to expand the understanding of RVFV N biology.

5.4 Summary

- A panel of mutants targeting residues conserved across the phlebovirus genus was generated.

- Mutant F149A was essential yet still performed all known functions of N protein indicating unknown protein-protein interaction effected.

- Mutant F11A had no minigenome activity yet also performed all known functions. F11A showed activity in multimerisation despite previous evidence indicating it as an essential residue for multimerisation.

- Mutant Y30A showed increased activity yet reduced RNA binding capacity. Y30A also had multimerisation capacity yet Y30A had been implicated as an important residue for both RNA binding and multimerisation. Mutant N181 also showed increased minigenome activity and reduced RNA binding, indicating inverse relationship between RNA binding and minigenome activity.

- D34A had reduced minigenome activity and performed all known functions. The residue being surface exposed may indicate a disrupted host protein interaction.

- delN1-14 showed no minigenome activity but retained multimerisation capacity. delN1-31 lost the ability to form higher order multimers, thus the stability of N-N interactions is likely centred around the 2^{nd} alpha helix within the N-terminal arm.

- This panel of mutants has provided a strong basis for future studies, informing on conserved residues that have revealed the complexities of RNP formation and successful transcription and replication capacity of RVFV N.

Chapter 6 RVFV and the WNT Signalling Pathway

6.1 Introduction

Understanding the interaction between host cell proteins and viruses is exceptionally important; disrupting these interactions may unveil novel intervention strategies for both drug treatment and vaccination. All viruses require the interaction of host cell machinery to replicate but also require host proteins for receptor binding, entry, penetration of the endosome, budding and release. A whole genome siRNA screen identifying host interactors of the phlebovirus UUKV had over 370 candidate genes. Many of the interactors were with the components of ribosomal machinery and RNA-binding proteins, as expected for an RNA virus, however, there were further interactions highlighted involved in entry, endosomal acidification and trafficking (Meier et al., 2014). Proteomics studies designed to assess bunyavirus host protein interactions are limited. Previous studies are often broad in scope and focus primarily on host proteins found packaged within the virion or directly interacting with the non-structural protein NSs (Nuss et al., 2014). These studies most commonly identified cytoskeletal proteins within the RVFV virions, such as integrin subunits and integrin regulatory proteins. These integrins have a predicted involvement with viral budding and egress, however, further study is limited. Additionally, proteins from the Ras superfamily were found within the virion correlating evidence for RVFV's use of caveola-mediated endocytosis for viral entry (Harmon et al., 2012).

Within RVFV research, the nucleocapsid protein N has not been the subject of focus for host protein interactions. The non-structural proteins of many viruses are involved in interactions disrupting innate immune pathways important for the successful replication of the virus. Influenza virus replication for example, can be disrupted by the targeting of host-virus interactions; such as the inhibition of the Raf/MEK/ERK signalling cascade resulted in reduction of virus production (Pleschka et al., 2001). There have been over 80 compounds identified as potent inhibitors of influenza host-virus interactions (De Chassey et al., 2014). This highlights the efficacy of targeting host protein interactions for viral therapeutics. Nucleoproteins may also have antagonistic properties. The

arenavirus Junín virus (JUNV) nucleoprotein was shown to associate with the double-stranded RNA activated protein kinase (PKR) by sequestering PKR into viral factories preventing the phosphorylation of eIF2α and thus inhibiting a key antiviral pathway (King et al., 2017). A previous study using a proteomics approach to assess Crimean-Congo haemorrhagic fever virus (CCHFV), of the *Nairovirus* genus, *Bunyavirales* order, identified an important interaction with cellular chaperons of the HSP70 family. The inhibition of HSP70 function resulted in a significant titre reduction for Hazara virus, a distinct virus of the CCHFV serogroup (Surtees et al., 2016).

The primary aim of this study was to identify host protein interactions of RVFV nucleocapsid protein and to further elucidate the importance of said interactions on the replication efficiency of the virus. Furthermore, I wished to assess the impact of RVFV infection on the interactions, determining relocalisation of proteins and impact on cellular pathways with the outlook of informing on possible therapeutic targets. The WNT signalling pathway had previously been shown to have a role in RVFV infection, however the mechanism behind this function and its importance within the wider context of virus infection was unknown. Additionally, the wealth of molecular tools available for studying WNT allowed for more in depth study into the pathway. Thus WNT was the primary focus of this study.

6.1.1 Human WNT signalling pathway

The WNT (wingless/integrated) pathway is an important pathway in embryonic development, involved in numerous cell cycle and cell proliferation activities. While there are a number of minor WNT signalling pathways, the most critical and most studied signalling pathway is the canonical WNT signalling pathway involving the effector molecule ß-catenin which localises to the nucleus to act as a key transcriptional activator for numerous downstream developmental genes (Clevers and Nusse, 2012).

In the absence of the signalling molecule WNT at the surface of the cell, cytoplasmic ß-catenin is targeted for degradation by the Axin complex in the cytoplasm (Figure 6-1A). The Axin complex is composed of the scaffold protein Axin, glycogen synthase kinase 3 (GSK3), casein kinase 1 (CK1) and adenomatous polyposis coli gene product (APC). This complex binds ß-catenin, phosphorylating the terminal region, thereby allowing recognition by the E3 ubiquitin ligase subunit Trcp resulting in subsequent ubiquination and further proteosomal degradation (Aberle et al., 1997). This results in significantly reduced levels of cytoplasmic ß-catenin preventing transition to the nucleus. WNT activated genes are repressed by DNA-bound T cell factor/lymphoid enhancer factor (TCF/LEF) including the proteins Transducin-like-Enhancer (TLE) and histone deacetylase-1 (HDAC) that form a co-repressor complex functioning to remove the acetyl groups from the chromatin resulting in transcriptional repression (Daniels and Weis, 2005).

Conversely, extracellular WNT ligand will bind to the cell surface transmembrane receptor Frizzled (Fz) and its co-receptor low-density lipoprotein receptor-related protein 5 (LRP5) or LRP6. The generation of this complex recruits the scaffold protein Dishevelled (Dv1) which in turn phosphorylates LRP5/6 resulting in the further recruitment of the Axin complex to the receptor, preventing the degradation of cytoplasmic ß-catenin. The accumulation of ß-catenin allows migration into the nucleus where ß-catenin complexes with TCF/LEF promotor sites allowing transcription (Daniels and Weis, 2005).

The ß-catenin independent WNT signalling pathway (non-canonical) does not involve LRP5/6 sensors or ß-catenin yet still activates various signalling cascades involved in gene transcription. Two common non-canonical pathways are WNT/Ca^{2+} and WNT/PCP (planar cell polarity) also referred to as the Frizzled-PCP pathway. These pathways have cross-talk with the canonical signalling pathway, often inhibiting the pathway (Mcneill and Woodgett, 2010). Overexpression of Wnt5a, an activator of the non-canonical signalling pathway can block stabilization of ß-catenin (Torres et al., 1996). Conversely, inhibition of the canonical pathway can result in a potential activation of PCP (Rousset et al., 2001). Thus it is important to be aware the consequences of affecting one pathway on the other.

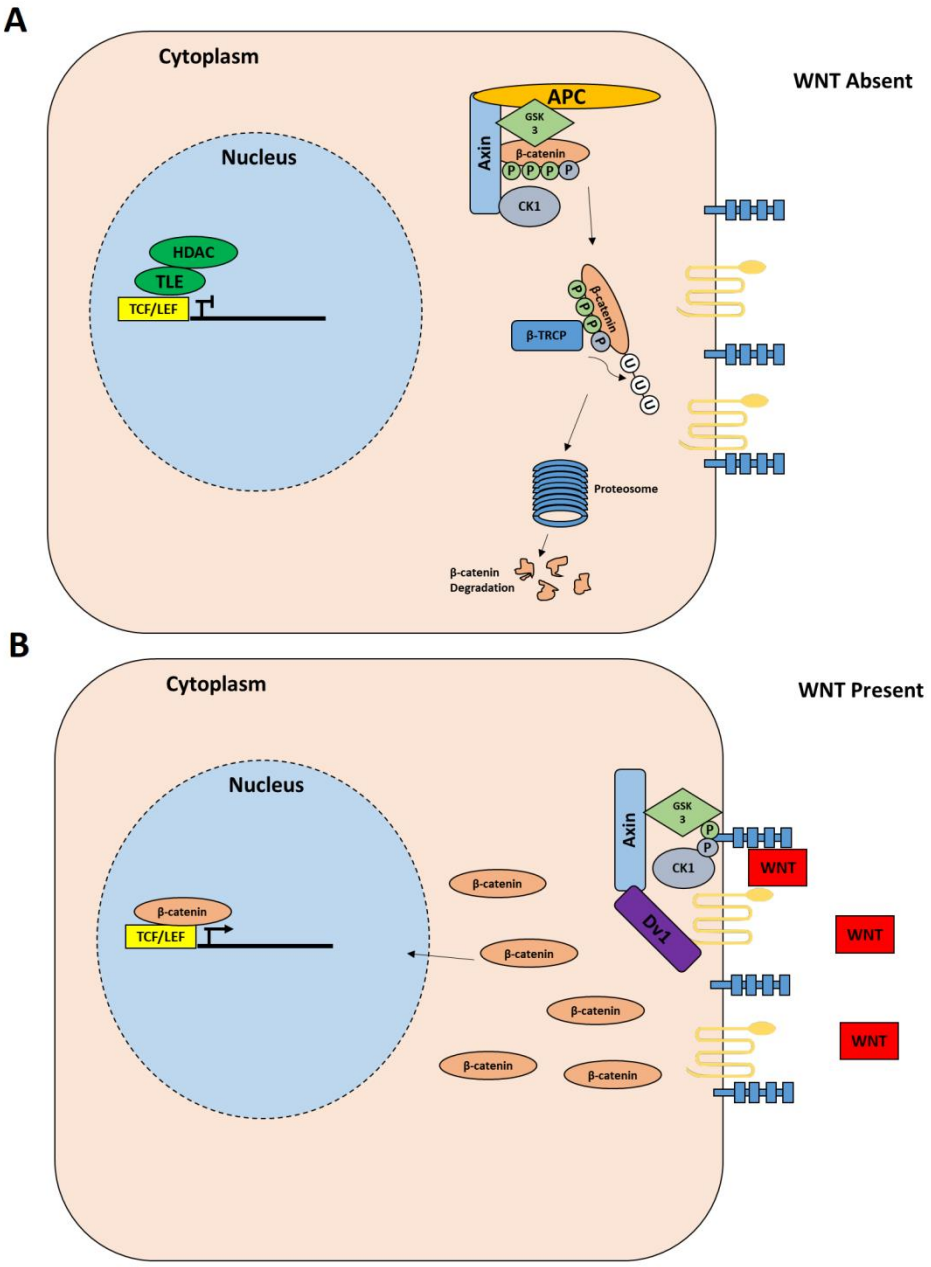

Figure 6-1. Canonical WNT signalling pathway.

A schematic representation of the canonical (ß-catenin dependent) WNT signalling pathway. (A) Signalling pathway in the absence of a WNT activator, resulting in the formation of the destruction complex and proteasomal degradation of ß-catenin preventing activation of downstream promoters. (B) Signalling pathway in the presence of a WNT activator (e.g. WNT3a) resulting in the stabilisation of ß-catenin and subsequent nuclear localisation binding to TCF/LEF promoters within the nucleus.

6.1.2 WNT in health and disease

The dysregulation of WNT is known to be involved in carcinogenesis and other diseases (Table 6-1). Most prominently, the APC gene, a suppressor of WNT signalling is commonly mutated in human cancers resulting in stabilisation of ß-catenin and subsequent activation of the pathway (Polakis, 2007). Additionally, Axin1 and Axin2 are also mutated in a number of human cancers, again due to the negative regulatory nature of the proteins on the WNT pathway, thus their dysregulation results in a subsequent activation of the pathway (Salahshor and Woodgett, 2005). One such Axin1 mutant showed a reduced binding of GSK3b preventing the formation of the destruction complex and another Axin1 substitution mutation interfered with Axin's interaction with Disheveled (Webster et al., 2000).

WNT has also been implicated in a number of bone diseases (Table 6-1). WNT activates osteoblasts and thus the inhibition or over activation of the pathway can result in abnormally low or high bone mass. This is evidenced by a loss-of-function mutation in LRP6 linked to osteoporosis (Mani et al., 2007), or a deleted Frizzled in patients diagnosed with Williams-Beuren syndrome, a disease characterised by low bone density (Wang et al., 1999). WNT dysregulation has also been associated in metabolic disease, particularly type II diabetes. Single nucleotide polymorphisms (SNPs) in TCF7L2 are a strong risk determinant for the disease (Tong et al., 2009).

Protein	Mutation Type	Associated Disease
PORCN	Loss-of-function	X-linked focal dermal hypoplasia
WNT3	Loss-of-function	Tetra-amelia
WNT4	Loss-of-function	Mullerian duct regression and virilisation
WNT5B	Loss-of-function	Type II diabetes
WNT7A	Loss-of-function	Fuhrmann syndrome
WNT10A	Loss-of-function	Odonto-onchyo-dermal hypoplasia
WNT10B	Loss-of-function	Obesity
RSPO1	Loss-of-function	XX sex reversal with palmoplantar hyperkeratosis
RSPO4	Loss-of-function	Autosomal-recessive anonychia and hyponychia congenital
SOST	Loss-of-function	High bone mass, sclerosteosis, Van Buchem disease
Norrin (NDP)	Loss-of-function	Famililal exudative vitreoretinopathy
LRP5	Gain-of-function	Hyperparathyroid tumors, High bone mass
LRP5	Loss-of-function	Osteoporosis-pseudoglioma, eye vascular effects
LRP6	Loss-of-function	Early coronary disease and osteoporosis
FZD4	Loss-of-function	Familial exudative vitreoretinopathy
FZD9	Loss-of-function	Williams-Beuren Syndrome
TSPAN12	Loss-of-function	Familial exudative vitreoretinopathy
APCDD1	Loss-of-function	Hereditary hypothrochosis simplex
Axin1	Loss-of-function	Caudal duplication, cancer
Axin2	Loss-of-function	Tooth agenesis, cancer
APC	Loss-of-function	Familial adenomatous polyposis, cancer
WTX	Loss-of-function	Wilms tumour, OCTS
B-catenin	Gain-of-function	Cancer
LEF1	Loss-of-function	Sebaceous skin tumour
TCF4	Gain-of-function	Type II diabetes, colon cancer

Table 6-1. Diseases associated with WNT component dysfunction.

6.1.3 Viral response to WNT signalling

While there are many studies implicating the WNT pathways importance in various viral infections, how these viruses utilise and interact with the WNT pathway to facilitate their replication and transmission is relatively unknown. There are however a number of proposed ways with which viruses can interact with the WNT pathway. The first is cellular or viral miRNAs targeting WNT genes. It has been shown that miR-34 family of miRNAs repress the WNT/ß-catenin signalling pathway and furthermore this repression has demonstrated strong anti-viral effects against a number of viruses including dengue virus (DENV), West Nile virus (WNV), ZIKV, alphaviruses and herpesviruses (Smith et al., 2017). There is indication that the WNT signalling pathway can influence the type-1 interferon pathway in response to viral infection. This cross-talk between signalling pathways occurs with phosphorylated GSK3ß interacting with TBK1, however in the activation of the WNT pathway, GSK3 ßs recruitment to the cell surface receptors prevents further phosphorylation of TBK1, reducing downstream IRF3 phosphorylation and a reduction in IFN stimulation (Wang et al., 2008). This is hypothesised to function as a negative feedback loop preventing overstimulation of the host inflammatory response. Inhibition of WNT signalling, in the case of the microRNA miR-34, enhances IFN stimulation (Smith et al., 2017). Furthermore, inhibition of GSK3ß by LiCl leads to the enhancement of IFN-ß (Marcato et al., 2016). However, a further study has indicated this is mediated through TCF/ ß-catenin complexes rather than IRF3 previously suggested (Wang et al., 2013).

The second method in which viruses can affect WNT signalling is through inhibition or activation at the epigenetic level. Aberrant WNT signalling caused by many viruses including hepatitis B virus (HBV) and Epstein-Barr viruses are thought to be a key component in carcinogenesis. In HBV infection, the downregulation of secreted frizzled-related proteins (SFRPs), antagonists of WNT signalling, facilitated through the binding of hepatitis B X protein (HBx) resulted in the activation of WNT pathway and further hepatocarcinogenesis (Xie et al., 2014).

Viruses can also relocalise ß-catenin or other WNT pathway components preventing or increasing downstream activation. In porcine circovirus-like virus

P1 infection, WNT is inhibited through expression of a VP1 protein that prevents ß-catenin from entering the nucleus and accessing the TCF/LEF promoters (Zhu et al., 2018). Additionally hepatitis C virus (HCV) core protein and non-structural 4B protein (NS4B) were shown to enhance the nuclear translocation of ß-catenin thereby enhancing WNT gene transcription (Jiang et al., 2017).

Finally, viruses can also directly interact with WNT pathway components, inhibiting or activating downstream WNT. In Karposi-Sarcoma Herpesvirus (KSHV) it has been shown that the viral protein kinase (vPK) interacts with ß-catenin directly reducing its affinity to bind to TCF binding sites resulting in reduced mRNA of downstream WNT products (Cha et al., 2018).

There are a number of other studies that have not identified a mechanism for the interaction of the virus with the WNT pathway, however, have determined that the pathway is important for viral replication. Influenza A virus has been shown to have significantly increased replication with WNT activated by Wnt3a, and has been shown to have a marked reduction in replication in ß-catenin knockout cells or with the use of iCRT14 Wnt inhibitor, an inhibitor that targets the interaction between ß-catenin and TCF4 (More et al., 2018).

The interactions between RVFV nucleocapsid protein and host proteins are a promising target for antiviral therapies due to the decreased likelihood of resistance developing. The low rate of genetic change within host cells, coupled with the highly conserved nature of the nucleocapsid protein may result in a longer period of effectiveness for targeting therapeutics. Additionally, by targeting host proteins it massively increases the repertoire of therapeutic targets and may allow the discovery of broad acting drugs that disrupt interactions across different virus genus or families.

6.2 Results

6.2.1 RVFV N proteomics studies reveals new interactions

To investigate the interaction partners of RVFV N, an immunoprecipitation of N using an anti-N antibody was performed 16 hours post infection from RVFV MP12-infected A549 cells. The control immunoprecipitation was performed on uninfected cells using the same anti-N antibody (Brennan et al., 2011b). Following pulldown, triplicate samples were analysed by mass spectrometry to identify host proteins captured by RVFV N. Using a label free quantification approach, analysed by MaxQuant, we identified 24 potential protein interactors (Table 6-2), determined by the presence of at least two peptides of the potential interactor in 3 or more infected samples and absent or reduced quantities in control samples. Along with host protein interactions, N also interacted with the viral proteins L, Gn and NSs to varying degrees, as was expected. By using the protein-protein interaction database STRING to analyse any potential complexes or interactions between the identified proteins we selected a smaller panel of proteins to investigate further (Figure 6-2). Many of the host interactors included ribosomal proteins and heat shock proteins that are often found in proteomic studies of RNA viruses. The smaller selected panel of proteins included: Scaffold attachment factor B (SAFB), Annexin A1 (ANXA1), Annexin A2 (ANXA2), Polyadenylate binding protein 1 (PABP1), Polyadenylate binding protein 4 (PABP4) and ß-catenin (CTNB1).

Protein Interactor	Abbreviation	Average RVFV LFQ Intensity	Average Negative Control LFQ Intensity	Ratio
Annexin A1	ANXA1	7545908.333	0	N/A
Protein S100-A8	S100A8	3629366.667	0	N/A
Heat shock protein beta-1	HSPB1	2456790	0	N/A
Zinc finger protein Rlf	RLF	1472300	0	N/A
Protein S100-A9	S100A9	1256713.333	0	N/A
Heterogeneous nuclear ribonucleoprotein H	HRNRPH1	898650	0	N/A
Dermcidin	DCD	805200	0	N/A
Histone H3.2	HIST2H3A	664940	0	N/A
Annexin A2	ANXA2	487846.6667	0	N/A
Histone H3.3	H3F3A	450430	0	N/A
60S ribosomal protein L15	RPL15	412100	0	N/A
Polyadenylate-binding protein 4	PABPC4 (PABP4)	395853.3333	0	N/A
Catenin beta-1	CTNNB1 (CTNB1)	393190	0	N/A
Scaffold attachment factor B1	SAFB2	294216.6667	0	N/A
Polyadenylate-binding protein 1	PABPC1 (PABP1)	11668633	313250	37.25023
Heterogeneous nuclear ribonucleoproteins A2/B1	HNRNPA2/B1	1012630	267973.3	3.778846
Putative uncharacterized protein PSMG3-AS1	PSMG3-AS1	10661000	5119400	2.082471
Histidine-rich glycoprotein	HRG	3766067	1826967	2.061377
Uncharacterized protein KIAA1671	KIAA1671	4.59E+08	2.7E+08	1.702327
Heterogeneous nuclear ribonucleoproteins C1/C2	HNRNPC1/C2	10039533	6163383	1.6289
Heterogeneous nuclear ribonucleoprotein M	HNRNPM	2412933	1557940	1.548797

Table 6-2. Potential interaction partners of RVFV N protein.

Protein interactions identified by Mass-spectrometry using a label-free quantification approach. LFQ intensities shown are the average of three experimental repeats. Full proteomics data available via ProteomeXchange (Project accession: PXD010423).

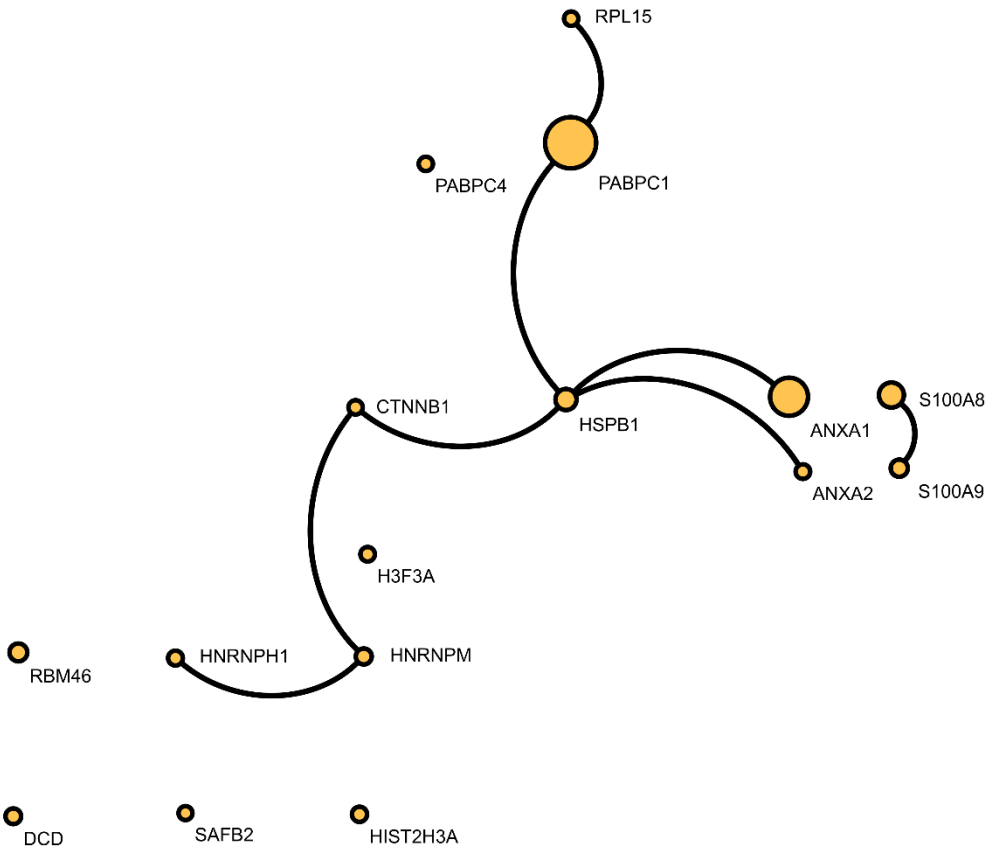

Figure 6-2. Cytoscape interaction diagram of RVFV N protein.

A549 cells were infected with RVFV MP12 at MOI 5 and immunoprecipitated using anti-N rabbit polyclonal antibody 16 hpi. Potential interactors were determined by evaluating LFQ intensities 30 fold or greater in infected samples compared with samples from uninfected cells. Interactions were assessed by STRING analysis, with each link representing a potential interaction identified through experimentation. The size of nodes indicates relative abundance of protein.

6.2.2 siRNA screen of potential interactors

The effect of potential protein interactions on viral replication was assessed by utilising an siRNA screen targeted against the panel of interactors. A549 cells were transfected with siRNA targeting each protein interactor, 72 hours post transfection cells were infected with *Renilla* luciferase expressing RVFV MP12delNSs:*hRen* at MOI 0.01. Luciferase values were assessed 24 hours post infection. The interactions with CTNB1, ANXA1, ANXA2, PABP1 and SAFB were all important for the replication of the virus and showed significant reduction in luciferase, however the silencing of PABP4 and DCD showed no effect on the reporter virus (Figure 6-3).

Additionally, an siRNA screen was performed using the T7 RNA polymerase based minigenome system in Huh-T7-Lunet cells to evaluate the impact of protein interactions on the formation of RNP complexes specifically (Figure 6-4). Huh-T7-Lunet cells were transfected with siRNAs targeting each protein interactor. After 24 hours, cells were transfected with pTM1 N, pTM1 L, pTVT7-GM:*hRen* and pTM1-FF-Luc. At 24 hours post transfection, cells were harvested and luciferase measured. The variability of the minigenome activity resulted in no significance of knockdown interactors; however, there was a trend for silencing of Anxa1, PABP4 and SAFB to have a reducing effect on the luciferase levels in the minigenome system.

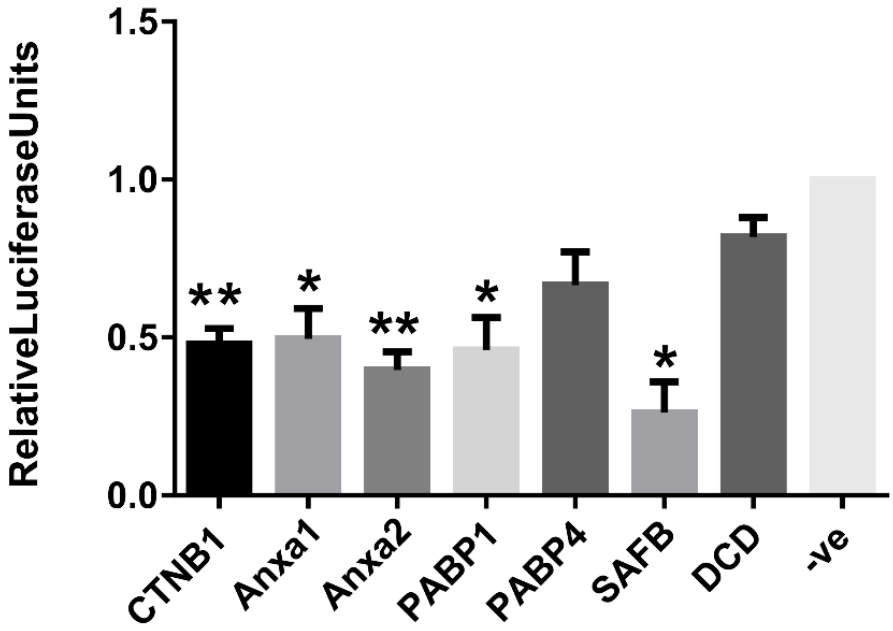

Figure 6-3. siRNA screen of potential N protein interactors infected with RVFV reporter

A549 cells were transfected with gene specific siRNAs or negative siRNA (-ve) for 72 hours before infection with RVFV MP12delNSs:*Rluc* reporter virus at MOI 0.01. Values of triplicate experiments were normalised to scrambled siRNA control. *denotes $p<0.05$, **$p<0.001$ using Student's T-test.

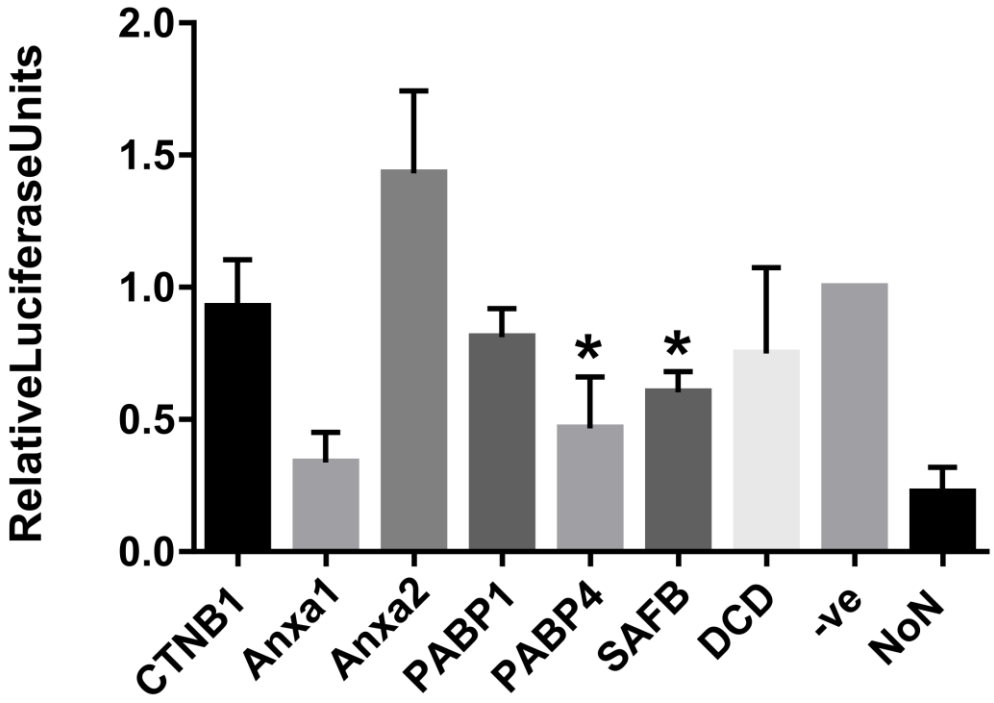

Figure 6-4. siRNA screen of potential N protein interactors utilising an RVFV minigenome system.

Huh-T7-Lunet cells were transfected with gene specific siRNAs or negative siRNA (-ve). At 24 hours post transfection with siRNA, cells were further transfected with RVFV pTM1 N, pTM1 L, pTVT7-GM:*hRen* and pTM1-FF-Luc. After 24 hours, cells were lysed and luciferase values measured. Values of triplicate experiments presented were normalised to negative siRNA control. Significance was determined by Student t-test were * denotes $p<0.05$.

6.2.3 RVFV impact on the Wnt pathway

Evaluation of previous literature and ß-catenin's impact in the siRNA screen on RVFV replication indicated that ß-catenin indeed does play a role in RVFV infection (Harmon et al., 2016). Thus, to investigate RVFV's role and influence on the canonical Wnt signalling pathway, of which ß-catenin is the main effector molecule (6.1.1), a TOPFlash (TF) system was employed. TOPFlash reporter plasmid utilises a pTA-Luc (Clontech) backbone with 7 TCF/LEF (AGATCAAAGG) binding sites, with a 5 nucleotide (GGGTA) spacer between each site driving the expression of the firefly luciferase gene (Veeman et al., 2003). Stable ß-catenin, upon WNT pathway activation, binds to TCF/LEF promoters driving firefly expression resulting in measurable luciferase.

A549, Huh-T7-Lunet and HEK 293FT cells were transfected with TF for 24 hours and subsequently infected with RVFV MP12 or eGFP expressing RVFV MP12delNSs:eGFP at MOI 1. The MP12delNSs:eGFP was used to determine the effects of NSs on the WNT pathway and to reduce the effects of general host transcriptional shut down on the assay. Cells were lysed and luminescence measured at 7 and 24 hours post infection. All three cell lines showed reduction in luciferase activity after both 7 and 24 hours (Figure 6-5). A549 cells displayed moderate reduction in activity after 7 hours and had significantly reduced activity compared with uninfected cells 24 hours post infection using both RVFV MP12 and RVFV MP12delNSs:eGFP, the former displaying slightly higher reduction in activity. Infection in both Huh-T7-Lunet and HEK 293FT cells resulted in significant inhibition of the WNT pathway at 7 and 24 hours post infection with both RVFV MP12 and RVFV MP12delNSs:eGFP.

Furthermore, to determine if the inhibition of WNT was an RVFV specific effect or could be a characteristic of bunyaviruses in general, A549, Huh-T7-Lunet and HEK 293FT cells were transfected with TF for 24 hours and subsequently infected with BUNV or BUNVdelNSs at MOI 1. At 7 and 24 hours post infection, cells were lysed, and luciferase measured (Figure 6-6). Interestingly, there was a more varied cell specific effect. In A549 infection, BUNV showed significant reduction in the WNT pathway only after 24 hours, and this effect was not observed with BUNVdelNSs. However, in Huh-T7-Lunets there appeared to be a discreet activation of the pathway for BUNVdelNSs after 7 hours, however after 24 hours

both BUNV and BUNVdelNSs showed significant inhibition of the WNT pathway. In HEK 293FT cells, neither BUNV nor BUNVdelNSs showed significant inhibition of the pathway after 7 or 24 hours.

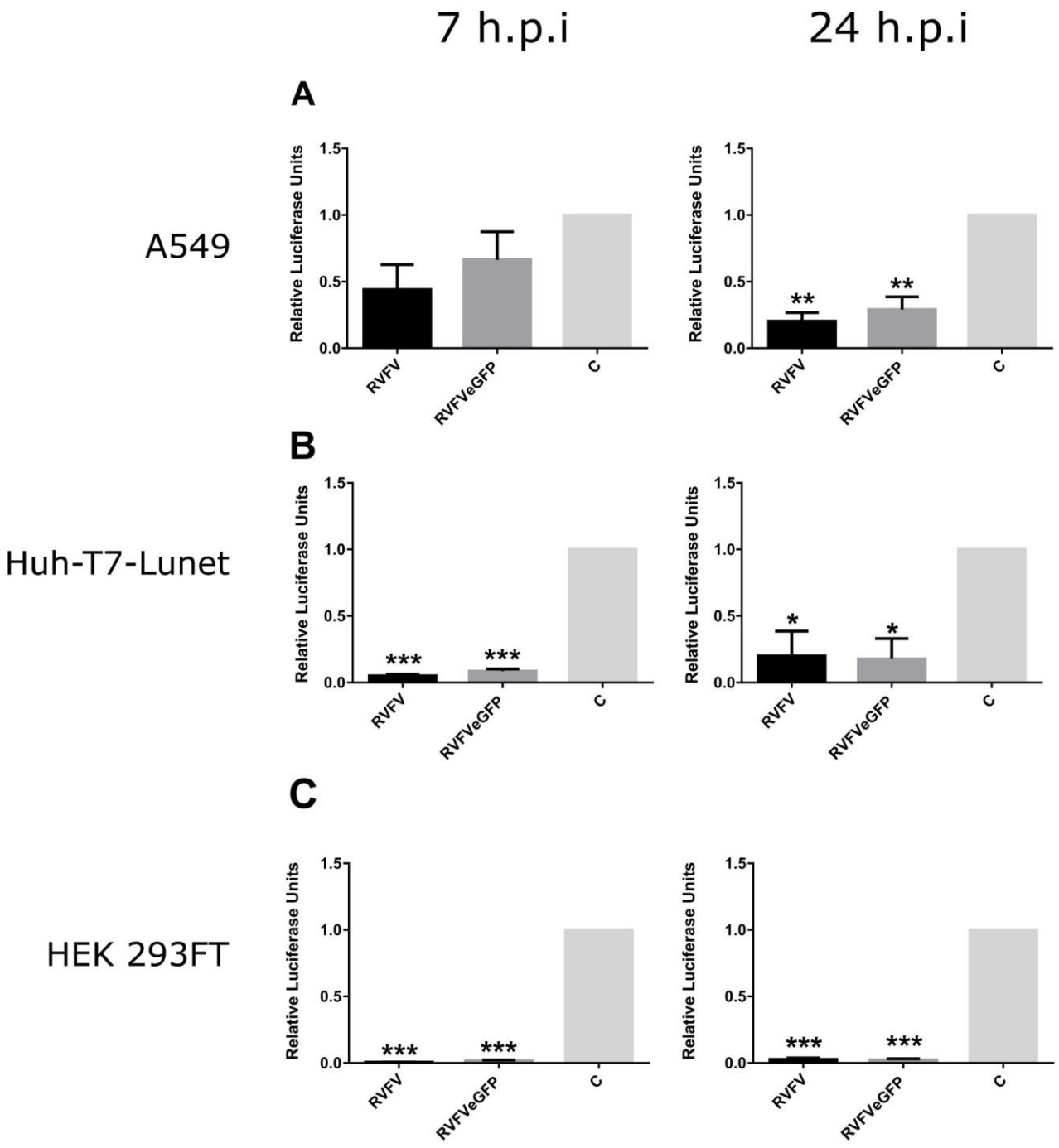

Figure 6-5. RVFV infection inhibits TOPFlash reporter activity in multiple cell types.

(A) A549, (B) Huh-T7-Lunet and (C) HEK 293FT cells were transfected with TCF/LEF WNT pathway reporter plasmid TOPFlash. At 24 hours post transfection, cells were infected with RVFV MP12 (RVFV), RVFV MP12delNSs:eGFP (RVFVeGFP) or mock (C) at MOI 1. Cells were lysed at 7 h (left panel) and 24 h (right panel) post infection and luciferase measured. Values of triplicate experiments were normalised to mock infected cells. *denotes $p<0.05$, **$p<0.001$, ***$p<0.0001$ using Student's T test.

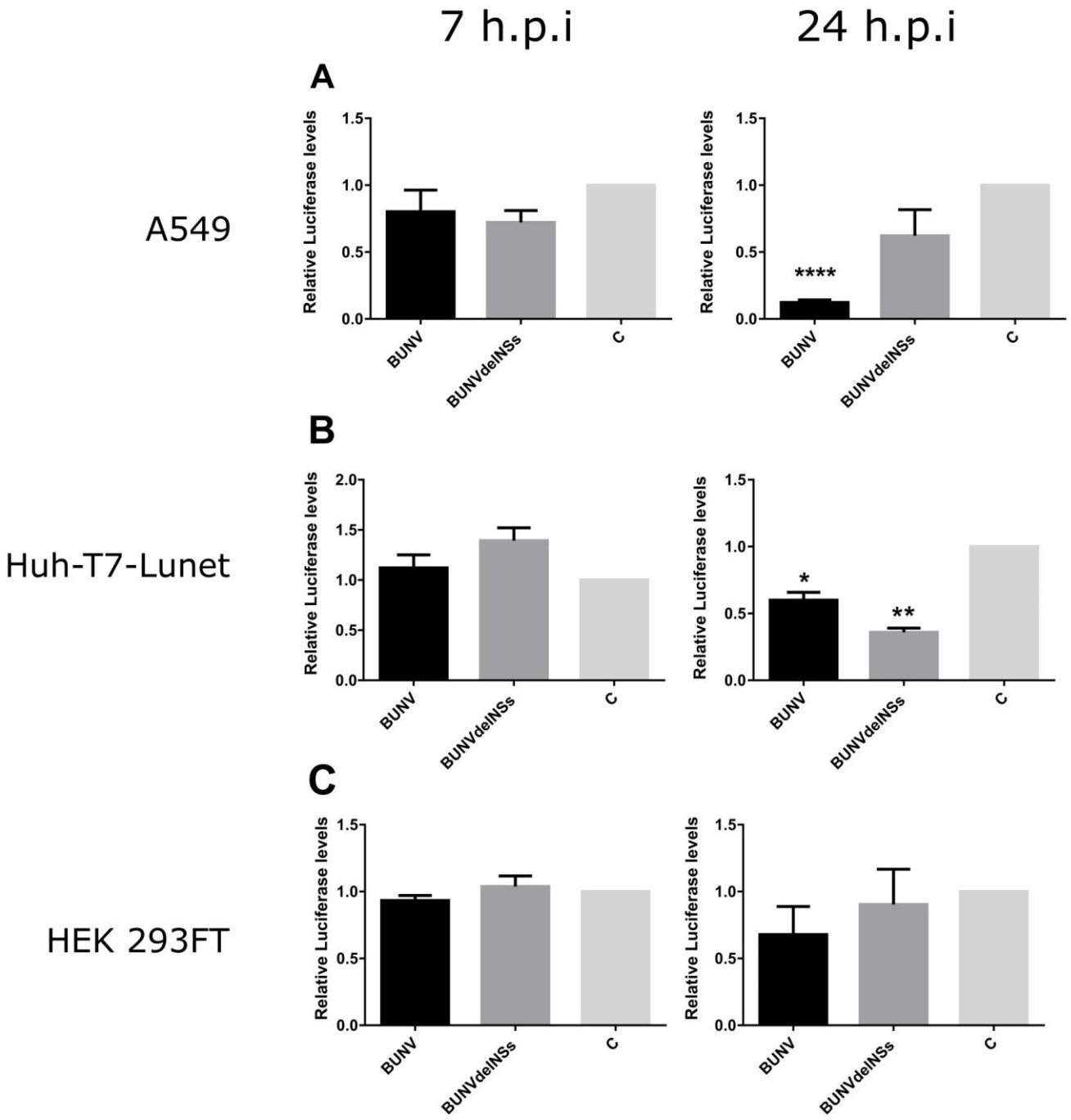

Figure 6-6. BUNV- specific inhibition of TOPFlash activity.

The three cell types, A549s (A), Huh-T7-Lunets (B) and HEK 293FTs (C) were transfected with the TOPFlash WNT activity reporter plasmid. At 24 hours post transfection cells were infected with BUNV, BUNVdelNSs or mock infected (C). At 7 h (left panel) and 24 h (right panel) post infection the cells were harvested and luciferase measured. Values of triplicate experiments were normalised to mock infected (C). *denotes $P<0.05$, **$P<0.001$, ****$P<0.00001$ determined by Student's T-test.

By utilising RVFV MP12delNSs:*hRen*, a reporter virus expressing *Renilla* luciferase in place of the NSs gene, it was possible to further determine the importance of ß-catenin for RVFV replication. Additionally, the generation of ß-catenin KO A549 cells provides confirmation of knockout and thus additional evidence that RVFV requires ß-catenin for successful replication. A549 ß-catenin KO and A549 control cells were treated with PBS/FBS or Wnt3a recombinant activator 1 hour pre-infection. Subsequently, cells were infected with RVFV MP12delNSs:*hRen* at MOI 0.01 (Figure 6-7). After 7, 24 and 48 hours cells were lysed and luminescence measured. After 7 hours, there was no effect on the replication of RVFV MP12delNSs:*hRen* by either the pre-activation or inhibition of the WNT pathway. At 24 hours post infection, RVFV showed reduced *Renilla* luciferase activity in A549 ß-catenin KO cells as compared to control. However, the activation with Wnt3a did not affect viral replication. Interestingly, at 48 hours post infection, there was a further decrease in viral replication in ß-catenin KO cells compared with control but also there was a significant yet mild increase in replication within cells treated with Wnt3a.

Furthermore, it was important to assess the effect of ß-catenin knockdown or activation on BUNV, to evaluate if the effect seen in RVFV is virus specific or can be seen in another virus family (Figure 6-8). A549 cells were transfected with siRNA targeting ß-catenin or treated with Wnt3a recombinant activator. At 72 hours post transfection, cells were infected with BUNV-expressing Nanoluc luciferase at MOI 1. At 24 hours post infection, cells were lysed and luciferase measured. Interestingly, the knockdown of ß-catenin or the activation of the WNT pathway had no effect on BUNV viral replication.

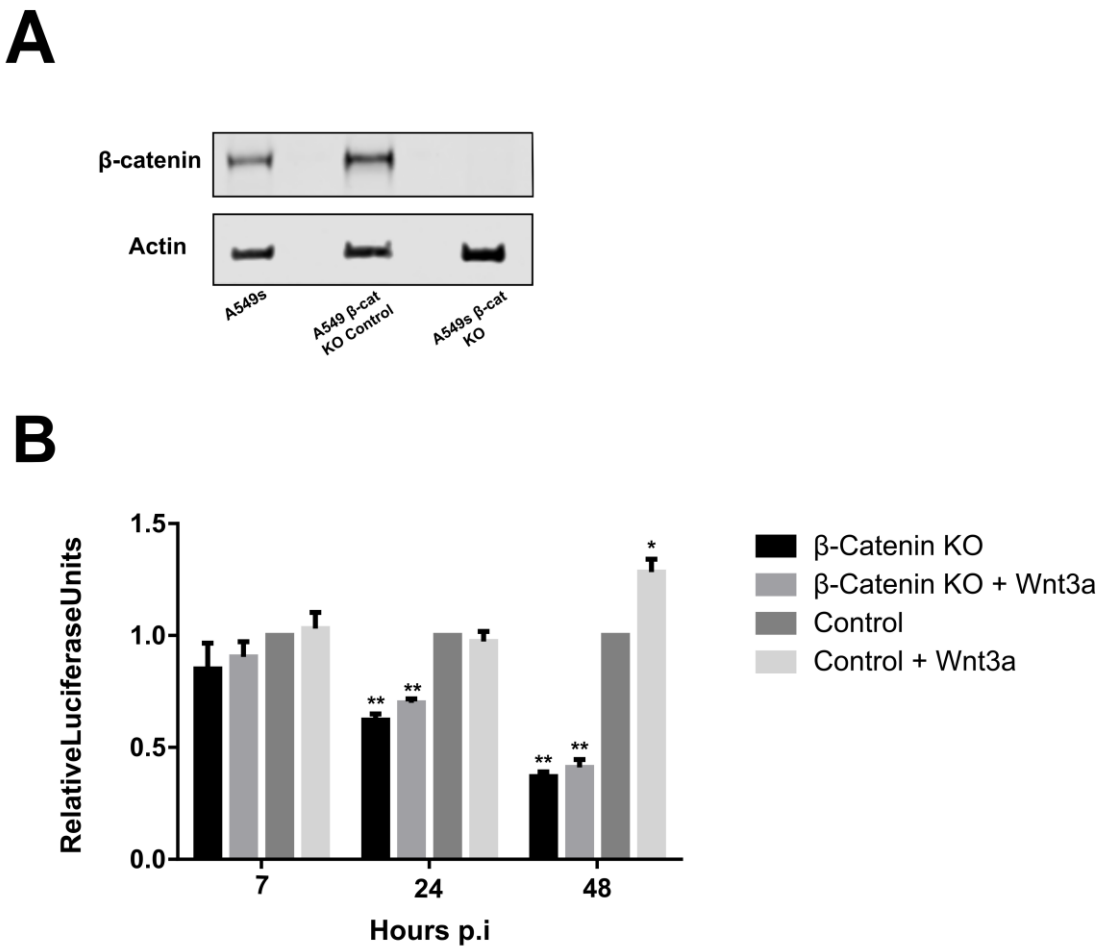

Figure 6-7. β-catenin knockout reduces RVFV reporter infection

(A) Western blot of A549 β-catenin KO and A549 β-catenin KO control cells. β-catenin was knocked out using CRISPR/Cas9 and single cell populations selected. Negative control cells contain non-functional lentiviral cassette. Representative image of three experimental repeats shown. (B) A549 β-catenin knockout or control cells were pre-treated 1 hour prior to infection with Wnt3a activator or with PBS/FBS mix. Cells were subsequently infected with RVFV MP12delNSs:*hRen* at MOI 0.01. After 7, 24 or 48 hours post infection cells were lysed and luciferase measured. Values of triplicate experiments were normalised to mock treated A549 β-catenin KO control cells separately for each time point. *denotes $p<0.05$, **$p<0.001$ using Student's T-test.

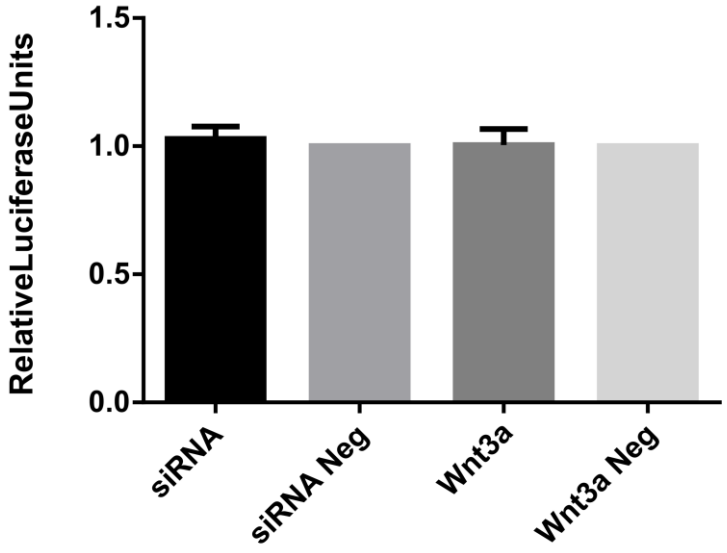

Figure 6-8. Effects of Knockdown or activation of WNT on BUNV infection

A549 cells were transfected with siRNA, negative siRNA or treated with Wnt3a activator or PBS/FBS mix (Neg) 24 hours prior to infection. Cells were subsequently infected with BUNV Nanoluc and at 24 hours post infection, cells were lysed and luciferase measured. Values of triplicate experiments were normalised to Wnt3a negative control.

It has been hypothesised that RVFVs inhibition of the WNT pathway may be an effect of general cell death rather than specific pathway inhibition. Thus, a cell viability assay was performed (Figure 6-9). A549, Huh-T7-Lunet and HEK 293FT cells were infected with RVFV MP12, RVFV MP12delNSs:eGFP, Mock or treated with 2 µg/ml puromycin. At 7 hours and 24 hours post infection, luciferase based cell viability assay was measured. After 7 hours, there was no evidence of cell death in A549s, Huh-T7-Lunets or HEK293 FTs infected with either RVFV MP12 or the delNSs virus. At 24 hours post infection, there was evidence of gradual minor cell death in A549s and Huh-T7-Lunets infected with RVFV MP12 and RVFV MP12delNSs:eGFP. There appeared to be more significant cell death in HEK 293FT cells when infected with RVFV MP12 however the effect was less pronounced in RVFV MP12delNSs:eGFP infected cells.

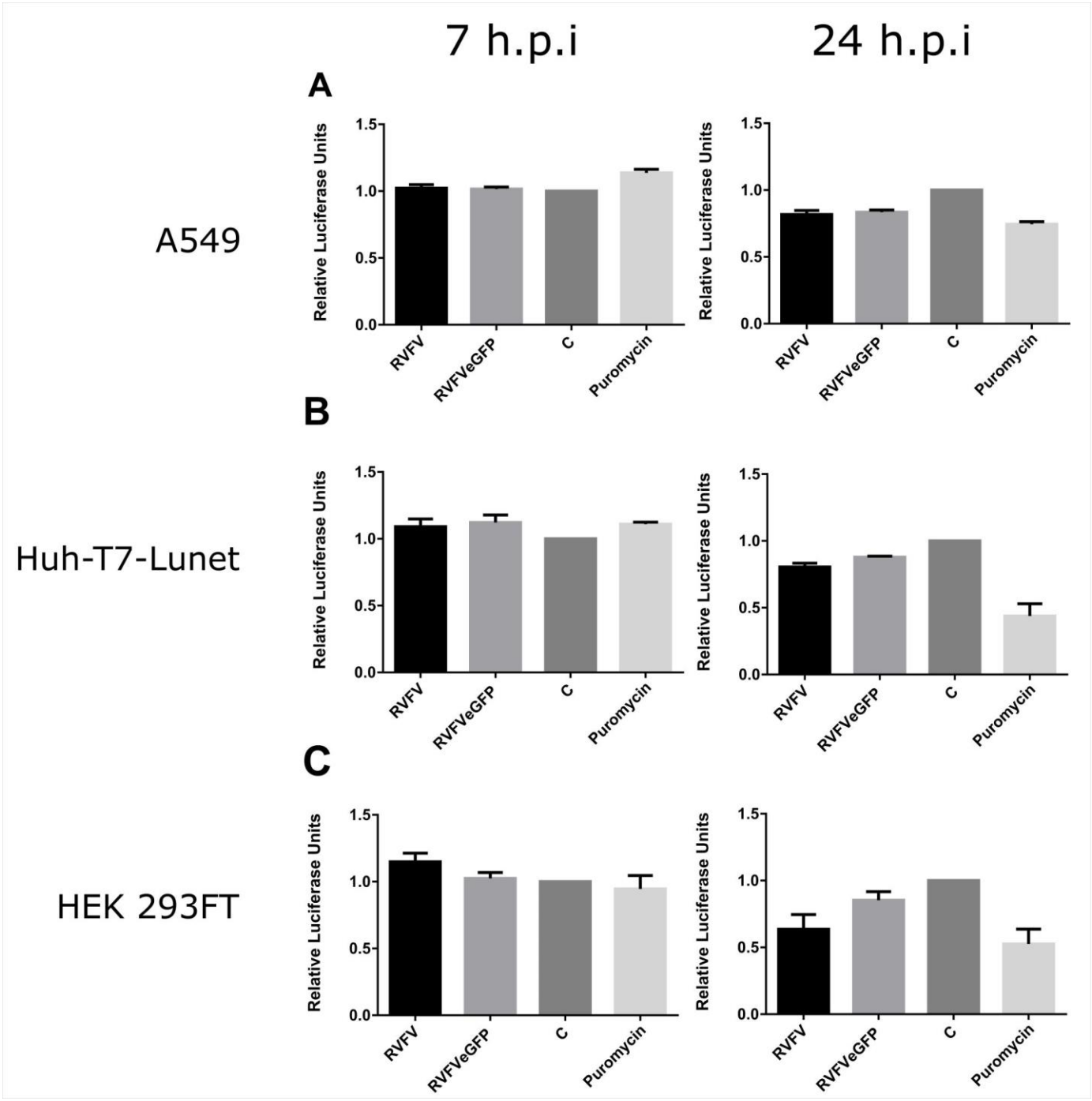

Figure 6-9. Viability of RVFV and RVFVdelNSs:eGFP infected cells

(A) A549s, (B) Huh-T7-Lunets and (C) HEK 293FTs were infected with RVFV MP12, RVFV MP12delNSs:eGFP, Mock infected at MOI 1 or treated with Puromycin. After 7 h (left panel) or 24 h (right panel) cells were harvested and luciferase measured. Values of triplicate experiments shown. No significance was determined by Student t-test.

The interaction between ß-catenin and RVFV appears to have a proviral effect on replication, in addition to proteomics data suggesting a direct interaction with the nucleoprotein, suggested that there may be co-localisation between RVFV N, RNP complexes and ß-catenin. A549 cells were infected with RVFV MP12 or RVFV MP12delNSs:eGFP at MOI 1. At 24 hours post infection, cells were fixed and probed with anti-N rabbit polyclonal antibody and anti-ß-catenin mouse monoclonal antibody. There was no evidence of direct co-localisation between ß-catenin and RVFV N (Figure 6-10). There was however distinct relocalisation of ß-catenin from the plasma membrane to a diffuse pattern across the cytoplasm.

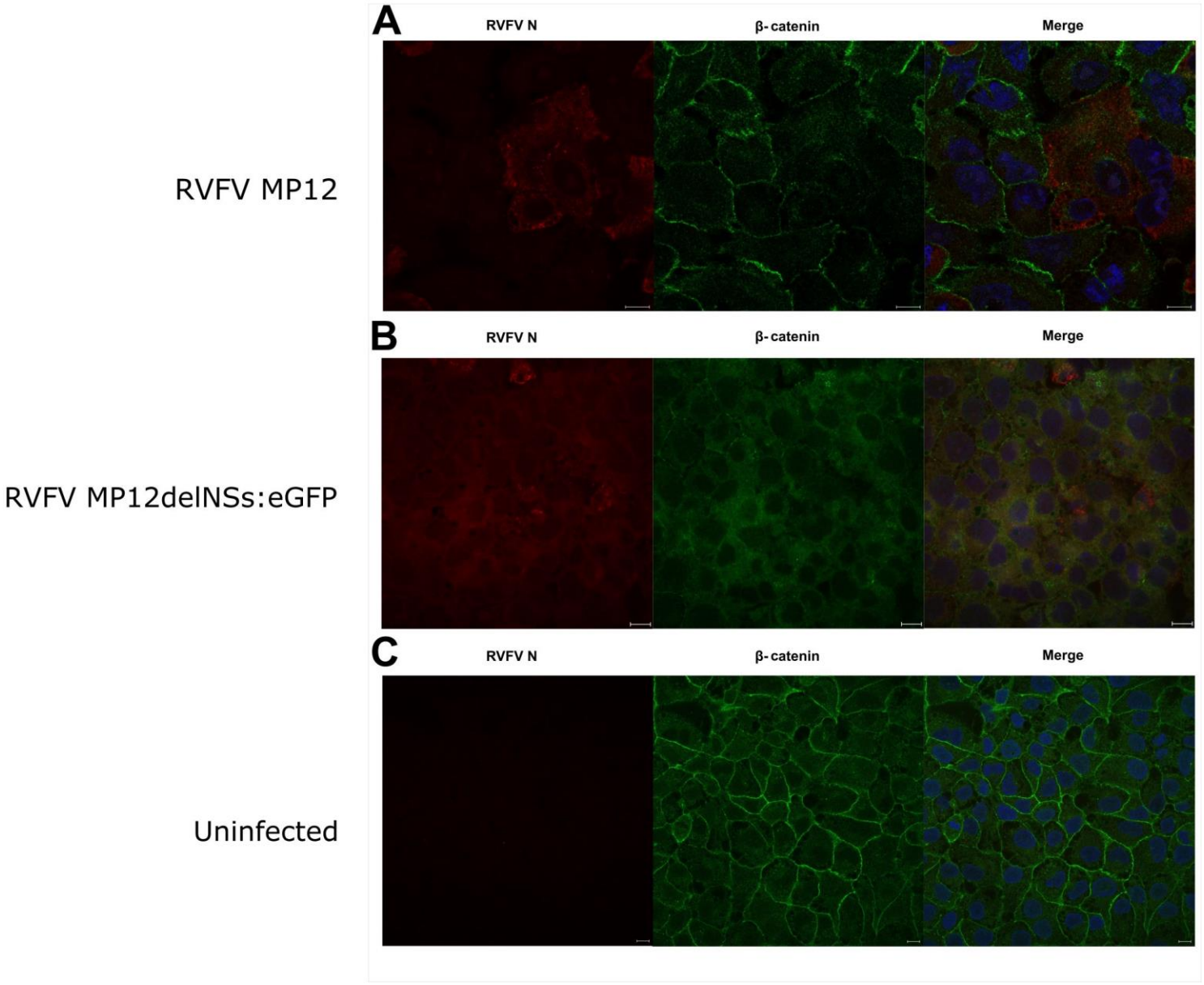

Figure 6-10. β-catenin localisation during RVFV infection.

(A) A549 cells infected with RVFV MP12 at MOI 1, cross-section displaying side by side comparison of infected and uninfected cells. (B) A549 cells infected with RVFV MP12delNSs:eGFP at MOI 1. (C) Uninfected A549 cells. RVFV MP12 N shown in red, β-catenin is shown in green and DRAQ7 DNA nuclear dye in blue. Representative images shown of three experiments.

6.3 Discussion

The mutagenesis study carried out during this project indicated there may be novel protein-protein interactions between N and host proteins that may involve residues located on surface of N. The proteomics study here identified a number of interesting and intriguing interactions. Annexin A1 (ANXA1) is involved in the innate immune response as an effector of glucocorticoid-mediated responses and as a regulator of the inflammatory response. Additionally, ANXA1 contributes to the adaptive immune response by enhancing signalling cascades triggered by T-cell activation, and further T-cell differentiation and proliferation. ANXA1 has also been implicated in the reorganization of the actin cytoskeleton, endosomal trafficking and apoptosis. ANXA1 has been implicated as an important host protein interactor for a number of viruses. For example, influenza A replication is enhanced in the presence of ANXA1. ANXA1 co-localises with early and late endosomes near the nucleus and has been shown to enhance trafficking of the virus to the nucleus evidenced from increased nuclear accumulation of viral nucleoprotein (Arora et al., 2016). ANXA1 was also identified in a proteomic screen of HIV infected cells, however there was no further study about its effects (Pathak et al., 2009). Interestingly, a study of HCV susceptibility of different liver cell types showed that HCV virus production was significantly reduced in cell lines stably expressing exogenous ANXA1. The study further demonstrated that ANXA1 specifically inhibits HCV RNA replication (Hiramoto et al., 2015). This indicates that ANXA1 does not have a specific proviral or antiviral function and therefore each viral species may interact with ANXA1 in different ways.

Annexin A2 (ANXA2) was also a potential interactor of RVFV N as evidenced from the proteomic study. It has a wide array of functions, primarily the linking of membrane complexes with the actin cytoskeleton and the exocytosis of intracellular proteins. ANXA2 has been shown to form complexes with S100A10 on the cell surface of macrophages and is important for HIV-1 infection of macrophages through the binding of HIV-1 gag proteins. The silencing of ANXA2 by RNAi significantly inhibits HIV-1 infection (Ryzhova et al., 2006, Woodham et al., 2016). In HPV-16 infection, the S100A10 heterotetramer with ANXA2 is required for entry into HeLa cells, as evidenced by small molecule inhibitors ability to block this interaction (Woodham et al., 2015). ANXA2 was shown to

interact with classical swine fever virus (CSFV) glycoprotein E2 and the silencing of ANXA2 reduced viral replication whereas overexpression enhanced replication. However, RNA replication was not affected and the binding to CSFV NS5A implicated ANXA2 as being involved in viral assembly (Sheng et al., 2015). ANXA2s interaction has also been hypothesised to be associated with CSFV cellular entry (Yang et al., 2015). ANXA2 has also been identified as a RNA binding protein involved in modulating frameshift activity in Infectious Bronchitis Virus (IFV) infection (Kwak et al., 2011).

Poly(A) binding protein 1 (PABP1) has been previously identified as an important protein within RVFV infection. PABP1 was shown to relocalise to the nucleus upon RVFV infection through the interaction with non-structural protein S (NSs). An siRNA screen showed no change in RVFV positive cells, however, the sequestration of PABP1 was hypothesised to influence the cellular environment to promote viral protein production (Copeland et al., 2013). This relocalisation is considered to block mRNA export, an important host cell process and targeted by many viruses (Copeland et al., 2015). The mechanism of interaction between NSs, PABP1 and host cell mRNA relocalisation has not been elucidated, however, it was observed that N alone was able to alter mRNA localisation though this was hypothesised to be an artefact (Copeland et al., 2015). With further evidence of direct PABP1 and N interaction, there may be another avenue of study to assess mRNA export mechanisms during RVFV infection.

The interaction with Poly(A) binding protein 4 (PABP4), eukaryotic initiation factor (eIF4E) and eukaryotic initiation factor 4G (eIF4G) is important for efficient translation of 5’ capped and 3’ poly(A) tailed cellular mRNAs. Viruses often have distinct mechanisms to initiate translation within host cells, such as the utilisation of a highly structured 3’ untranslated region (UTR) that functionally replaces the poly(A) tail of some positive stranded RNA viruses (Edgil et al., 2003). The UTR regions of the negative-stranded BUNV have also been shown to mediate efficient translation of viral mRNAs though this interaction is independent of PABP (Blakqori et al., 2009).

Scaffold attachment factor B (SAFB) functions as a nuclear matrix protein (NMP) that binds to scaffold or matrix attachment region DNA elements (S/MAR DNA), thus, it is thought to be important in assembling a transcriptome complex near

actively transcribed genes (Debril et al., 2005). They have also been implicated in a number of cellular processes including chromatin organization, transcriptional regulation, stress response and RNA splicing (Oesterreich, 2003). There is limited documentation on any interaction between viral infections and SAFB, however, it has been shown to be a target of the immediate-early protein BICP22 in bovine herpesvirus 1 infection (Saydam et al., 2006).

The antimicrobial peptide Dermicidin (DCD) was found to be an interactor, though likely to be a contaminant, and was thus chosen as a likely negative control for further interaction studies. DCD is an antimicrobial peptide secreted by sweat glands and transported to the epidermal surface to disrupt the colonization of early skin pathogens (Schittek et al., 2001). DCD has been found previously in viral proteomics of HIV host protein interactors, though no further study was conducted (Pathak et al., 2009). Additionally, DCD was found to be upregulated in influenza A infection of A549 cells (Coombs et al., 2010).

Lastly, the effector molecule of the WNT signalling pathway, ß-catenin, was identified within this proteomics study as an interactor of RVFV N protein. As mentioned previously, the WNT signalling pathway is important for a number of key cellular processes such as cell homeostasis and it affects over 100 downstream genes. The disruption of the WNT pathway has been implicated in cancer, tumorigenesis and metabolic diseases (Reya and Clevers, 2005, Kanazawa et al., 2004).

The identification of ß-catenin, ANXA1, ANXA2, PABP1, PABP4 and SAFB as important for viral infection was a significant finding. The previous identification of PABP4 and ß-catenin as being involved in RVFV replication validates the proteomic results whilst uncovering new information. This provides a number of avenues with which to pursue elucidating the interactions of RVFV N protein. A comparison between the RVFV reporter virus siRNA screen and the minigenome screen may indicate a more significant involvement of PABP4 and SAFB on the actual formation of the RNP complexes, whereas it is more likely ANXA2 is involved in entry/exit processes not evaluated in the minigenome assay. The minigenome siRNA screens general lack of significance may be a result of a number of factors worthy of further investigations. The siRNA transfection was performed for 24 hours, which may not be sufficient time for full knockdown, as

evidenced from siRNA of ß-catenin which required a minimum of 70 hours post transfection of siRNAs to reach a sufficient level of knockdown. Additionally, the difference in cell types may further suggest cell specific interactions identified.

The focus of this study on ß-catenin was primarily due to previous studies identifying the importance of the protein for RVFV infection, and the abundance of high quality molecular tools to help evaluate the interaction. A whole genome siRNA screen identified the knockdown of ß-catenin to result in a significant reduction in viral replication (Harmon et al., 2016). Thus, the full knockout of ß-catenin and siRNA screen knockdown provided further evidence that ß-catenin plays a role in the RVFV replication cycle. Additionally, Harmon *et al* identified small molecule inhibitors IWR-1 and JW67 that stabilise the ß-catenin destruction complex and through this action reduce ß-catenin levels and therefore reduce RVFV replication. In our study, we showed that activation of the pathway has a minor effect on RVFV replication after 48 hours. Further assessment of RVFV MP12 viral titre in the presence of WNT3a may be important. Particularly as there may be a more pronounced positive effect on viral replication, due to the increased inhibition of the WNT pathway of RVFV compared to RVFVdelNSs:eGFP. Interestingly, this effect is RVFV specific and does not extend to the *Orthobunyavirus* genus, as BUNV shows no change in replication dynamics in ß-catenin knockdown cells or upon activation of the WNT pathway with Wnt3a activator (Figure 6-8). Further study may investigate other members of the *Phlebovirus* genus, such as the closely related TOSV or members of the tick-borne group, UUKV or SFTSV. Evaluating the effect on other phleboviruses may provide opportunities to test WNT pathway inhibitors as therapeutics upon phlebovirus infection, or may be a factor differentiating phleboviruses from other members of the *Phenuviridae* family.

Another study on WNT in RVFV infection utilised a mouse model to investigate RVFV ZH548 effect on IFN-ß production and the WNT pathway (Marcato et al., 2016). This study found no significant fold change in the mRNA production of ß-catenin and differing profiles of WNT gene regulation between infection with RVFV MP12 and RVFV ZH548. In contrast, Harmon *et al* using a HEK 293T cell model infected with RVFV MP12 found a small but significant 1.8 fold upregulation of ß-catenin mRNA. This indicates that RVFVs effect on the WNT

pathway may be virus strain or cell specific. Further study could investigate the variation in general expression levels of ß-catenin within different tissue or cell types and investigate a correlation between RVFV infectivity. It has been proposed that the importance of ß-catenin in the context of viral infection involves the activation of IFN-ß however this is contradictory to the knockout of ß-catenin reducing RVFV replication and thus, it is likely to be a more complex mechanism.

This study identified RVFV MP12 and RVFV MP12delNSs:eGFP inhibit the TOPFlash WNT reporter system and thus, inhibit the WNT pathway at 7 and 24 hours post in infection in three distinct cell types. In contrast, Harmon *et al* showed a distinct activation of the WNT pathway by these viruses up to 7 hours post infection in HEK 293T cells. The inhibition of the WNT pathway is not an artefact of general cell death (Figure 6-9). The RVFV non-structural protein S (NSs) has been shown to bind to WNT pathway genes through use of a CHIP-seq assay. This binding includes WNT ligands, negative regulators of ß-catenin (such as GSK3b) and ß-catenin itself amongst others (Benferhat et al., 2012). This may contribute to WNTs inhibition, however the inhibition effect is seen in the NSs deletion mutant RVFV MP12delNSs:eGFP, thus NSs effect is likely non-specific to WNT signalling and performs other primary functions. The inhibition of WNT by RVFV MP12delNSs:eGFP also indicates that the effect is not due to general host translational shutoff by NSs. Additionally, BUNV and BUNVdelNSs showed cell specific inhibition of the WNT pathway, with BUNV inhibiting WNT in A549 cells after 24 hours but BUNVdelNSs having no significant effect. The inhibition by both BUNV and BUNVdelNSs after 24 hours in Huh-T7-Lunet cells and no inhibition in HEK 293FT cells indicates a cell specific inhibition of the WNT pathway that may be a non-specific effect of BUNV infection (Figure 6-6). The interplay between RVFVs use of ß-catenin for efficient replication and RVFVs inhibition of the WNT pathway is unclear. It may be inhibition of WNT signalling is a side effect of RVFVs interaction with ß-catenin, or that the modulation of WNT signalling itself is important for replication.

ß-catenin has been implicated as a target in a number of viral infections. The herpesvirus human cytomegalovirus (HCMV) inhibits the ß-catenin signalling pathway and relocalises ß-catenin to form aggregates at a central juxtanuclear

location (Angelova et al., 2012). Furthermore, HIV-1 tat protein has been shown to induce an inhibitory effect on the canonical WNT signalling pathway in astrocytes (Henderson et al., 2012), however, the activation of ß-catenin reduces HIV-1 replication (Narasipura et al., 2012). Thus, it is clear that there are no overall anti-viral or pro-viral effects portrayed by ß-catenin, and viruses impact the pathway in a multitude of different ways.

This study also found that ß-catenin loses its distinct localisation at the plasma membrane upon infection with RVFV MP12 or RVFV MP12delNSs:eGFP. RVFV may therefore sequester ß-catenin early in infection and thus interfere with ß-catenin's localisation to the nucleus upon activation. ß-catenin was not found to co-localise with RVFV N at 24 hours post infection (Figure 6-10), however, the speed of activation with WNT activator Wnt3a may indicate this interaction occurs earlier in infection. The diffuse nature of RVFV N throughout the cytoplasm may obscure any specific ß-catenin interaction. Additionally, this interaction may not be a direct interaction with the nucleocapsid, and could be in complex with other viral proteins such as L or Gn. Further investigation into the interaction dynamics of N and ß-catenin is required.

The important nature of the identified protein interactors, and their implication in other viral-host protein interactions make each target an interesting point of study. An understanding of these interactions may reveal new targets for antiviral therapy. This is evident from the impact of WNT inhibitors on RVFV infection (Harmon et al., 2016), and thus by understanding the mechanism behind the interaction, it provides a platform with which to discover new inhibitors or improve existing drugs. Additionally, this study uncovered more RVFV N protein interactors, informing on the basic molecular biology of the virus with which further studies can investigate the therapeutic potential of targeting these interactions.

6.4 Summary

- A proteomics study was performed on RVFV N protein in A549 cells, revealing potential host-pathogen protein-protein interactions.

- Knockdown of host proteins CTNB1, ANXA1, ANXA2, PABP1 and SAFB reduced RVFV replication. Minigenome activity was reduced in PABP4 and SAFB knockdown cells.

- RVFV and RVFVdelNSs:eGFP inhibit the WNT pathway in A549, Huh-T7-Lunet and HEK 293FT cell lines. The effect seen in RVFVdelNSs:eGFP indicates this is not general transcriptional shutdown.

- BUNV inhibitions the WNT pathway in A549 and Huh-T7-Lunet cells after 24 hours but not HEK 293FTs. This is likely a non-specific effect of BUNV NSs.

- Knockout of ß-catenin reduces RVFV replication, activation of WNT shows a moderate increase in RVFV replication after 48 hours.

- Inhibition or activation of WNT has no effect on BUNV.

- RVFV infection delocalises ß-catenin from the plasma membrane resulting in a diffuse staining pattern throughout the cytoplasm, likely resulting in the inhibition of the WNT pathway.

Chapter 7 *Bunyavirales* N effect on exo-siRNA pathway

7.1 Introduction

Arbovirus infection of arthropod vectors requires an important balance between viral replication and survival of the vector. Replication of such viruses does not cause obvious pathogenesis within the vector allowing a long duration infection, maximising the virus transmissibility. It is hypothesised that the innate immune response of the invertebrate host is essential for controlling viremia and thus a stable and persistent infection. There are a number of important innate immune responses identified in mosquitos, particularly; the exogeneous siRNA pathway (exo-siRNA) of different RNA interference (RNAi) mechanisms are very efficient against viruses. Briefly, the siRNA pathway functions by identification of long (viral) dsRNA within the cytoplasm by an endo-ribonuclease known as Dicer 2 (Dcr2). Dcr2 cleaves the dsRNA into short interfering RNA (siRNA) fragments of 21 nucleotides (nt) in length which are loaded to the RNA-induced silencing complex (RISC) made up of the Argonaut 2 (Ago2) protein and a complex of Dcr2, R2D2 and other associated proteins (Hammond et al., 2000, Dana et al., 2017, Liu et al., 2004). The passenger strand of the siRNA duplex is degraded and the RISC complex remains bound to the guide strand. This RISC complex recognises (viral) RNA fragments complementary to the bound fragment and targets these for cleavage. The guide strand is thought to be retained allowing degradation of subsequent targets. The result is a knockdown of RNA transcripts that can disrupt viral replication. Research into antiviral RNAi pathways in insects has predominantly focussed on the model organism *Drosophila melanogaster*, however key parts of these pathways are also present in aedine mosquitos (Blair and Olson, 2015, Kemp and Imler, 2009).

The effect of RNAi silencing on viral replication in vector systems has been extensively investigated. RVFV infection of *Aedes albopictus* and *Aedes aegypti* based cell lines, U4.4 and Aag2 respectively, revealed the siRNA response to infection was partially responsible for establishing persistence of the virus (Léger et al., 2013). A similar effect was shown in dengue type 2 (DENV2) infection of the Aag2 cell line, with DENV2 circumventing the RNAi pathway without completely evading it, thus indicating RNAi is involved in the balance of viral

persistence within the vector to aid successful transmission (Sánchez-Vargas et al., 2009). This is further evident by assessment of mosquito fitness upon suppression of RNAi effector molecules and subsequent infection with the alphavirus Sindbis virus (SINV), which showed a marked decrease in mosquito fitness, again showing the importance of the siRNA pathway for viral maintenance within the viral vector (Myles et al., 2008). Another key piece of evidence supporting RNAi as a regulator of virus infection in the vector is the rapid evolutionary arms race of RNAi genes, indicating the importance of RNAi as an antiviral mechanism (Campbell et al., 2008, Obbard et al., 2006). Regarding *Phenuiviridae*, virus specific small RNAs have been shown to be produced in mosquito cells during RVFV infection (Dietrich et al., 2017). Additionally, knocking out the RNAi components enhances RVFV replication, however no viral suppressor of RNAi was identified (Dietrich et al., 2017).

The nature of RVFV N protein's ability to non-specifically bind RNA lead to the hypothesis that N may non-specifically bind siRNA or precursors thereof, resulting in the suppression but not complete reduction of the siRNA pathway required for the persistence of RVFV within the mosquito vector. The nucleocapsid could also directly interact with siRNA machinery. The capsid protein of *Flavivirus* yellow fever virus (YFV) has recently been identified as a viral suppressor of siRNA through potential inhibition of Dicer-2s cleavage ability by non-specifically binding double stranded RNA (dsRNA) (Samuel et al., 2016). Additionally, it has previously been shown that BUNV NSs does not function to suppress the RNAi response in *Ae. aegypti* suggesting any suppression by BUNV may come from the nucleocapsid or other viral proteins (Samuel et al., 2016).

The capability of YFV capsid to interfere with the siRNA pathway suggested that the function may utilised by other members of the *Flavivirus* genus, within the *Flaviviridae* family, such as the Zika virus (ZIKV). ZIKV was first isolated in Uganda in 1947 (Dick et al., 1952), however, a recent epidemic that started in South America in 2015 signalled a need for thorough investigation from the research community (Petersen et al., 2016). ZIKV has a typical flavivirus genome organization, a single-stranded positive sense RNA molecule with a single open reading frame encoding three structural proteins; precursor membrane (prM) protein, envelope (E) and capsid (C) protein, along with seven non-structural

proteins (Shi and Gao, 2017). The prM protein is thought to be involved in E protein folding before subsequent cleavage in the golgi network into the pr peptide and M protein (Tian et al., 2016). Zika E protein is the major virion surface protein involved in binding to host cell receptors and membrane fusion (Dai et al., 2016). The Zika C protein comprises the viral capsid in an icosahedral shape surround by a lipid bilayer derived from the host cell. The non-structural proteins primary function is to form the replicative complex and to antagonise the host immune response. NS1 and NS4A are involved in viral replication (Lindenbach and Rice, 1999). NS2A, NS2B and NS4B have currently unknown functions (Zhu et al., 2016). NS3 is involved in polyprotein processing and is important for viral replication. NS5 functions as an RNA-dependent RNA polymerase with cap snatching functions while also suppressing IFN signalling (Grant et al., 2016, Faye et al., 2014).

Infection with ZIKV primarily results in asymptomatic infection though can cause mild febrile illness as seen with other flaviviruses such as dengue fever. However, there has been an association between incidences of microcephaly, Guillain-Barré Syndrome and other congenital abnormalities in infants born from ZIKV infected mothers during ZIKV outbreaks (Cao-Lormeau et al., 2016, Brasil et al., 2016). This suggests ZIKV specific neural tropism not found in other flaviviruses and the ability to cross the placental barrier (Wang et al., 2017).

Semliki Forest Virus (SFV) is a mosquito-borne alphavirus of the *Togaviridae* family. SFV is closely related to Chikungunya virus and is often used as a model system for viral pathogenesis and viral encephalitis (Atkins et al., 1999). SFV encodes for 4 non-structural proteins in addition to the structural proteins under a subgenomic promotor. A designed reporter SFV contains a second duplicated subgenomic promotor which allows for further expression of proteins of interest (Varjak et al., 2017a). The virulent SFV6 strain (Ferguson et al., 2015), a mutant of the prototype SFV4 strain, was used as a model virus in this study for its ability to grow to high titres and susceptibility to genetic manipulation.

The expression of ZIKV C by recombinant SINV was shown to cause a significant disease phenotype in infected mosquitos, though the mechanism behind this phenotype has not been established (Samuel et al., 2016). Elucidating the

suppression of the RNAi response in vector systems may provide avenues for generation of suitable vaccine candidates.

7.2 Results

The replication enhancing effect of flavivirus C proteins has been previously described (Samuel et al., 2016), though this effect has not been observed with members of the *Bunyaviridae* family. Thus, to test the hypothesis that RVFV N, BUNV N or ZIKV C proteins inhibited the antiviral response in mosquitos we first cloned the full length ORF of RVFV N, BUNV N and ZIKV C behind the duplicated subgenomic promoter in the alphavirus Semliki Forest Virus (SFV) genome. Additionally, the tombusvirus p19 protein, known to bind siRNAs (Attarzadeh-Yazdi et al., 2009, Silhavy et al., 2002), was cloned into SFV as a positive control and eGFP expressing SFV was used as a negative control. These viruses also expressed *Renilla* luciferase, which was cloned together with duplicated cleavage sites between the non-structural proteins nsP3 and nsP4 within the viral genome. Aag2 cell line was infected at a low MOI (0.01) with recombinant SFV expressing each protein of interest to monitor the spread of SFV by measurement of *Renilla* levels (*RLuc*) (Figure 7-1). The expression of ZIKV C resulted in enhanced replication of SFV, interestingly this effect was significantly greater than resulted from the expression of the RNAi suppressor p19. Both RVFV N and BUNV N showed inhibition of viral replication, with reduced replication compared with the SFV eGFP control.

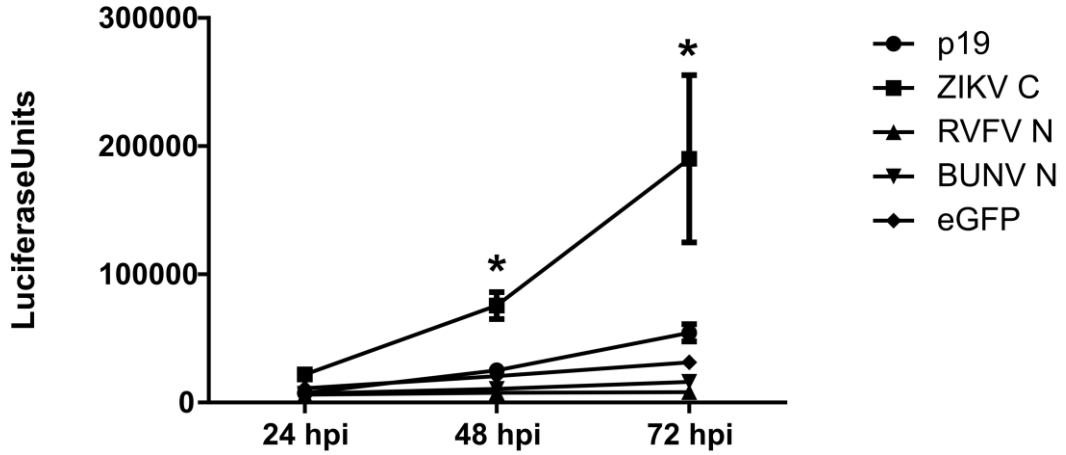

Figure 7-1. Increased replication efficiency of recombinant SFV expressing Zika C.

Aag2 cells were infected with SFV6(3H)-*RLuc*-2SG-p19, SFV6(3H)-*RLuc*-2SG-ZIKV_C, SFV6(3H)-*RLuc*-2SG-RVFV_N, SFV6(3H)-*RLuc*-2SG-BUNV_N or SFV6(3H)-*RLuc*-2SG-eGFP at MOI 0.01. Replication of recombinant SFV was determined by measurement of *Renilla* luciferase *(RLuc*) activity at each time point. Experiment was performed three times in quadruplicate. Significance determined by Student's t-test, where * denotes $p<0.05$.

The lack of viral enhancement of SFV expressing BUNV N or RVFV N changed the focus of investigation to p19 and ZIKV C To further assess the replication enhancing activity of ZIKV C, AF319 cells (a derivate cell line of Aag2 cells with the key RNAi effector molecule Dicer2 knocked out (Varjak et al., 2017b)) and its parental cell line AF5 cells (Varjak et al., 2017b) were infected at MOI 0.01 (Figure 7-2) or MOI 0.001 (Figure 7-3) to assess the replication of ZIKV C in RNAi defective cells. p19 expressing SFV showed increased replication in AF5 cells, however, lost the enhancing effect in RNAi deficient AF319 cells. SFV expressing ZIKV C showed increased replication in AF5 cells as expected. Surprisingly, the virus also showed significantly increased replication in AF319 cells indicating that the infection enhancing activity of ZIKV C is not related to or active against the antiviral RNAi response within the mosquito cells. The enhanced replication was more pronounced at MOI 0.001 compared with MOI 0.01.

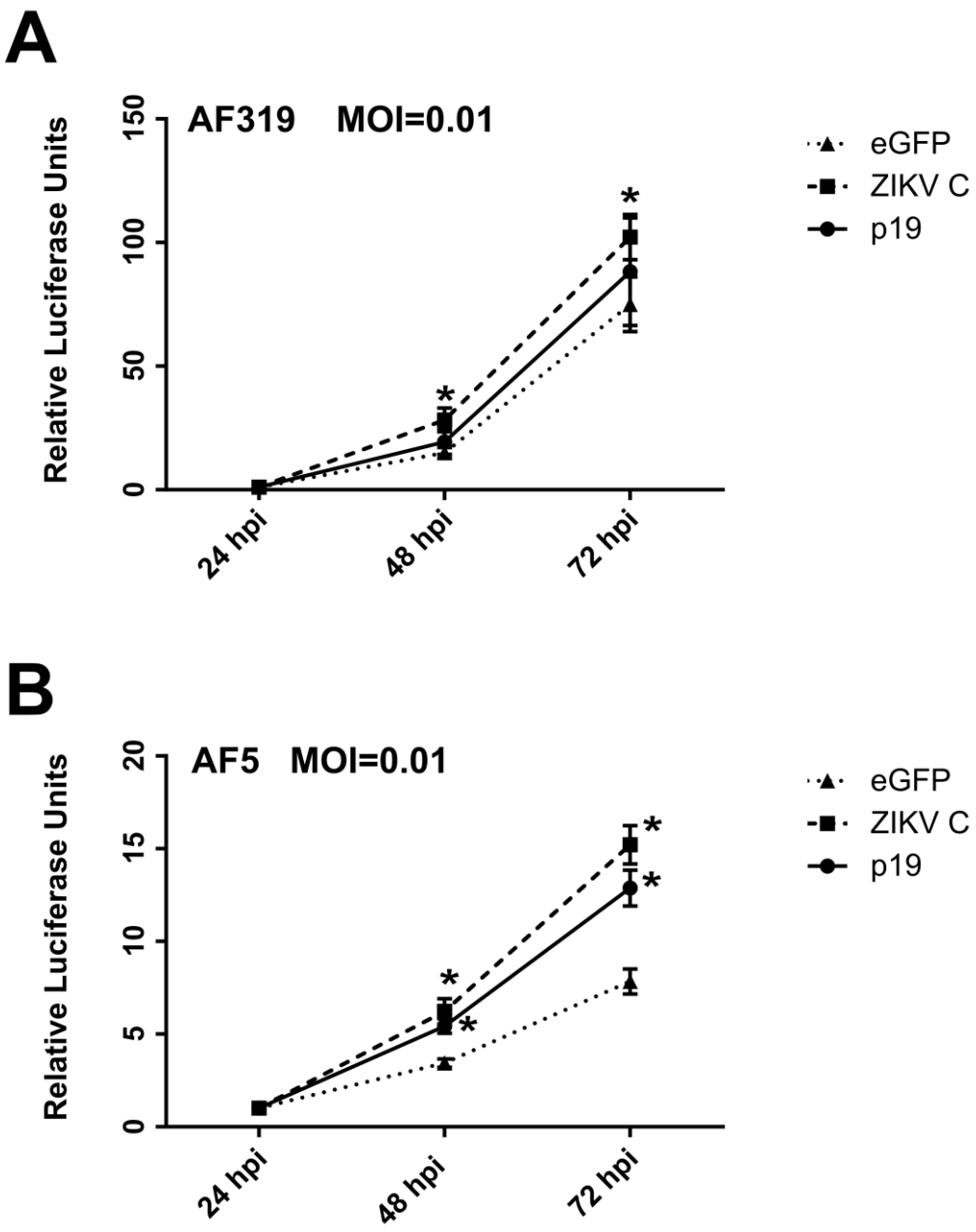

Figure 7-2. Infection of AF5 and AF319 cells with recombinant SFV6 at MOI 0.01

AF319 (A) and AF5 (B) cells were infected with SFV6(3H)-*RLuc*-2SG-p19, SFV6(3H)-*RLuc*-2SG-ZIKV_C or SFV6(3H)-*RLuc*-2SG-eGFP at MOI 0.01. Cells were harvested at respective time points and *Renilla* luciferase levels measured. Experiments were repeated three times in quadruplicate. Mean values are shown and error bars depict standard error. Significance determined by Student's t-test, where * denotes $p<0.05$.

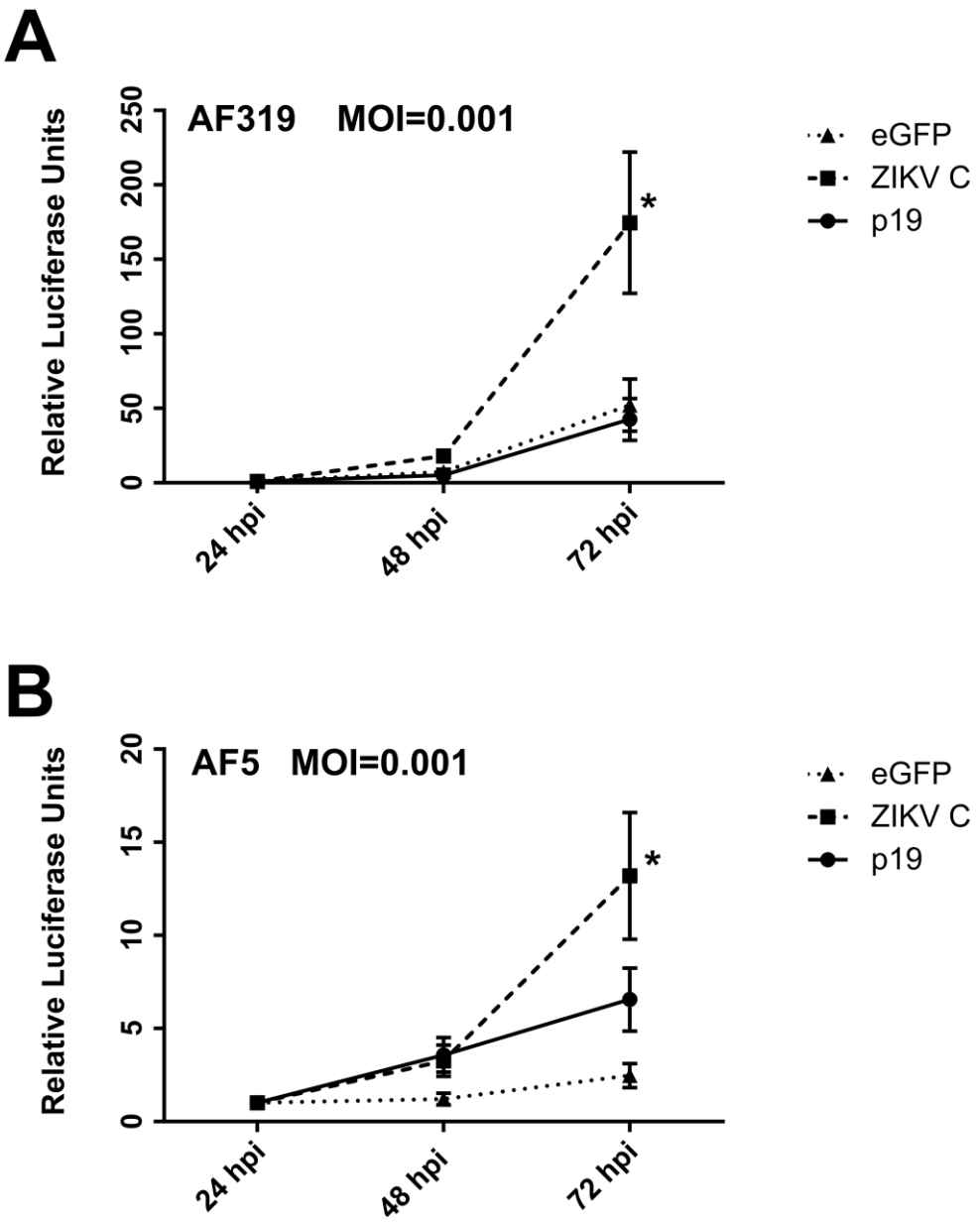

Figure 7-3. Infection of AF5 and AF319 cells with recombinant SFV6 at MOI 0.001

AF319 (A) and AF5 (B) cells were infected with SFV6(3H)-*RLuc*-2SG-p19, SFV6(3H)-*RLuc*-2SG-ZIKV_C or SFV6(3H)-*RLuc*-2SG-eGFP at MOI 0.001. Cells were harvested at respective time points and *Renilla* luciferase measured. Experiments were repeated three times in quadruplicate. Mean values are shown and error bars depict standard error. Significance determined by Student's t-test, where * denotes $p<0.05$.

Although RVFV N did not show any enhancing effects on reporter virus, it was of interest to determine if ZIKV C has any effect on the RNAi pathway. For this, Aag2 cells were infected with recombinant SFV expressing ZIKV C, p19 or eGFP. At 24 hours post infection, cells were transfected with a plasmid expressing firefly luciferase (*Fluc*) and *Fluc* specific dsRNAs or siRNAs, dsRNAs against LacZ or siRNAs against Hygromycin B resistance gene were used as control, respectively. In the case of an active RNAi system, the transfection of *Fluc* specific dsRNA or siRNA will result in the targeted destruction of *Fluc* transcripts. The transfection of dsRNA resulted in knockdown of *Fluc* transcripts for both p19 and ZIKV C. The transfection of siRNA and subsequent knockdown of *Fluc* transcripts was inhibited by p19, which showed approximately 20% activity compared with 5% activity in the eGFP control. The *Fluc* activity in the presence of ZIKV C interestingly showed similar knockdown to eGFP, thus showing ZIKV C's replication enhancing activity is unlikely to be related to the RNAi response.

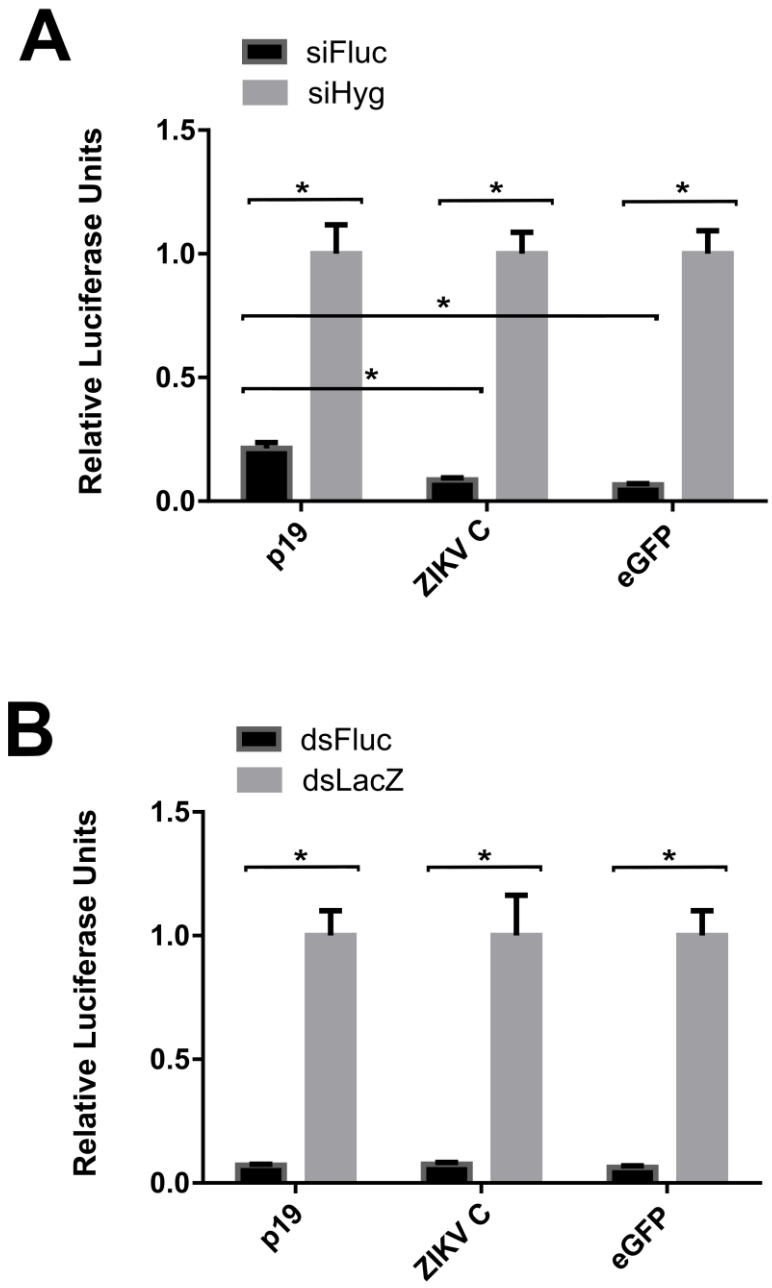

Figure 7-4. ZIKV capsid C has no effect on the exo-siRNA pathway

Aag2 cells were infected with SFV6(3H)-*RLuc*-2SG-p19, SFV6(3H)-*RLuc*-2SG-ZIKV_C or SFV6(3H)-*RLuc*-2SG-eGFP at MOI 1. At 24 hours post infection, cells were transfected with (A) siRNAs against *Fluc* (siFluc) or Hygromycin B resistance gene (siHyg) (B) dsRNA against *Fluc* (dsFluc) or LacZ (dsLacZ), in addition to an *Fluc*-expressing reporter plasmid. Cells were lysed 24 hours post-transfection and *Fluc* activity measured. Experiment was repeated three times in quadruplicate and mean shown with error bars indicating the standard error. Significance was determined by two-way ANOVA with * denoting $p<0.05$.

7.3 Discussion

It is important for viruses to balance supressing host antiviral responses and host survivability for the successful transmission of the pathogen. There are a number of proteins encoded by viruses that function to counter the RNAi defence known as Viral suppressors of RNA silencing (VSRs) (Wu et al., 2010, Csorba et al., 2015). VSRs have diverse mechanisms in suppressing the RNAi response. The primary mechanism appears to be the binding of dsRNA by VSRs and this is evident in a number of VSRs including influenza A virus NS1 (Bucher et al., 2004). Interestingly, tombusvirus p19s mode of action is unique, where p19 has a high affinity for duplexed siRNA and has much weaker affinity for dsRNA longer than 22 nt, implying size specific recognition and binding of siRNA (Vargason et al., 2003, Ye et al., 2003). There is some evidence for VSRs expressed by arboviruses; the dengue non-structural protein NS4B is described to interact with RNAi machinery resulting in inhibition of the pathway (Kakumani et al., 2013), the sfRNA encoded by flaviviruses also has RNAi inhibitory activity (Schnettler et al., 2012) and YFV C is a candidate VSR (Samuel et al., 2016).

RVFV N and BUNV N both bind ssRNA and dsRNA in an unspecific manner, with limited evidence of preference to either (Osborne and Elliott, 2000). However, there was no evidence for a proviral effect in comparison to eGFP expressing SFV. In fact, both RVFV N and BUNV N showed distinct antiviral properties which may be a result of the non-specific binding of SFV transcripts preventing efficient viral replication, however, this requires further study, alternatively, the effect could be an artefact. The replication enhancing effect of SINV expressing ZIKV C had previously been described and was suggested to be the result of RNAi silencing as seen for YFV (Samuel et al., 2016). YFV C was shown to bind dsRNA *in vitro* and thus interfere with cleavage by Dicer thereby inhibiting the RNAi response. Interestingly, ZIKV C proviral effect was evident in Dicer2 knockout A319 cells and an RNAi reporter assay showed ZIKV C had no effect on dsRNA or siRNA mediated silencing. Therefore, the mechanism of ZIKV C replication enhancing effect is unknown. This highlights that despite the evidence that many flavivirus C proteins provide replication enhancing effects to alphaviruses, their means can be different.

Interestingly, p19 had no silencing effect upon the transfection of dsRNA into the reporter system. This is likely due to p19s mechanism of specifically binding duplexed siRNA, and thus the silencing effect was more pronounced when siRNA was transfected directly, resulting in an abundance of available targets for p19s inhibitory activity. ZIKV C replication enhancing activity was significantly higher than the effect provided by p19, suggesting that the ZIKV C enhancement of infection by an unknown mechanism has a more significant effect than overcoming the antiviral properties of RNAi.

Understanding the mechanisms governing persistence of viruses within their vectors allows the exploitation of interactions, particularly those which impact the innate immune system. These interactions can be investigated as therapeutic targets or as mechanisms for vector control.

7.4 Summary

- Recombinant SFV reporter viruses expressing RVFV N, BUNV N and ZIKV C proteins along with positive and negative controls were generated.

- RVFV N and BUNV N reduced replication of SFV in Aag2 mosquito cells and are not likely to display RNAi-antagonistic activities.

- ZIKV C significantly increased replication of SFV in Aag2 cells.

- ZIKV C showed significantly increased replication of SFV in AF5 cells with functional siRNA pathway and in A319 cells with impaired Dcr2. This effect was more pronounced in low MOI infections.

- ZIKV C showed no inhibitory effect on the siRNA pathway

Chapter 8 General Discussion

8.1 Project Outcomes

The main focus and primary aim of this project was to inform on the fundamental processes involved in the replication cycle of RVFV with particular focus on the nucleocapsid protein N, and its potential interactions within host cells during infection.

At the beginning of the project, we sought to identify conserved regions of the nucleocapsid protein that may act as interaction domains between the nucleocapsid and RVFV or host proteins. By performing a sequence alignment and assessment of the 3D structure, five residues were selected for further investigation (Chapter 5). I used a site-directed mutagenesis approach to perform alanine substitutions for these key nucleocapsid residues, as well as two N-terminal arm deletions that had previously been indicated as functional (unpublished data). By performing crosslinking, RNA binding, immunoprecipitation assays and utilising minigenome reporter systems, I identified two novel functional residues, F11 and F149 that, despite performing all known functions of RVFV N, showed no activity in the minigenome assay when mutated to alanine. Unfortunately, despite multiple attempts of virus rescue it was not possible within the project's timeframe to utilise reverse genetics systems to rescue RVFV containing each mutation. This was due to laboratory wide issues rescuing wildtype RVFV. Ultimately, by informing on the RVFV N functional residues we provided useful data for further study, particularly with regards to potential interaction sites of RVFV with host proteins. Furthermore, the discovery of the mutant Y30A with increased replication capacity, despite reduced RNA binding, could open avenues for replication competent attenuated vaccines.

Previous studies investigating RVFV host protein interactions have mostly been limited to RVFV NSs and understanding its antagonistic properties. I was interested in elucidating the interactions of RVFV N protein with an aim to identify interactions essential for the RVFV life cycle. Using a proteomics-based approach, I identified 23 potential host protein interactors with RVFV N in A549 cells during infection, 2 of which had been previously identified as having a role

in RVFV virus-host interaction and 21 were newly identified. This initial study provides a basis for further investigation into RVFV N roles. After testing each interaction by siRNA knockdown, I identified interactions involved in RVFV replication. This screen allowed me to make an informed decision on which interactions would be most relevant for further investigations. The large body of previous research on the WNT pathway, the availability of molecular tools and a prior indication of the WNT pathway's importance in RVFV infection made ß-catenin a prime candidate for further experiments.

By employing a TOPFlash reporter assay, I informed on RVFV's inhibition of the WNT pathway and by developing a CRISPR-Cas9 ß-catenin knockout cell line I provided a useful tool for further study of interactions between RVFV and WNT pathway. Using the knockout A549 cell line, I highlighted the impact of ß-catenin for efficient RVFV replication. Additionally, I identified a small but enhancement of RVFV replication upon WNT pathway activation. Utilising a confocal microscopy-based approach, I identified a change in localisation of ß-catenin from the plasma membrane during the infection to a cytoplasmic disperse localisation. This study has identified ß-catenin as an important interactor of RVFV N protein that is involved in modulating replication of RVFV. The disruption of this interaction or the WNT pathway itself may provide therapeutic potential to RVFV infection.

During the course of this PhD, a study on YFV revealed dsRNA binding properties of its capsid protein that allowed YFV to evade the RNAi response in mosquito cells (Samuel et al., 2016). In light of this, it was hypothesised that RVFV and BUNVs non-specific binding of RNA may also influence the RNAi response in a similar manner. I cloned RVFV N, BUNV N and ZIKV C into the subgenomic region of a reporter SFV. By utilising these reporter viruses, I identified RVFV N and BUNV N both provided a fitness disadvantage, however, ZIKV C showed greatly increased viral replication. I continued investigation into ZIKV C and identified its replication enhancing activity unrelated to the RNAi antagonistic activity. Uncovering the mechanism behind the replication enhancing activity of ZIKV C will increase our understanding of ZIKV C's modulation of viral replication within the mosquito vector. Hover, clearly bunyavirus N proteins are not likely to have RNAi antagonistic activity.

8.2 Future Studies

The importance of RVFV is highlighted by the constant threat of outbreaks across the continent of Africa. This is evidenced by a significant outbreak in Niger in 2016 that infected both humans and ruminants and most recently, evidence of ongoing human infection in Uganda, July 2018. The lack of therapeutics and vaccines is an ever-present issue that will be amplified by the potential spread of RVFV vector mosquitos into southern Europe.

The identification of essential functional residues within RVFV N opens many avenues for future research. In particular, the generated panel of mutants can be combined with the siRNA screen designed from the proteomics screen, focusing on mutants F11A and F149A. The cloning of mutants F11A and F149A into a plasmid backbone containing a mammalian promoter such as a CMV promoter would allow expression within A549 cells and other mammalian cell systems. Overexpression of these mutants within A549 cells, application of the siRNA screen and subsequent immunoprecipitation of RVFV N mutants, followed by probing using antibodies against potential interactors such as β-catenin would inform on whether these residues disrupt specific interactions. Alternatively, using a proteomics approach on immunoprecipitated mutant N proteins and comparing between the wildtype interaction panel one can make an informed decision on any interactions that may be disrupted, which can lead to therapeutic targets or viruses/replicons that can be manipulated or selected for via specific interactions. This could lead to novel restricted vaccination strains. The lack of licenced RVFV vaccines is a persistent issue. While RVFV MP12 is a well-studied attenuated vaccine candidate, RVFV MP12 retains some virulence and has been shown to result in fetal death in sheep (Morrill et al., 2013). Thus, recombinant RVFV MP12 N mutants with specific cell ranges may unveil potential vaccine candidates that might reduce issues of virulence.

The siRNA experiment itself allows a number of interesting leads for follow up studies. Annexin A1 and A2 have been shown to be important in many viral infections. Annexin A2 knockout reduced virus reporter activity however it did not affect the formation of viral RNPs or viral replication directly (Chapter 6). As ANXA2 has RNA binding activity and has been shown to be involved in the frameshift efficiency of viral proteins (Kwak et al., 2011), it may be involved in

altering the balance of GnGc expression and its various cleavage products, resulting in reduced particle formation. ANXA2 may also interact with the formation of viral particles directly at the Golgi apparatus. By employing VLP assays, one can elucidate ANXA2s interaction with RVFV during the virus life cycle. Additionally, the use of immunoprecipitation to pulldown ANXA2 from RVFV infected cells may reveal if the interaction with N is direct or mediated by viral glycoproteins. Additionally, by dissociating and sequencing the RNA bound to ANXA2, we may uncover specific RVFV bound sequence motifs.

The identification of PABP1 and PABP4 are also significant and can be investigated further. Investigating the direct interaction of RVFV N and PABP1 may be important. The overexpression of PABP1 promotes human cytomegalovirus (HCMV) protein synthesis (Perez et al., 2011), thus, it may support a similar function in RVFV infection. A recent study generated and characterized an RNA substrate that binds to PABP with high specificity impairing PABP function (Barragán-Iglesias et al., 2018). Utilising such a substrate would allow investigation into the mechanism of interaction with RVFV N and its impact on RVFV replication.

The limited study on SAFBs interaction within virus infection implies a more explorative study to untangle the importance of SAFB for RVFV replication. SAFBs function in healthy cells is binding of DNA elements for transcription and its involvement in RNA splicing may play a role in RVFV infection. Using confocal microscopy to identify the intracellular localisation of SAFB in relation to RVFV N at varying timepoints during RVFV infection would inform on the relationship during RVFV replication.

During this study, I focused on one specific interactor, and I identified ß-catenin to be important for RVFV replication. The presence of ß-catenin is required for efficient viral replication. Currently the downstream effect of RVFV infection on the WNT pathway is not clearly understood. By utilising qPCR, one can assess many of the downstream genes for which ß-catenin is a transcription factor for. In turn, each of these downstream genes may also influence RVFV infection. Furthermore, RNASeq of A549 cells after infection by RVFV would provide a global overview of RNA transcription that may allow the identification of new co-factors related to ß-catenin and the regulation of the WNT pathway. The

relocalisation of ß-catenin during RVFV infection can be studied further, in particular using confocal microscopy combined with live cell imaging to assess earlier timepoints during RVFV infection. Confocal imagery of RVFV N and ß-catenin at early timepoints may allow observation of the direct infection between these two proteins. A more thorough analysis of WNT pathway activation and the dynamics of RVFV infection would inform on the observed RVFV replication enhancing effect of WNT activation. Such an effect may be timepoint specifc or cell specific. The relocalisation may be due to the invagination of the plasma membrane during the virus particles entry into endosomes, or by some other mechanism. Understanding this process would allow specific targeting of the ß-catenin – RVFV interaction at timepoints where the interaction is the most important for the virus lifecycle.

The identification of RVFV N and BUNV N not acting as RNAi antagonists indicates that non-specific binding of RNA transcripts is not sufficient as a mechanism for RNAi antagonism. Additionally, the discovery of ZIKV C as a significant proviral protein that also does not work through the antagonism of the RNAi response in mosquitos implies that capsid or nucleocapsid proteins may not have general RNAi antagonistic properties. Further work is required to evaluate RVFVs interaction with mosquito cell proteins that allow the balance between efficient viral replication and mosquito cell fitness.

Work from this PhD provided new insights into the mechanisms, molecular characterisations and host protein interactions of RVFV nucleocapsid protein. By expanding the knowledge of RVFVs interaction with host cell pathways, I have provided a strong basis for future study and the potential development of therapeutics. The interaction of ß-catenin with RVFV is a strong candidate for intervention strategies. Understanding these processes is important as RVFV continues to be a public health threat.

Chapter 9 Appendices

9.1 Oligonucleotides

Table 9-1. Oligonucleotide primers used for generation of RVFV nucleocapsid mutant plamsids

Primer	Sequence (5' → 3')	Purpose
PTM1 Plus ATG Rev	[Phos]CATGGTATTATCGTGTTTTTCAAAGGAAAAC	Site directed mutagenesis of pTM1-RVFV_N sequence
PTM1 N-2-15-Fwd	GTGGACCGCAATGAGATTGAACAGTGGGTC	
PTM1 N2-30 Fwd	AAGGGTTTGATGCCCGTAGAGTTATCGAAC	
PTM1 P11A Fwd	GCCGCTGCTCAAGCAGTGGACCGC	Site directed mutagenesis of pTM1-RVFV_N sequence
PTM1 P11A Rev	[Phos]CTGGATCGCAAGCTCTTGATAG	
Y30 Fwd	GGTCCGAGAGTTTGCTGCTCAAGGGTTTGA	Site directed mutagenesis of pTM1-RVFV_N sequence
Y30 Rev	TCAAACCCTTGAGCAGCAAACTCTCGGACC	
Asp34Ala Fwd	CCGCCCGTAGAGTTATCGAAC	Site directed mutagenesis of pTM1-RVFV_N sequence
Asp34Ala Rev	CAAACCCTTGATAAGCAAACTC	
Phe149Ala Fwd	GCCGCTGGCATGGTGGATCCTTC	Site directed mutagenesis of pTM1-RVFV_N sequence
Phe149Ala Rev	GCTGGGGTGCATCATATGCCTC	
Asp181Ala Fwd	GCCCCAAACCTCCGAGGTAGAAC	Site directed mutagenesis of pTM1-RVFV_N sequence
Asp181Ala Rev	GATGACCCGGGAGAACTGCAGC	

Primer	Sequence (5’ → 3’)	Purpose
p14 P11A Fwd	CAAGAGCTTGGATCCAGGCCGCTGCTCAAGCAGTGGAC	Site directed mutagenesis of p14-RVFV_N sequence
p14 P11A Rev	GTCCACTGCTTGAGCAGCCGGCTGGATCGCAAGCTCTTG	
p14 Asp34Ala Fwd	CCGCCCGTAGAGTTATCGAAC	Site directed mutagenesis of p14-RVFV_N sequence
p14 Asp34Ala Rev	[Phos]CAAACCCTTGATAAGCAAACTC	
p14 Phe149Ala Fwd	GCCGCTGGCATGGTGGATCCTTC	Site directed mutagenesis of p14-RVFV_N sequence
p14 Phe149Ala Rev	[Phos]GCTGGGGTGCATCATATGCCTC	
p14 Asp181Ala Fwd	GCCCCAAACCTCCGAGGTAGAAC	Site directed mutagenesis of p14-RVFV_N sequence
p14 Asp181Ala Rev	[Phos]GATGACCCGGGAGAACTGCAGC	

Table 9-2. Oligonucleotide primers used for generation of SFV6 constructs.

Primer	Sequence (5' → 3')	Purpose
Zika_C Fwd	CGTTAATACAGGATCCATGAAAAACCCAAAAAAGAAATCC	Insertion of ZIKV C sequence before subgenomic region of SFV6 plasmid
Zika_C Rev	CTACCCTAACGGATCCTTATGCCATAGCTGTGGTCAGCAG	
Bun_N Fwd	CGTTAATACAGGATCCATGATTGAGTTGGAATTTCATGATG	Insertion of BUNV N sequence before subgenomic region of SFV6 plasmid
Bun_N Rev	CTACCCTAACGGATCCTTACATGTTGATTCCGAATTTAG	
Rift_N Fwd	CGTTAATACAGGATCCATGGACAACTATCAAGAGCTTGCG	Insertion of RVFV N sequence before subgenomic region of SFV6 plasmid
Rift_N Rev	CTACCCTAACGGATCCTTAGGCTGCTGTCTTGTAAGCCTG	
eGFP Fwd	CGTTAATACAGGATCCATGGTGAGCAAGGGCGAGGAGCTG	Insertion of eGFP sequence before subgenomic region of SFV6 plasmid
eGFP Rev	CTACCCTAACGGATCCTTACTTGTACAGCTCGTCCATGCC	
P19 Fwd	CGTTAATACAGGATCCATGGAACGAGCTATACAAGGA	Insertion of P19 sequence before subgenomic region of SFV6 plasmid
P19 Rev	CTACCCTAACGGATCCTTACTCGCTTTCTTTTTCGAAG	

9.2 Sequence Alignment

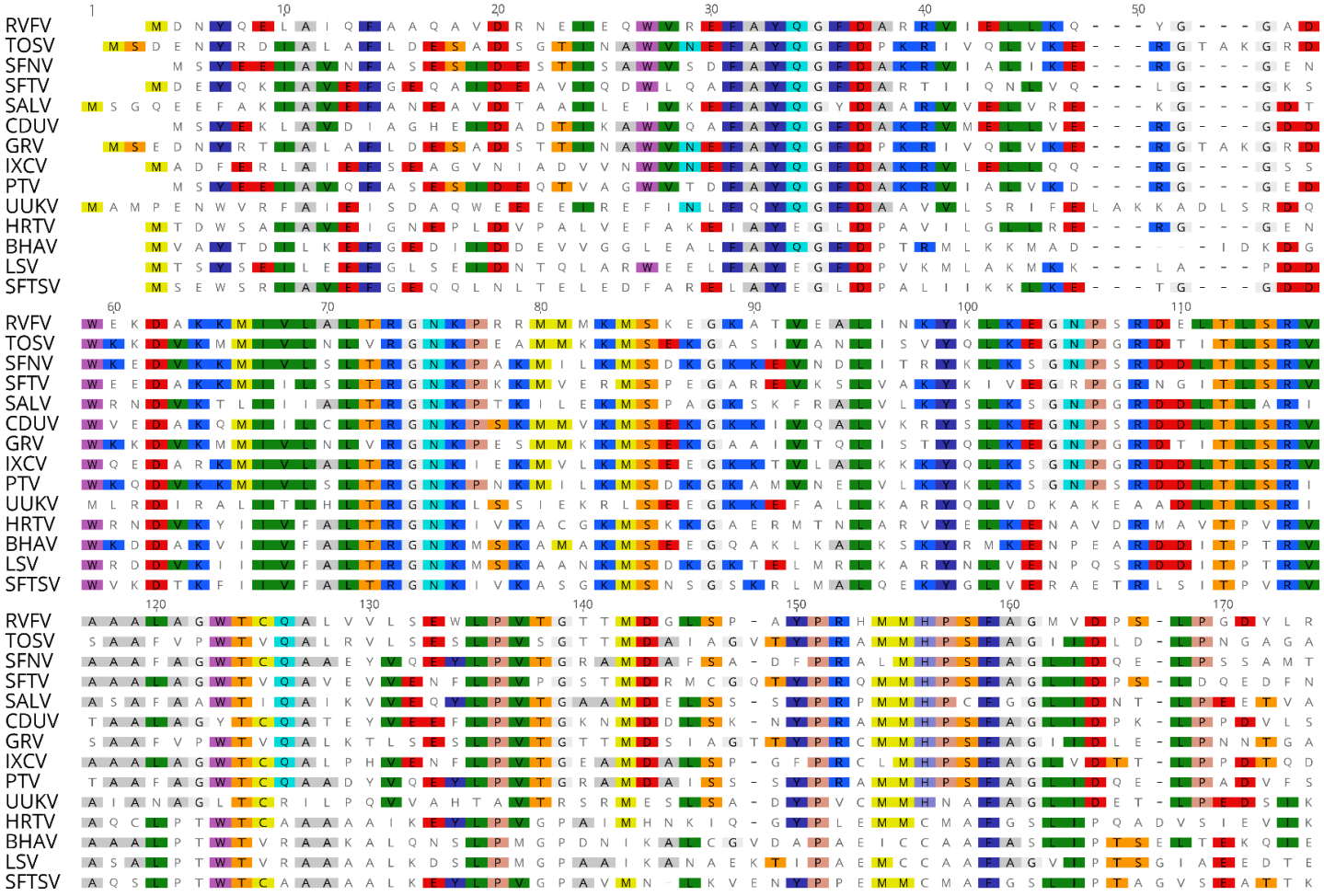

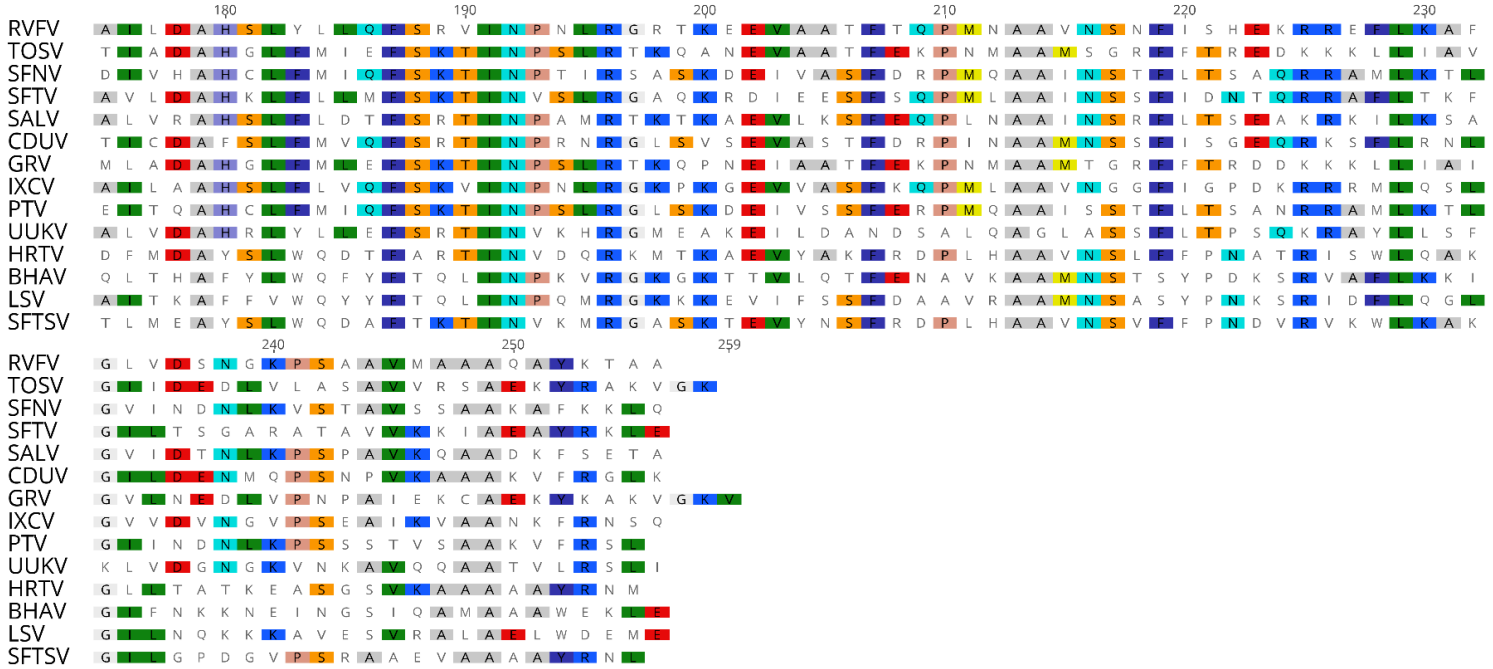

Figure 9-1. Complete sequence alignment of *Phlebovirus* N sequences

Phlebovirus N Genbank sequences were aligned using Geneious. Conserved amino acids are colour highlighted. Amino acid positioning relative to UUKV N.

References

(Cdc), C. F. D. C. A. P. 2000a. Outbreak of Rift Valley fever--Saudi Arabia, August-October, 2000. *MMWR Morb Mortal Wkly Rep,* 49, 905-8.

(Cdc), C. F. D. C. A. P. 2000b. Outbreak of Rift Valley fever--Yemen, August-October 2000. *MMWR Morb Mortal Wkly Rep,* 49, 1065-6.

Aberle, H., Bauer, A., Stappert, J., Kispert, A. & Kemler, R. 1997. beta-catenin is a target for the ubiquitin-proteasome pathway. *EMBO J,* 16, 3797-804.

Adam, I. & Karsany, M. S. 2008. Case report: Rift Valley Fever with vertical transmission in a pregnant Sudanese woman. *J Med Virol,* 80, 929.

Albariño, C. G., Bird, B. H. & Nichol, S. T. 2007. A shared transcription termination signal on negative and ambisense RNA genome segments of Rift Valley fever, sandfly fever Sicilian, and Toscana viruses. *J Virol,* 81, 5246-56.

Albornoz, A., Hoffmann, A. B., Lozach, P. Y. & Tischler, N. D. 2016. Early Bunyavirus-Host Cell Interactions. *Viruses,* 8.

Alfadhli, A., Love, Z., Arvidson, B., Seeds, J., Willey, J. & Barklis, E. 2001. Hantavirus nucleocapsid protein oligomerization. *J Virol,* 75, 2019-23.

Andersson, A. M. & Pettersson, R. F. 1998. Targeting of a short peptide derived from the cytoplasmic tail of the G1 membrane glycoprotein of Uukuniemi virus (Bunyaviridae) to the Golgi complex. *J Virol,* 72, 9585-96.

Angelova, M., Zwezdaryk, K., Ferris, M., Shan, B., Morris, C. A. & Sullivan, D. E. 2012. Human cytomegalovirus infection dysregulates the canonical Wnt/ß-catenin signaling pathway. *PLoS Pathog,* 8, e1002959.

Arora, S., Lim, W., Bist, P., Perumalsamy, R., Lukman, H. M., Li, F., Welker, L. B., Yan, B., Sethi, G., Tambyah, P. A., Fairhurst, A. M., Alonso, S. & Lim, L. H. 2016. Influenza A virus enhances its propagation through the modulation of

Annexin-A1 dependent endosomal trafficking and apoptosis. *Cell Death Differ,* 23**,** 1243-56.

Atkins, G. J., Sheahan, B. J. & Liljeström, P. 1999. The molecular pathogenesis of Semliki Forest virus: a model virus made useful? *J Gen Virol,* 80 (Pt 9)**,** 2287-97.

Attarzadeh-Yazdi, G., Fragkoudis, R., Chi, Y., Siu, R. W., Ulper, L., Barry, G., Rodriguez-Andres, J., Nash, A. A., Bouloy, M., Merits, A., Fazakerley, J. K. & Kohl, A. 2009. Cell-to-cell spread of the RNA interference response suppresses Semliki Forest virus (SFV) infection of mosquito cell cultures and cannot be antagonized by SFV. *J Virol,* 83**,** 5735-48.

Baer, A., Shafagati, N., Benedict, A., Ammosova, T., Ivanov, A., Hakami, R. M., Terasaki, K., Makino, S., Nekhai, S. & Kehn-Hall, K. 2016. Protein Phosphatase-1 regulates Rift Valley fever virus replication. *Antiviral Res,* 127**,** 79-89.

Barr, J. N. 2007. Bunyavirus mRNA synthesis is coupled to translation to prevent premature transcription termination. *RNA,* 13**,** 731-6.

Barr, J. N., Elliott, R. M., Dunn, E. F. & Wertz, G. W. 2003. Segment-specific terminal sequences of Bunyamwera bunyavirus regulate genome replication. *Virology,* 311**,** 326-38.

Barr, J. N., Rodgers, J. W. & Wertz, G. W. 2006. Identification of the Bunyamwera bunyavirus transcription termination signal. *J Gen Virol,* 87**,** 189-98.

Barragán-Iglesias, P., Lou, T. F., Bhat, V. D., Megat, S., Burton, M. D., Price, T. J. & Campbell, Z. T. 2018. Inhibition of Poly(A)-binding protein with a synthetic RNA mimic reduces pain sensitization in mice. *Nat Commun,* 9**,** 10.

Barski, M., Brennan, B., Miller, O. K., Potter, J. A., Vijayakrishnan, S., Bhella, D., Naismith, J. H., Elliott, R. M. & Schwarz-Linek, U. 2017. Rift Valley fever phlebovirus NSs protein core domain structure suggests molecular basis for nuclear filaments. *Elife,* 6.

Benferhat, R., Josse, T., Albaud, B., Gentien, D., Mansuroglu, Z., Marcato, V., Souès, S., Le Bonniec, B., Bouloy, M. & Bonnefoy, E. 2012. Large-scale chromatin immunoprecipitation with promoter sequence microarray analysis of the interaction of the NSs protein of Rift Valley fever virus with regulatory DNA regions of the host genome. *J Virol,* 86**,** 11333-44.

Billecocq, A., Gauliard, N., Le May, N., Elliott, R. M., Flick, R. & Bouloy, M. 2008. RNA polymerase I-mediated expression of viral RNA for the rescue of infectious virulent and avirulent Rift Valley fever viruses. *Virology,* 378**,** 377-84.

Billecocq, A., Spiegel, M., Vialat, P., Kohl, A., Weber, F., Bouloy, M. & Haller, O. 2004. NSs protein of Rift Valley fever virus blocks interferon production by inhibiting host gene transcription. *J Virol,* 78**,** 9798-806.

Bird, B. H., Albariño, C. G., Hartman, A. L., Erickson, B. R., Ksiazek, T. G. & Nichol, S. T. 2008. Rift valley fever virus lacking the NSs and NSm genes is highly attenuated, confers protective immunity from virulent virus challenge, and allows for differential identification of infected and vaccinated animals. *J Virol,* 82**,** 2681-91.

Bird, B. H., Ksiazek, T. G., Nichol, S. T. & Maclachlan, N. J. 2009. Rift Valley fever virus. *J Am Vet Med Assoc,* 234**,** 883-93.

Bird, B. H. & Nichol, S. T. 2012. Breaking the chain: Rift Valley fever virus control via livestock vaccination. *Curr Opin Virol,* 2**,** 315-23.

Blair, C. D. & Olson, K. E. 2015. The role of RNA interference (RNAi) in arbovirus-vector interactions. *Viruses,* 7**,** 820-43.

Blakqori, G., Van Knippenberg, I. & Elliott, R. M. 2009. Bunyamwera orthobunyavirus S-segment untranslated regions mediate poly(A) tail-independent translation. *J Virol,* 83**,** 3637-46.

Botros, B., Omar, A., Elian, K., Mohamed, G., Soliman, A., Salib, A., Salman, D., Saad, M. & Earhart, K. 2006. Adverse response of non-indigenous cattle of

European breeds to live attenuated Smithburn Rift Valley fever vaccine. *J Med Virol,* 78, 787-91.

Bouloy, M. & Weber, F. 2010. Molecular biology of rift valley Fever virus. *Open Virol J,* 4, 8-14.

Bowden, T. A., Bitto, D., Mclees, A., Yeromonahos, C., Elliott, R. M. & Huiskonen, J. T. 2013. Orthobunyavirus ultrastructure and the curious tripodal glycoprotein spike. *PLoS Pathog,* 9, e1003374.

Brasil, P., Pereira, J. P., Moreira, M. E., Ribeiro Nogueira, R. M., Damasceno, L., Wakimoto, M., Rabello, R. S., Valderramos, S. G., Halai, U. A., Salles, T. S., Zin, A. A., Horovitz, D., Daltro, P., Boechat, M., Raja Gabaglia, C., Carvalho De Sequeira, P., Pilotto, J. H., Medialdea-Carrera, R., Cotrim Da Cunha, D., Abreu De Carvalho, L. M., Pone, M., Machado Siqueira, A., Calvet, G. A., Rodrigues Baião, A. E., Neves, E. S., Nassar De Carvalho, P. R., Hasue, R. H., Marschik, P. B., Einspieler, C., Janzen, C., Cherry, J. D., Bispo De Filippis, A. M. & Nielsen-Saines, K. 2016. Zika Virus Infection in Pregnant Women in Rio de Janeiro. *N Engl J Med,* 375, 2321-2334.

Brennan, B., Li, P. & Elliott, R. M. 2011a. Generation and characterization of a recombinant Rift Valley fever virus expressing a V5 epitope-tagged RNA-dependent RNA polymerase. *J Gen Virol,* 92, 2906-13.

Brennan, B., Rezelj, V. V. & Elliott, R. M. 2017. Mapping of Transcription Termination within the S Segment of SFTS Phlebovirus Facilitated Generation of NSs Deletant Viruses. *J Virol,* 91.

Brennan, B., Welch, S. R. & Elliott, R. M. 2014. The consequences of reconfiguring the ambisense S genome segment of Rift Valley fever virus on viral replication in mammalian and mosquito cells and for genome packaging. *PLoS Pathog,* 10, e1003922.

Brennan, B., Welch, S. R., Mclees, A. & Elliott, R. M. 2011b. Creation of a recombinant Rift Valley fever virus with a two-segmented genome. *J Virol,* 85, 10310-8.

Bridgen, A. & Elliott, R. M. 1996. Rescue of a segmented negative-strand RNA virus entirely from cloned complementary DNAs. *Proc Natl Acad Sci U S A,* 93, 15400-4.

Bucher, E., Hemmes, H., De Haan, P., Goldbach, R. & Prins, M. 2004. The influenza A virus NS1 protein binds small interfering RNAs and suppresses RNA silencing in plants. *J Gen Virol,* 85, 983-91.

Buchholz, U. J., Finke, S. & Conzelmann, K. K. 1999. Generation of bovine respiratory syncytial virus (BRSV) from cDNA: BRSV NS2 is not essential for virus replication in tissue culture, and the human RSV leader region acts as a functional BRSV genome promoter. *J Virol,* 73, 251-9.

Busquets, N., Xavier, F., Martín-Folgar, R., Lorenzo, G., Galindo-Cardiel, I., Del Val, B. P., Rivas, R., Iglesias, J., Rodríguez, F., Solanes, D., Domingo, M. & Brun, A. 2010. Experimental infection of young adult European breed sheep with Rift Valley fever virus field isolates. *Vector Borne Zoonotic Dis,* 10, 689-96.

Campbell, C. L., Black, W. C., Hess, A. M. & Foy, B. D. 2008. Comparative genomics of small RNA regulatory pathway components in vector mosquitoes. *BMC Genomics,* 9, 425.

Cao-Lormeau, V. M., Blake, A., Mons, S., Lastere, S., Roche, C., Vanhomwegen, J., Dub, T., Baudouin, L., Teissier, A., Larre, P., Vial, A. L., Decam, C., Choumet, V., Halstead, S. K., Willison, H. J., Musset, L., Manuguerra, J. C., Despres, P., Fournier, E., Mallet, H. P., Musso, D., Fontanet, A., Neil, J. & Ghawché, F. 2016. Guillain-Barré Syndrome outbreak associated with Zika virus infection in French Polynesia: a case-control study. *Lancet,* 387, 1531-1539.

Caplen, H., Peters, C. J. & Bishop, D. H. 1985. Mutagen-directed attenuation of Rift Valley fever virus as a method for vaccine development. *J Gen Virol,* 66 (Pt 10), 2271-7.

Capobianco Dondona, A., Aschenborn, O., Pinoni, C., Di Gialleonardo, L., Maseke, A., Bortone, G., Polci, A., Scacchia, M., Molini, U. & Monaco, F. 2016.

Rift Valley Fever Virus among Wild Ruminants, Etosha National Park, Namibia, 2011. *Emerg Infect Dis,* 22, 128-30.

Carnec, X., Ermonval, M., Kreher, F., Flamand, M. & Bouloy, M. 2014. Role of the cytosolic tails of Rift Valley fever virus envelope glycoproteins in viral morphogenesis. *Virology,* 448, 1-14.

Carter, S. D., Surtees, R., Walter, C. T., Ariza, A., Bergeron, É., Nichol, S. T., Hiscox, J. A., Edwards, T. A. & Barr, J. N. 2012. Structure, function, and evolution of the Crimean-Congo hemorrhagic fever virus nucleocapsid protein. *J Virol,* 86, 10914-23.

Cha, S., Kang, M. S. & Seo, T. 2018. KSHV vPK inhibits Wnt signaling via preventing interactions between ß-catenin and TCF4. *Biochem Biophys Res Commun,* 497, 381-387.

Chengula, A. A., Mdegela, R. H. & Kasanga, C. J. 2013. Socio-economic impact of Rift Valley fever to pastoralists and agro pastoralists in Arusha, Manyara and Morogoro regions in Tanzania. *Springerplus,* 2, 549.

Choi, Y., Kwon, Y. C., Kim, S. I., Park, J. M., Lee, K. H. & Ahn, B. Y. 2008. A hantavirus causing hemorrhagic fever with renal syndrome requires gC1qR/p32 for efficient cell binding and infection. *Virology,* 381, 178-83.

Chung, H. C., Nguyen, V. G., Goede, D., Park, C. H., Kim, A. R., Moon, H. J., Park, S. J., Kim, H. K. & Park, B. K. 2014. Gouleako and Herbert viruses in pigs, Republic of Korea, 2013. *Emerg Infect Dis,* 20, 2072-5.

Clevers, H. & Nusse, R. 2012. Wnt/beta-catenin signaling and disease. *Cell,* 149, 1192-205.

Coetzer, J. A. 1982. The pathology of Rift Valley fever. II. Lesions occurring in field cases in adult cattle, calves and aborted foetuses. *Onderstepoort J Vet Res,* 49, 11-7.

Collett, M. S. 1986. Messenger RNA of the M segment RNA of Rift Valley fever virus. *Virology,* 151, 151-6.

Coombs, K. M., Berard, A., Xu, W., Krokhin, O., Meng, X., Cortens, J. P., Kobasa, D., Wilkins, J. & Brown, E. G. 2010. Quantitative proteomic analyses of influenza virus-infected cultured human lung cells. *J Virol,* 84, 10888-906.

Copeland, A. M., Altamura, L. A., Van Deusen, N. M. & Schmaljohn, C. S. 2013. Nuclear relocalization of polyadenylate binding protein during rift valley fever virus infection involves expression of the NSs gene. *J Virol,* 87, 11659-69.

Copeland, A. M., Van Deusen, N. M. & Schmaljohn, C. S. 2015. Rift Valley fever virus NSS gene expression correlates with a defect in nuclear mRNA export. *Virology,* 486, 88-93.

Csorba, T., Kontra, L. & Burgyán, J. 2015. viral silencing suppressors: Tools forged to fine-tune host-pathogen coexistence. *Virology,* 479-480, 85-103.

Cusi, M. G., Savellini, G. G. & Zanelli, G. 2010. Toscana virus epidemiology: from Italy to beyond. *Open Virol J,* 4, 22-8.

Cyr, N., De La Fuente, C., Lecoq, L., Guendel, I., Chabot, P. R., Kehn-Hall, K. & Omichinski, J. G. 2015. A ΩXaV motif in the Rift Valley fever virus NSs protein is essential for degrading p62, forming nuclear filaments and virulence. *Proc Natl Acad Sci U S A,* 112, 6021-6.

Cêtre-Sossah, C., Pédarrieu, A., Guis, H., Defernez, C., Bouloy, M., Favre, J., Girard, S., Cardinale, E. & Albina, E. 2012. Prevalence of Rift Valley Fever among ruminants, Mayotte. *Emerg Infect Dis,* 18, 972-5.

Dai, L., Song, J., Lu, X., Deng, Y. Q., Musyoki, A. M., Cheng, H., Zhang, Y., Yuan, Y., Song, H., Haywood, J., Xiao, H., Yan, J., Shi, Y., Qin, C. F., Qi, J. & Gao, G. F. 2016. Structures of the Zika Virus Envelope Protein and Its Complex with a Flavivirus Broadly Protective Antibody. *Cell Host Microbe,* 19, 696-704.

Dana, H., Chalbatani, G. M., Mahmoodzadeh, H., Karimloo, R., Rezaiean, O., Moradzadeh, A., Mehmandoost, N., Moazzen, F., Mazraeh, A., Marmari, V., Ebrahimi, M., Rashno, M. M., Abadi, S. J. & Gharagouzlo, E. 2017. Molecular Mechanisms and Biological Functions of siRNA. *Int J Biomed Sci,* 13**,** 48-57.

Daniels, D. L. & Weis, W. I. 2005. Beta-catenin directly displaces Groucho/TLE repressors from Tcf/Lef in Wnt-mediated transcription activation. *Nat Struct Mol Biol,* 12**,** 364-71.

Daubney, R., Hudson, J. R. & Garnham, P. C. 1931. Enzootic hepatitis or rift valley fever. An undescribed virus disease of sheep cattle and man from east africa

The Journal of Pathology and Bacteriology Volume 34, Issue 4. *The Journal of Pathology and Bacteriology* [Online], 34. Available: http://onlinelibrary.wiley.com/doi/10.1002/path.1700340418/abstract [Accessed 01].

De Boer, S. M., Kortekaas, J., De Haan, C. A., Rottier, P. J., Moormann, R. J. & Bosch, B. J. 2012a. Heparan sulfate facilitates Rift Valley fever virus entry into the cell. *J Virol,* 86**,** 13767-71.

De Boer, S. M., Kortekaas, J., Spel, L., Rottier, P. J., Moormann, R. J. & Bosch, B. J. 2012b. Acid-activated structural reorganization of the Rift Valley fever virus Gc fusion protein. *J Virol,* 86**,** 13642-52.

De Chassey, B., Meyniel-Schicklin, L., Vonderscher, J., André, P. & Lotteau, V. 2014. Virus-host interactomics: new insights and opportunities for antiviral drug discovery. *Genome Med,* 6**,** 115.

Debril, M. B., Dubuquoy, L., Feige, J. N., Wahli, W., Desvergne, B., Auwerx, J. & Gelman, L. 2005. Scaffold attachment factor B1 directly interacts with nuclear receptors in living cells and represses transcriptional activity. *J Mol Endocrinol,* 35**,** 503-17.

Deutsch, E. W., Csordas, A., Sun, Z., Jarnuczak, A., Perez-Riverol, Y., Ternent, T., Campbell, D. S., Bernal-Llinares, M., Okuda, S., Kawano, S., Moritz, R. L., Carver, J. J., Wang, M., Ishihama, Y., Bandeira, N., Hermjakob, H. & Vizcaíno, J. A. 2017. The ProteomeXchange consortium in 2017: supporting the cultural change in proteomics public data deposition. *Nucleic Acids Res,* 45**,** D1100-D1106.

Dick, G. W., Kitchen, S. F. & Haddow, A. J. 1952. Zika virus. I. Isolations and serological specificity. *Trans R Soc Trop Med Hyg,* 46**,** 509-20.

Dietrich, I., Jansen, S., Fall, G., Lorenzen, S., Rudolf, M., Huber, K., Heitmann, A., Schicht, S., Ndiaye, E. H., Watson, M., Castelli, I., Brennan, B., Elliott, R. M., Diallo, M., Sall, A. A., Failloux, A. B., Schnettler, E., Kohl, A. & Becker, S. C. 2017. RNA Interference Restricts Rift Valley Fever Virus in Multiple Insect Systems. *mSphere,* 2.

Dong, H., Li, P., Elliott, R. M. & Dong, C. 2013. Structure of Schmallenberg orthobunyavirus nucleoprotein suggests a novel mechanism of genome encapsidation. *J Virol,* 87**,** 5593-601.

Edgil, D., Diamond, M. S., Holden, K. L., Paranjape, S. M. & Harris, E. 2003. Translation efficiency determines differences in cellular infection among dengue virus type 2 strains. *Virology,* 317**,** 275-90.

Eifan, S., Schnettler, E., Dietrich, I., Kohl, A. & Blomström, A. L. 2013. Non-structural proteins of arthropod-borne bunyaviruses: roles and functions. *Viruses,* 5**,** 2447-68.

Eifan, S. A. & Elliott, R. M. 2009. Mutational analysis of the Bunyamwera orthobunyavirus nucleocapsid protein gene. *J Virol,* 83**,** 11307-17.

Ellenbecker, M., Sears, L., Li, P., Lanchy, J. M. & Lodmell, J. S. 2012. Characterization of RNA aptamers directed against the nucleocapsid protein of Rift Valley fever virus. *Antiviral Res,* 93**,** 330-9.

Elliott, R. M. 2014. Orthobunyaviruses: recent genetic and structural insights. *Nat Rev Microbiol,* 12**,** 673-85.

Ellis, D. S., Shirodaria, P. V., Fleming, E. & Simpson, D. I. 1988. Morphology and development of Rift Valley fever virus in Vero cell cultures. *J Med Virol,* 24**,** 161-74.

Endris, R. G., Tesh, R. B. & Young, D. G. 1983. Transovarial transmission of Rio Grande virus (Bunyaviridae: Phlebovirus) by the sand fly, Lutzomyia anthophora. *Am J Trop Med Hyg,* 32**,** 862-4.

Faye, O., Freire, C. C., Iamarino, A., De Oliveira, J. V., Diallo, M., Zanotto, P. M. & Sall, A. A. 2014. Molecular evolution of Zika virus during its emergence in the 20(th) century. *PLoS Negl Trop Dis,* 8**,** e2636.

Ferguson, M. C., Saul, S., Fragkoudis, R., Weisheit, S., Cox, J., Patabendige, A., Sherwood, K., Watson, M., Merits, A. & Fazakerley, J. K. 2015. Ability of the Encephalitic Arbovirus Semliki Forest Virus To Cross the Blood-Brain Barrier Is Determined by the Charge of the E2 Glycoprotein. *J Virol,* 89**,** 7536-49.

Ferron, F., Li, Z., Danek, E. I., Luo, D., Wong, Y., Coutard, B., Lantez, V., Charrel, R., Canard, B., Walz, T. & Lescar, J. 2011. The hexamer structure of Rift Valley fever virus nucleoprotein suggests a mechanism for its assembly into ribonucleoprotein complexes. *PLoS Pathog,* 7**,** e1002030.

Fill, M. A., Compton, M. L., Mcdonald, E. C., Moncayo, A. C., Dunn, J. R., Schaffner, W., Bhatnagar, J., Zaki, S. R., Jones, T. F. & Shieh, W. J. 2017. Novel Clinical and Pathologic Findings in a Heartland Virus-Associated Death. *Clin Infect Dis,* 64**,** 510-512.

Filone, C. M., Hanna, S. L., Caino, M. C., Bambina, S., Doms, R. W. & Cherry, S. 2010. Rift valley fever virus infection of human cells and insect hosts is promoted by protein kinase C epsilon. *PLoS One,* 5**,** e15483.

Fontana, J., López-Montero, N., Elliott, R. M., Fernández, J. J. & Risco, C. 2008. The unique architecture of Bunyamwera virus factories around the Golgi complex. *Cell Microbiol,* 10**,** 2012-28.

Freiberg, A. N., Sherman, M. B., Morais, M. C., Holbrook, M. R. & Watowich, S. J. 2008. Three-dimensional organization of Rift Valley fever virus revealed by cryoelectron tomography. *J Virol,* 82**,** 10341-8.

Garcin, D., Lezzi, M., Dobbs, M., Elliott, R. M., Schmaljohn, C., Kang, C. Y. & Kolakofsky, D. 1995. The 5' ends of Hantaan virus (Bunyaviridae) RNAs suggest a prime-and-realign mechanism for the initiation of RNA synthesis. *J Virol,* 69**,** 5754-62.

Garry, C. E. & Garry, R. F. 2004. Proteomics computational analyses suggest that the carboxyl terminal glycoproteins of Bunyaviruses are class II viral fusion protein (beta-penetrenes). *Theor Biol Med Model,* 1**,** 10.

Gauliard, N., Billecocq, A., Flick, R. & Bouloy, M. 2006. Rift Valley fever virus noncoding regions of L, M and S segments regulate RNA synthesis. *Virology,* 351**,** 170-9.

Gavrilovskaya, I. N., Shepley, M., Shaw, R., Ginsberg, M. H. & Mackow, E. R. 1998. beta3 Integrins mediate the cellular entry of hantaviruses that cause respiratory failure. *Proc Natl Acad Sci U S A,* 95**,** 7074-9.

Gear, J. H. 1979. Hemorrhagic fevers, with special reference to recent outbreaks in southern Africa. *Rev Infect Dis,* 1**,** 571-91.

Georges, T. M., Justin, M., Victor, M., Marie, K. J., Mark, R. & Léopold, M. M. K. 2018. Seroprevalence and Virus Activity of Rift Valley Fever in Cattle in Eastern Region of Democratic Republic of the Congo. *J Vet Med,* 2018**,** 4956378.

Gerrard, S. R., Bird, B. H., Albariño, C. G. & Nichol, S. T. 2007. The NSm proteins of Rift Valley fever virus are dispensable for maturation, replication and infection. *Virology,* 359**,** 459-65.

Gerrard, S. R. & Nichol, S. T. 2002. Characterization of the Golgi retention motif of Rift Valley fever virus G(N) glycoprotein. *J Virol,* 76**,** 12200-10.

Gould, E., Pettersson, J., Higgs, S., Charrel, R. & De Lamballerie, X. 2017. Emerging arboviruses: Why today? *One Health,* 4**,** 1-13.

Grant, A., Ponia, S. S., Tripathi, S., Balasubramaniam, V., Miorin, L., Sourisseau, M., Schwarz, M. C., Sánchez-Seco, M. P., Evans, M. J., Best, S. M. & García-Sastre, A. 2016. Zika Virus Targets Human STAT2 to Inhibit Type I Interferon Signaling. *Cell Host Microbe,* 19**,** 882-90.

Guu, T. S., Zheng, W. & Tao, Y. J. 2012. Bunyavirus: structure and replication. *Adv Exp Med Biol,* 726**,** 245-66.

Habjan, M., Penski, N., Spiegel, M. & Weber, F. 2008. T7 RNA polymerase-dependent and -independent systems for cDNA-based rescue of Rift Valley fever virus. *J Gen Virol,* 89**,** 2157-66.

Habjan, M., Penski, N., Wagner, V., Spiegel, M., Overby, A. K., Kochs, G., Huiskonen, J. T. & Weber, F. 2009. Efficient production of Rift Valley fever virus-like particles: The antiviral protein MxA can inhibit primary transcription of bunyaviruses. *Virology,* 385**,** 400-8.

Hammond, S. M., Bernstein, E., Beach, D. & Hannon, G. J. 2000. An RNA-directed nuclease mediates post-transcriptional gene silencing in Drosophila cells. *Nature,* 404**,** 293-6.

Harmon, B., Bird, S. W., Schudel, B. R., Hatch, A. V., Rasley, A. & Negrete, O. A. 2016. A Genome-Wide RNA Interference Screen Identifies a Role for Wnt/β-Catenin Signaling during Rift Valley Fever Virus Infection. *J Virol,* 90**,** 7084-97.

Harmon, B., Schudel, B. R., Maar, D., Kozina, C., Ikegami, T., Tseng, C. T. & Negrete, O. A. 2012. Rift Valley fever virus strain MP-12 enters mammalian host cells via caveola-mediated endocytosis. *J Virol,* 86**,** 12954-70.

Harrington, D. G., Lupton, H. W., Crabbs, C. L., Peters, C. J., Reynolds, J. A. & Slone, T. W. 1980. Evaluation of a formalin-inactivated Rift Valley fever vaccine in sheep. *Am J Vet Res,* 41**,** 1559-64.

Henderson, L. J., Sharma, A., Monaco, M. C., Major, E. O. & Al-Harthi, L. 2012. Human immunodeficiency virus type 1 (HIV-1) transactivator of transcription through its intact core and cysteine-rich domains inhibits Wnt/β-catenin signaling in astrocytes: relevance to HIV neuropathogenesis. *J Neurosci,* 32**,** 16306-13.

Hepojoki, J., Strandin, T., Wang, H., Vapalahti, O., Vaheri, A. & Lankinen, H. 2010. Cytoplasmic tails of hantavirus glycoproteins interact with the nucleocapsid protein. *J Gen Virol,* 91**,** 2341-50.

Hiramoto, H., Dansako, H., Takeda, M., Satoh, S., Wakita, T., Ikeda, M. & Kato, N. 2015. Annexin A1 negatively regulates viral RNA replication of hepatitis C virus. *Acta Med Okayama,* 69**,** 71-8.

Hobson-Peters, J., Warrilow, D., Mclean, B. J., Watterson, D., Colmant, A. M., Van Den Hurk, A. F., Hall-Mendelin, S., Hastie, M. L., Gorman, J. J., Harrison, J. J., Prow, N. A., Barnard, R. T., Allcock, R., Johansen, C. A. & Hall, R. A. 2016. Discovery and characterisation of a new insect-specific bunyavirus from Culex mosquitoes captured in northern Australia. *Virology,* 489**,** 269-81.

Hofmann, H., Li, X., Zhang, X., Liu, W., Kühl, A., Kaup, F., Soldan, S. S., González-Scarano, F., Weber, F., He, Y. & Pöhlmann, S. 2013. Severe fever with thrombocytopenia virus glycoproteins are targeted by neutralizing antibodies and can use DC-SIGN as a receptor for pH-dependent entry into human and animal cell lines. *J Virol,* 87**,** 4384-94.

Hollidge, B. S., Nedelsky, N. B., Salzano, M. V., Fraser, J. W., González-Scarano, F. & Soldan, S. S. 2012. Orthobunyavirus entry into neurons and other mammalian cells occurs via clathrin-mediated endocytosis and requires trafficking into early endosomes. *J Virol,* 86**,** 7988-8001.

Hornak, K. E., Lanchy, J. M. & Lodmell, J. S. 2016. RNA Encapsidation and Packaging in the Phleboviruses. *Viruses,* 8.

Hornung, V., Ellegast, J., Kim, S., Brzózka, K., Jung, A., Kato, H., Poeck, H., Akira, S., Conzelmann, K. K., Schlee, M., Endres, S. & Hartmann, G. 2006. 5'-Triphosphate RNA is the ligand for RIG-I. *Science,* 314, 994-7.

Huiskonen, J. T., Hepojoki, J., Laurinmäki, P., Vaheri, A., Lankinen, H., Butcher, S. J. & Grünewald, K. 2010. Electron cryotomography of Tula hantavirus suggests a unique assembly paradigm for enveloped viruses. *J Virol,* 84, 4889-97.

Hutchinson, K. L., Peters, C. J. & Nichol, S. T. 1996. Sin Nombre virus mRNA synthesis. *Virology,* 224, 139-49.

Ikegami, T. 2012. Molecular biology and genetic diversity of Rift Valley fever virus. *Antiviral Res,* 95, 293-310.

Ikegami, T. 2017. Rift Valley fever vaccines: an overview of the safety and efficacy of the live-attenuated MP-12 vaccine candidate. *Expert Rev Vaccines,* 16, 601-611.

Ikegami, T., Hill, T. E., Smith, J. K., Zhang, L., Juelich, T. L., Gong, B., Slack, O. A., Ly, H. J., Lokugamage, N. & Freiberg, A. N. 2015. Rift Valley Fever Virus MP-12 Vaccine Is Fully Attenuated by a Combination of Partial Attenuations in the S, M, and L Segments. *J Virol,* 89, 7262-76.

Ikegami, T. & Makino, S. 2011. The pathogenesis of Rift Valley fever. *Viruses,* 3, 493-519.

Ikegami, T., Won, S., Peters, C. J. & Makino, S. 2007. Characterization of Rift Valley fever virus transcriptional terminations. *J Virol,* 81, 8421-38.

Jiang, X. H., Xie, Y. T., Cai, Y. P., Ren, J. & Ma, T. 2017. Effects of hepatitis C virus core protein and nonstructural protein 4B on the Wnt/ß-catenin pathway. *BMC Microbiol,* 17, 124.

Junglen, S., Marklewitz, M., Zirkel, F., Wollny, R., Meyer, B., Heidemann, H., Metzger, S., Annan, A., Dei, D., Leendertz, F. H., Oppong, S. & Drosten, C. 2015. No Evidence of Gouléako and Herbert Virus Infections in Pigs, Côte d'Ivoire and Ghana. *Emerg Infect Dis,* 21, 2190-3.

Kading, R. C., Crabtree, M. B., Bird, B. H., Nichol, S. T., Erickson, B. R., Horiuchi, K., Biggerstaff, B. J. & Miller, B. R. 2014. Deletion of the NSm virulence gene of Rift Valley fever virus inhibits virus replication in and dissemination from the midgut of Aedes aegypti mosquitoes. *PLoS Negl Trop Dis,* 8, e2670.

Kainulainen, M., Habjan, M., Hubel, P., Busch, L., Lau, S., Colinge, J., Superti-Furga, G., Pichlmair, A. & Weber, F. 2014. Virulence factor NSs of rift valley fever virus recruits the F-box protein FBXO3 to degrade subunit p62 of general transcription factor TFIIH. *J Virol,* 88, 3464-73.

Kakumani, P. K., Ponia, S. S., S, R. K., Sood, V., Chinnappan, M., Banerjea, A. C., Medigeshi, G. R., Malhotra, P., Mukherjee, S. K. & Bhatnagar, R. K. 2013. Role of RNA interference (RNAi) in dengue virus replication and identification of NS4B as an RNAi suppressor. *J Virol,* 87, 8870-83.

Kalveram, B., Lihoradova, O. & Ikegami, T. 2011. NSs protein of rift valley fever virus promotes posttranslational downregulation of the TFIIH subunit p62. *J Virol,* 85, 6234-43.

Kanazawa, A., Tsukada, S., Sekine, A., Tsunoda, T., Takahashi, A., Kashiwagi, A., Tanaka, Y., Babazono, T., Matsuda, M., Kaku, K., Iwamoto, Y., Kawamori, R., Kikkawa, R., Nakamura, Y. & Maeda, S. 2004. Association of the gene encoding wingless-type mammary tumor virus integration-site family member 5B (WNT5B) with type 2 diabetes. *Am J Hum Genet,* 75, 832-43.

Katz, A., Freiberg, A. N., Backstrom, V., Schulz, A. R., Mateos, A., Holm, L., Pettersson, R. F., Vaheri, A., Flick, R. & Plyusnin, A. 2010a. Oligomerization of Uukuniemi virus nucleocapsid protein. *Virol J,* 7, 187.

Katz, A., Freiberg, A. N., Backström, V., Schulz, A. R., Mateos, A., Holm, L., Pettersson, R. F., Vaheri, A., Flick, R. & Plyusnin, A. 2010b. Oligomerization of Uukuniemi virus nucleocapsid protein. *Virol J,* 7**,** 187.

Kaul, A., Woerz, I., Meuleman, P., Leroux-Roels, G. & Bartenschlager, R. 2007. Cell culture adaptation of hepatitis C virus and in vivo viability of an adapted variant. *J Virol,* 81**,** 13168-79.

Kemp, C. & Imler, J. L. 2009. Antiviral immunity in drosophila. *Curr Opin Immunol,* 21**,** 3-9.

King, B. R., Hershkowitz, D., Eisenhauer, P. L., Weir, M. E., Ziegler, C. M., Russo, J., Bruce, E. A., Ballif, B. A. & Botten, J. 2017. A Map of the Arenavirus Nucleoprotein-Host Protein Interactome Reveals that Junín Virus Selectively Impairs the Antiviral Activity of Double-Stranded RNA-Activated Protein Kinase (PKR). *J Virol,* 91.

Kohl, A., Dunn, E. F., Lowen, A. C. & Elliott, R. M. 2004. Complementarity, sequence and structural elements within the 3' and 5' non-coding regions of the Bunyamwera orthobunyavirus S segment determine promoter strength. *J Gen Virol,* 85**,** 3269-78.

Kraemer, M. U., Sinka, M. E., Duda, K. A., Mylne, A. Q., Shearer, F. M., Barker, C. M., Moore, C. G., Carvalho, R. G., Coelho, G. E., Van Bortel, W., Hendrickx, G., Schaffner, F., Elyazar, I. R., Teng, H. J., Brady, O. J., Messina, J. P., Pigott, D. M., Scott, T. W., Smith, D. L., Wint, G. R., Golding, N. & Hay, S. I. 2015. The global distribution of the arbovirus vectors Aedes aegypti and Ae. albopictus. *Elife,* 4**,** e08347.

Krautkrämer, E. & Zeier, M. 2008. Hantavirus causing hemorrhagic fever with renal syndrome enters from the apical surface and requires decay-accelerating factor (DAF/CD55). *J Virol,* 82**,** 4257-64.

Kreher, F., Tamietti, C., Gommet, C., Guillemot, L., Ermonval, M., Failloux, A. B., Panthier, J. J., Bouloy, M. & Flamand, M. 2014. The Rift Valley fever

accessory proteins NSm and P78/NSm-GN are distinct determinants of virus propagation in vertebrate and invertebrate hosts. *Emerg Microbes Infect,* 3, e71.

Kwak, H., Park, M. W. & Jeong, S. 2011. Annexin A2 binds RNA and reduces the frameshifting efficiency of infectious bronchitis virus. *PLoS One,* 6, e24067.

Labeaud, A. D., Muiruri, S., Sutherland, L. J., Dahir, S., Gildengorin, G., Morrill, J., Muchiri, E. M., Peters, C. J. & King, C. H. 2011. Postepidemic analysis of Rift Valley fever virus transmission in northeastern kenya: a village cohort study. *PLoS Negl Trop Dis,* 5, e1265.

Lara, E., Billecocq, A., Leger, P. & Bouloy, M. 2011. Characterization of wild-type and alternate transcription termination signals in the Rift Valley fever virus genome. *J Virol,* 85, 12134-45.

Laughlin, L. W., Meegan, J. M., Strausbaugh, L. J., Morens, D. M. & Watten, R. H. 1979. Epidemic Rift Valley fever in Egypt: observations of the spectrum of human illness. *Trans R Soc Trop Med Hyg,* 73, 630-3.

Le May, N., Dubaele, S., Proietti De Santis, L., Billecocq, A., Bouloy, M. & Egly, J. M. 2004. TFIIH transcription factor, a target for the Rift Valley hemorrhagic fever virus. *Cell,* 116, 541-50.

Le May, N., Gauliard, N., Billecocq, A. & Bouloy, M. 2005. The N terminus of Rift Valley fever virus nucleoprotein is essential for dimerization. *J Virol,* 79, 11974-80.

Le May, N., Mansuroglu, Z., Léger, P., Josse, T., Blot, G., Billecocq, A., Flick, R., Jacob, Y., Bonnefoy, E. & Bouloy, M. 2008. A SAP30 complex inhibits IFN-beta expression in Rift Valley fever virus infected cells. *PLoS Pathog,* 4, e13.

Leonard, V. H., Kohl, A., Osborne, J. C., Mclees, A. & Elliott, R. M. 2005. Homotypic interaction of Bunyamwera virus nucleocapsid protein. *J Virol,* 79, 13166-72.

Lindenbach, B. D. & Rice, C. M. 1999. Genetic interaction of flavivirus nonstructural proteins NS1 and NS4A as a determinant of replicase function. *J Virol,* 73, 4611-21.

Liu, J., Carmell, M. A., Rivas, F. V., Marsden, C. G., Thomson, J. M., Song, J. J., Hammond, S. M., Joshua-Tor, L. & Hannon, G. J. 2004. Argonaute2 is the catalytic engine of mammalian RNAi. *Science,* 305, 1437-41.

Liu, Q., He, B., Huang, S. Y., Wei, F. & Zhu, X. Q. 2014. Severe fever with thrombocytopenia syndrome, an emerging tick-borne zoonosis. *Lancet Infect Dis,* 14, 763-772.

Lokugamage, N., Freiberg, A. N., Morrill, J. C. & Ikegami, T. 2012. Genetic subpopulations of Rift Valley fever virus strains ZH548 and MP-12 and recombinant MP-12 strains. *J Virol,* 86, 13566-75.

Lowen, A. C. & Elliott, R. M. 2005. Mutational analyses of the nonconserved sequences in the Bunyamwera Orthobunyavirus S segment untranslated regions. *J Virol,* 79, 12861-70.

Lowen, A. C., Noonan, C., Mclees, A. & Elliott, R. M. 2004. Efficient bunyavirus rescue from cloned cDNA. *Virology,* 330, 493-500.

Lozach, P. Y., Kühbacher, A., Meier, R., Mancini, R., Bitto, D., Bouloy, M. & Helenius, A. 2011. DC-SIGN as a receptor for phleboviruses. *Cell Host Microbe,* 10, 75-88.

Lozach, P. Y., Mancini, R., Bitto, D., Meier, R., Oestereich, L., Overby, A. K., Pettersson, R. F. & Helenius, A. 2010. Entry of bunyaviruses into mammalian cells. *Cell Host Microbe,* 7, 488-99.

Lumley, S., Horton, D. L., Hernandez-Triana, L. L. M., Johnson, N., Fooks, A. R. & Hewson, R. 2017. Rift Valley fever virus: strategies for maintenance, survival and vertical transmission in mosquitoes. *J Gen Virol,* 98, 875-887.

Ly, H. J. & Ikegami, T. 2016. Rift Valley fever virus NSs protein functions and the similarity to other bunyavirus NSs proteins. *Virol J,* 13**,** 118.

Ly, H. J., Lokugamage, N., Nishiyama, S. & Ikegami, T. 2017. Risk analysis of inter-species reassortment through a Rift Valley fever phlebovirus MP-12 vaccine strain. *PLoS One,* 12**,** e0185194.

Léger, P., Lara, E., Jagla, B., Sismeiro, O., Mansuroglu, Z., Coppée, J. Y., Bonnefoy, E. & Bouloy, M. 2013. Dicer-2- and Piwi-mediated RNA interference in Rift Valley fever virus-infected mosquito cells. *J Virol,* 87**,** 1631-48.

Léger, P., Tetard, M., Youness, B., Cordes, N., Rouxel, R. N., Flamand, M. & Lozach, P. Y. 2016. Differential Use of the C-Type Lectins L-SIGN and DC-SIGN for Phlebovirus Endocytosis. *Traffic,* 17**,** 639-56.

Macpherson, I. & Stoker, M. 1962. Polyoma transformation of hamster cell clones--an investigation of genetic factors affecting cell competence. *Virology,* 16**,** 147-51.

Madani, T. A., Al-Mazrou, Y. Y., Al-Jeffri, M. H., Mishkhas, A. A., Al-Rabeah, A. M., Turkistani, A. M., Al-Sayed, M. O., Abodahish, A. A., Khan, A. S., Ksiazek, T. G. & Shobokshi, O. 2003. Rift Valley fever epidemic in Saudi Arabia: epidemiological, clinical, and laboratory characteristics. *Clin Infect Dis,* 37**,** 1084-92.

Mandell, R. B. & Flick, R. 2010. Rift Valley fever virus: an unrecognized emerging threat? *Hum Vaccin,* 6**,** 597-601.

Mani, A., Radhakrishnan, J., Wang, H., Mani, M. A., Nelson-Williams, C., Carew, K. S., Mane, S., Najmabadi, H., Wu, D. & Lifton, R. P. 2007. LRP6 mutation in a family with early coronary disease and metabolic risk factors. *Science,* 315**,** 1278-82.

Marcato, V., Luron, L., Laqueuvre, L. M., Simon, D., Mansuroglu, Z., Flamand, M., Panthier, J. J., Souès, S., Massaad, C. & Bonnefoy, E. 2016. ß-Catenin Upregulates the Constitutive and Virus-Induced Transcriptional Capacity of the

Interferon Beta Promoter through T-Cell Factor Binding Sites. *Mol Cell Biol,* 36, 13-29.

Matsuno, K., Weisend, C., Travassos Da Rosa, A. P., Anzick, S. L., Dahlstrom, E., Porcella, S. F., Dorward, D. W., Yu, X. J., Tesh, R. B. & Ebihara, H. 2013. Characterization of the Bhanja serogroup viruses (Bunyaviridae): a novel species of the genus Phlebovirus and its relationship with other emerging tick-borne phleboviruses. *J Virol,* 87, 3719-28.

Mcneill, H. & Woodgett, J. R. 2010. When pathways collide: collaboration and connivance among signalling proteins in development. *Nat Rev Mol Cell Biol,* 11, 404-13.

Meier, R., Franceschini, A., Horvath, P., Tetard, M., Mancini, R., Von Mering, C., Helenius, A. & Lozach, P. Y. 2014. Genome-wide small interfering RNA screens reveal VAMP3 as a novel host factor required for Uukuniemi virus late penetration. *J Virol,* 88, 8565-78.

Mir, M. A., Duran, W. A., Hjelle, B. L., Ye, C. & Panganiban, A. T. 2008. Storage of cellular 5' mRNA caps in P bodies for viral cap-snatching. *Proc Natl Acad Sci U S A,* 105, 19294-9.

Mir, M. A. & Panganiban, A. T. 2004. Trimeric hantavirus nucleocapsid protein binds specifically to the viral RNA panhandle. *J Virol,* 78, 8281-8.

Mir, M. A. & Panganiban, A. T. 2006a. Characterization of the RNA chaperone activity of hantavirus nucleocapsid protein. *J Virol,* 80, 6276-85.

Mir, M. A. & Panganiban, A. T. 2006b. The bunyavirus nucleocapsid protein is an RNA chaperone: possible roles in viral RNA panhandle formation and genome replication. *RNA,* 12, 272-82.

More, S., Yang, X., Zhu, Z., Bamunuarachchi, G., Guo, Y., Huang, C., Bailey, K., Metcalf, J. P. & Liu, L. 2018. Regulation of influenza virus replication by Wnt/ß-catenin signaling. *PLoS One,* 13, e0191010.

Morrill, J. C., Jennings, G. B., Caplen, H., Turell, M. J., Johnson, A. J. & Peters, C. J. 1987. Pathogenicity and immunogenicity of a mutagen-attenuated Rift Valley fever virus immunogen in pregnant ewes. *Am J Vet Res,* 48**,** 1042-7.

Morrill, J. C., Laughlin, R. C., Lokugamage, N., Pugh, R., Sbrana, E., Weise, W. J., Adams, L. G., Makino, S. & Peters, C. J. 2013. Safety and immunogenicity of recombinant Rift Valley fever MP-12 vaccine candidates in sheep. *Vaccine,* 31**,** 559-65.

Morvan, J., Fontenille, D., Saluzzo, J. F. & Coulanges, P. 1991. Possible Rift Valley fever outbreak in man and cattle in Madagascar. *Trans R Soc Trop Med Hyg,* 85**,** 108.

Mottram, T. J., Li, P., Dietrich, I., Shi, X., Brennan, B., Varjak, M. & Kohl, A. 2017. Mutational analysis of Rift Valley fever phlebovirus nucleocapsid protein indicates novel conserved, functional amino acids. *PLoS Negl Trop Dis,* 11**,** e0006155.

Murakami, S., Terasaki, K., Narayanan, K. & Makino, S. 2012. Roles of the coding and noncoding regions of rift valley Fever virus RNA genome segments in viral RNA packaging. *J Virol,* 86**,** 4034-9.

Mutso, M., Saul, S., Rausalu, K., Susova, O., Žusinaite, E., Mahalingam, S. & Merits, A. 2017. Reverse genetic system, genetically stable reporter viruses and packaged subgenomic replicon based on a Brazilian Zika virus isolate. *J Gen Virol,* 98**,** 2712-2724.

Myles, K. M., Wiley, M. R., Morazzani, E. M. & Adelman, Z. N. 2008. Alphavirus-derived small RNAs modulate pathogenesis in disease vector mosquitoes. *Proc Natl Acad Sci U S A,* 105**,** 19938-43.

Müller, R., Poch, O., Delarue, M., Bishop, D. H. & Bouloy, M. 1994. Rift Valley fever virus L segment: correction of the sequence and possible functional role of newly identified regions conserved in RNA-dependent polymerases. *J Gen Virol,* 75 (Pt 6)**,** 1345-52.

Nakabayashi, H., Taketa, K., Miyano, K., Yamane, T. & Sato, J. 1982. Growth of human hepatoma cells lines with differentiated functions in chemically defined medium. *Cancer Res,* 42**,** 3858-63.

Nanyingi, M. O., Munyua, P., Kiama, S. G., Muchemi, G. M., Thumbi, S. M., Bitek, A. O., Bett, B., Muriithi, R. M. & Njenga, M. K. 2015. A systematic review of Rift Valley Fever epidemiology 1931-2014. *Infect Ecol Epidemiol,* 5**,** 28024.

Narasipura, S. D., Henderson, L. J., Fu, S. W., Chen, L., Kashanchi, F. & Al-Harthi, L. 2012. Role of β-catenin and TCF/LEF family members in transcriptional activity of HIV in astrocytes. *J Virol,* 86**,** 1911-21.

Narayanan, A., Popova, T., Turell, M., Kidd, J., Chertow, J., Popov, S. G., Bailey, C., Kashanchi, F. & Kehn-Hall, K. 2011. Alteration in superoxide dismutase 1 causes oxidative stress and p38 MAPK activation following RVFV infection. *PLoS One,* 6**,** e20354.

Nepomichene, T. N. J. J., Raharimalala, F. N., Andriamandimby, S. F., Ravalohery, J. P., Failloux, A. B., Heraud, J. M. & Boyer, S. 2018. Vector competence of Culex antennatus and Anopheles coustani mosquitoes for Rift Valley fever virus in Madagascar. *Med Vet Entomol,* 32**,** 259-262.

Nuss, J. E., Kehn-Hall, K., Benedict, A., Costantino, J., Ward, M., Peyser, B. D., Retterer, C. J., Tressler, L. E., Wanner, L. M., Mcgovern, H. F., Zaidi, A., Anthony, S. M., Kota, K. P., Bavari, S. & Hakami, R. M. 2014. Multi-faceted proteomic characterization of host protein complement of Rift Valley fever virus virions and identification of specific heat shock proteins, including HSP90, as important viral host factors. *PLoS One,* 9**,** e93483.

Nyakarahuka, L., De St Maurice, A., Purpura, L., Ervin, E., Balinandi, S., Tumusiime, A., Kyondo, J., Mulei, S., Tusiime, P., Lutwama, J., Klena, J. D., Brown, S., Knust, B., Rollin, P. E., Nichol, S. T. & Shoemaker, T. R. 2018. Prevalence and risk factors of Rift Valley fever in humans and animals from Kabale district in Southwestern Uganda, 2016. *PLoS Negl Trop Dis,* 12**,** e0006412.

Obbard, D. J., Jiggins, F. M., Halligan, D. L. & Little, T. J. 2006. Natural selection drives extremely rapid evolution in antiviral RNAi genes. *Curr Biol,* 16**,** 580-5.

Obijeski, J. F., Bishop, D. H., Palmer, E. L. & Murphy, F. A. 1976. Segmented genome and nucleocapsid of La Crosse virus. *J Virol,* 20**,** 664-75.

Oesterreich, S. 2003. Scaffold attachment factors SAFB1 and SAFB2: Innocent bystanders or critical players in breast tumorigenesis? *J Cell Biochem,* 90**,** 653-61.

Olal, D., Dick, A., Woods, V. L., Liu, T., Li, S., Devignot, S., Weber, F., Saphire, E. O. & Daumke, O. 2014. Structural insights into RNA encapsidation and helical assembly of the Toscana virus nucleoprotein. *Nucleic Acids Res,* 42**,** 6025-37.

Osborne, J. C. & Elliott, R. M. 2000. RNA binding properties of bunyamwera virus nucleocapsid protein and selective binding to an element in the 5' terminus of the negative-sense S segment. *J Virol,* 74**,** 9946-52.

Overby, A. K., Pettersson, R. F., Grünewald, K. & Huiskonen, J. T. 2008. Insights into bunyavirus architecture from electron cryotomography of Uukuniemi virus. *Proc Natl Acad Sci U S A,* 105**,** 2375-9.

Overby, A. K., Pettersson, R. F. & Neve, E. P. 2007. The glycoprotein cytoplasmic tail of Uukuniemi virus (Bunyaviridae) interacts with ribonucleoproteins and is critical for genome packaging. *J Virol,* 81**,** 3198-205.

Panganiban, A. T. & Mir, M. A. 2009. Bunyavirus N: eIF4F surrogate and cap-guardian. *Cell Cycle,* 8**,** 1332-7.

Pathak, S., De Souza, G. A., Salte, T., Wiker, H. G. & Asjö, B. 2009. HIV induces both a down-regulation of IRAK-4 that impairs TLR signalling and an up-regulation of the antibiotic peptide dermcidin in monocytic cells. *Scand J Immunol,* 70**,** 264-76.

Patterson, J. L., Holloway, B. & Kolakofsky, D. 1984. La Crosse virions contain a primer-stimulated RNA polymerase and a methylated cap-dependent endonuclease. *J Virol,* 52**,** 215-22.

Pepin, M., Bouloy, M., Bird, B. H., Kemp, A. & Paweska, J. 2010. Rift Valley fever virus(Bunyaviridae: Phlebovirus): an update on pathogenesis, molecular epidemiology, vectors, diagnostics and prevention. *Vet Res,* 41**,** 61.

Perez, C., Mckinney, C., Chulunbaatar, U. & Mohr, I. 2011. Translational control of the abundance of cytoplasmic poly(A) binding protein in human cytomegalovirus-infected cells. *J Virol,* 85**,** 156-64.

Perez-Riverol, Y., Xu, Q. W., Wang, R., Uszkoreit, J., Griss, J., Sanchez, A., Reisinger, F., Csordas, A., Ternent, T., Del-Toro, N., Dianes, J. A., Eisenacher, M., Hermjakob, H. & Vizcaíno, J. A. 2016. PRIDE Inspector Toolsuite: Moving Toward a Universal Visualization Tool for Proteomics Data Standard Formats and Quality Assessment of ProteomeXchange Datasets. *Mol Cell Proteomics,* 15**,** 305-17.

Petersen, E., Wilson, M. E., Touch, S., Mccloskey, B., Mwaba, P., Bates, M., Dar, O., Mattes, F., Kidd, M., Ippolito, G., Azhar, E. I. & Zumla, A. 2016. Rapid Spread of Zika Virus in The Americas--Implications for Public Health Preparedness for Mass Gatherings at the 2016 Brazil Olympic Games. *Int J Infect Dis,* 44**,** 11-5.

Phoenix, I., Lokugamage, N., Nishiyama, S. & Ikegami, T. 2016a. Mutational Analysis of the Rift Valley Fever Virus Glycoprotein Precursor Proteins for Gn Protein Expression. *Viruses,* 8.

Phoenix, I., Nishiyama, S., Lokugamage, N., Hill, T. E., Huante, M. B., Slack, O. A., Carpio, V. H., Freiberg, A. N. & Ikegami, T. 2016b. N-Glycans on the Rift Valley Fever Virus Envelope Glycoproteins Gn and Gc Redundantly Support Viral Infection via DC-SIGN. *Viruses,* 8.

Pietrantoni, A., Fortuna, C., Remoli, M. E., Ciufolini, M. G. & Superti, F. 2015. Bovine lactoferrin inhibits Toscana virus infection by binding to heparan sulphate. *Viruses,* 7**,** 480-95.

Pingen, M., Bryden, S. R., Pondeville, E., Schnettler, E., Kohl, A., Merits, A., Fazakerley, J. K., Graham, G. J. & Mckimmie, C. S. 2016. Host Inflammatory Response to Mosquito Bites Enhances the Severity of Arbovirus Infection. *Immunity,* 44**,** 1455-69.

Piper, M. E. & Gerrard, S. R. 2010. A novel system for identification of inhibitors of rift valley Fever virus replication. *Viruses,* 2**,** 731-47.

Piper, M. E., Sorenson, D. R. & Gerrard, S. R. 2011. Efficient cellular release of Rift Valley fever virus requires genomic RNA. *PLoS One,* 6**,** e18070.

Pleschka, S., Wolff, T., Ehrhardt, C., Hobom, G., Planz, O., Rapp, U. R. & Ludwig, S. 2001. Influenza virus propagation is impaired by inhibition of the Raf/MEK/ERK signalling cascade. *Nat Cell Biol,* 3**,** 301-5.

Polakis, P. 2007. The many ways of Wnt in cancer. *Curr Opin Genet Dev,* 17**,** 45-51.

Portolani, M., Sabbatini, A. M., Beretti, F., Gennari, W., Tamassia, M. G. & Pecorari, M. 2002. Symptomatic infections by toscana virus in the Modena province in the triennium 1999-2001. *New Microbiol,* 25**,** 485-8.

Raftery, M. J., Lalwani, P., Krautkrämer, E., Peters, T., Scharffetter-Kochanek, K., Krüger, R., Hofmann, J., Seeger, K., Krüger, D. H. & Schönrich, G. 2014. β2 integrin mediates hantavirus-induced release of neutrophil extracellular traps. *J Exp Med,* 211**,** 1485-97.

Raymond, D. D., Piper, M. E., Gerrard, S. R., Skiniotis, G. & Smith, J. L. 2012. Phleboviruses encapsidate their genomes by sequestering RNA bases. *Proc Natl Acad Sci U S A,* 109**,** 19208-13.

Raymond, D. D., Piper, M. E., Gerrard, S. R. & Smith, J. L. 2010. Structure of the Rift Valley fever virus nucleocapsid protein reveals another architecture for RNA encapsidation. *Proc Natl Acad Sci U S A,* 107, 11769-74.

Reguera, J., Gerlach, P., Rosenthal, M., Gaudon, S., Coscia, F., Günther, S. & Cusack, S. 2016. Comparative Structural and Functional Analysis of Bunyavirus and Arenavirus Cap-Snatching Endonucleases. *PLoS Pathog,* 12, e1005636.

Reguera, J., Weber, F. & Cusack, S. 2010. Bunyaviridae RNA polymerases (L-protein) have an N-terminal, influenza-like endonuclease domain, essential for viral cap-dependent transcription. *PLoS Pathog,* 6, e1001101.

Reya, T. & Clevers, H. 2005. Wnt signalling in stem cells and cancer. *Nature,* 434, 843-50.

Riblett, A. M., Blomen, V. A., Jae, L. T., Altamura, L. A., Doms, R. W., Brummelkamp, T. R. & Wojcechowskyj, J. A. 2016. A Haploid Genetic Screen Identifies Heparan Sulfate Proteoglycans Supporting Rift Valley Fever Virus Infection. *J Virol,* 90, 1414-23.

Rodriguez-Andres, J., Rani, S., Varjak, M., Chase-Topping, M. E., Beck, M. H., Ferguson, M. C., Schnettler, E., Fragkoudis, R., Barry, G., Merits, A., Fazakerley, J. K., Strand, M. R. & Kohl, A. 2012. Phenoloxidase activity acts as a mosquito innate immune response against infection with Semliki Forest virus. *PLoS Pathog,* 8, e1002977.

Rostal, M. K., Liang, J. E., Zimmermann, D., Bengis, R., Paweska, J. & Karesh, W. B. 2017. Rift Valley Fever: Does Wildlife Play a Role? *ILAR J,* 58, 359-370.

Rousset, R., Mack, J. A., Wharton, K. A., Axelrod, J. D., Cadigan, K. M., Fish, M. P., Nusse, R. & Scott, M. P. 2001. Naked cuticle targets dishevelled to antagonize Wnt signal transduction. *Genes Dev,* 15, 658-71.

Rusu, M., Bonneau, R., Holbrook, M. R., Watowich, S. J., Birmanns, S., Wriggers, W. & Freiberg, A. N. 2012. An assembly model of rift valley Fever virus. *Front Microbiol,* 3, 254.

Ryzhova, E. V., Vos, R. M., Albright, A. V., Harrist, A. V., Harvey, T. & González-Scarano, F. 2006. Annexin 2: a novel human immunodeficiency virus type 1 Gag binding protein involved in replication in monocyte-derived macrophages. *J Virol,* 80**,** 2694-704.

Salahshor, S. & Woodgett, J. R. 2005. The links between axin and carcinogenesis. *J Clin Pathol,* 58**,** 225-36.

Samuel, G. H., Wiley, M. R., Badawi, A., Adelman, Z. N. & Myles, K. M. 2016. Yellow fever virus capsid protein is a potent suppressor of RNA silencing that binds double-stranded RNA. *Proc Natl Acad Sci U S A,* 113**,** 13863-13868.

Saul, S., Ferguson, M., Cordonin, C., Fragkoudis, R., Ool, M., Tamberg, N., Sherwood, K., Fazakerley, J. K. & Merits, A. 2015. Differences in Processing Determinants of Nonstructural Polyprotein and in the Sequence of Nonstructural Protein 3 Affect Neurovirulence of Semliki Forest Virus. *J Virol,* 89**,** 11030-45.

Saydam, O., Steiner, F., Vogt, B. & Schwyzer, M. 2006. Host cell targets of immediate-early protein BICP22 of bovine herpesvirus 1. *Vet Microbiol,* 113**,** 185-92.

Schittek, B., Hipfel, R., Sauer, B., Bauer, J., Kalbacher, H., Stevanovic, S., Schirle, M., Schroeder, K., Blin, N., Meier, F., Rassner, G. & Garbe, C. 2001. Dermcidin: a novel human antibiotic peptide secreted by sweat glands. *Nat Immunol,* 2**,** 1133-7.

Schnell, M. J., Mebatsion, T. & Conzelmann, K. K. 1994. Infectious rabies viruses from cloned cDNA. *EMBO J,* 13**,** 4195-203.

Schnettler, E., Sterken, M. G., Leung, J. Y., Metz, S. W., Geertsema, C., Goldbach, R. W., Vlak, J. M., Kohl, A., Khromykh, A. A. & Pijlman, G. P. 2012. Noncoding flavivirus RNA displays RNA interference suppressor activity in insect and Mammalian cells. *J Virol,* 86**,** 13486-500.

Shatkin, A. J. 1976. Capping of eucaryotic mRNAs. *Cell,* 9**,** 645-53.

Sheng, C., Liu, X., Jiang, Q., Xu, B., Zhou, C., Wang, Y., Chen, J. & Xiao, M. 2015. Annexin A2 is involved in the production of classical swine fever virus infectious particles. *J Gen Virol,* 96**,** 1027-32.

Shi, X. & Elliott, R. M. 2009. Generation and analysis of recombinant Bunyamwera orthobunyaviruses expressing V5 epitope-tagged L proteins. *J Gen Virol,* 90**,** 297-306.

Shi, X., Van Mierlo, J. T., French, A. & Elliott, R. M. 2010. Visualizing the replication cycle of bunyamwera orthobunyavirus expressing fluorescent protein-tagged Gc glycoprotein. *J Virol,* 84**,** 8460-9.

Shi, Y. & Gao, G. F. 2017. Structural Biology of the Zika Virus. *Trends Biochem Sci,* 42**,** 443-456.

Shtanko, O., Nikitina, R. A., Altuntas, C. Z., Chepurnov, A. A. & Davey, R. A. 2014. Crimean-Congo hemorrhagic fever virus entry into host cells occurs through the multivesicular body and requires ESCRT regulators. *PLoS Pathog,* 10**,** e1004390.

Silhavy, D., Molnár, A., Lucioli, A., Szittya, G., Hornyik, C., Tavazza, M. & Burgyán, J. 2002. A viral protein suppresses RNA silencing and binds silencing-generated, 21- to 25-nucleotide double-stranded RNAs. *EMBO J,* 21**,** 3070-80.

Silvas, J. A. & Aguilar, P. V. 2017. The Emergence of Severe Fever with Thrombocytopenia Syndrome Virus. *Am J Trop Med Hyg,* 97**,** 992-996.

Simon, M., Johansson, C., Lundkvist, A. & Mirazimi, A. 2009. Microtubule-dependent and microtubule-independent steps in Crimean-Congo hemorrhagic fever virus replication cycle. *Virology,* 385**,** 313-22.

Simons, J. F. & Pettersson, R. F. 1991. Host-derived 5' ends and overlapping complementary 3' ends of the two mRNAs transcribed from the ambisense S segment of Uukuniemi virus. *J Virol,* 65**,** 4741-8.

Sindato, C., Karimuribo, E. & Mboera, L. E. 2011. The epidemiology and socio-economic impact of rift valley fever epidemics in Tanzania: a review. *Tanzan J Health Res,* 13, 305-18.

Smith, J. L., Jeng, S., Mcweeney, S. K. & Hirsch, A. J. 2017. A MicroRNA Screen Identifies the Wnt Signaling Pathway as a Regulator of the Interferon Response during Flavivirus Infection. *J Virol,* 91.

Smithburn, K. C. 1949. Rift Valley fever; the neurotropic adaptation of the virus and the experimental use of this modified virus as a vaccine. *Br J Exp Pathol,* 30, 1-16.

Surtees, R., Dowall, S. D., Shaw, A., Armstrong, S., Hewson, R., Carroll, M. W., Mankouri, J., Edwards, T. A., Hiscox, J. A. & Barr, J. N. 2016. Heat Shock Protein 70 Family Members Interact with Crimean-Congo Hemorrhagic Fever Virus and Hazara Virus Nucleocapsid Proteins and Perform a Functional Role in the Nairovirus Replication Cycle. *J Virol,* 90, 9305-16.

Sánchez-Vargas, I., Scott, J. C., Poole-Smith, B. K., Franz, A. W., Barbosa-Solomieu, V., Wilusz, J., Olson, K. E. & Blair, C. D. 2009. Dengue virus type 2 infections of Aedes aegypti are modulated by the mosquito's RNA interference pathway. *PLoS Pathog,* 5, e1000299.

Tamberg, N., Lulla, V., Fragkoudis, R., Lulla, A., Fazakerley, J. K. & Merits, A. 2007. Insertion of EGFP into the replicase gene of Semliki Forest virus results in a novel, genetically stable marker virus. *J Gen Virol,* 88, 1225-30.

Terasaki, K., Murakami, S., Lokugamage, K. G. & Makino, S. 2011. Mechanism of tripartite RNA genome packaging in Rift Valley fever virus. *Proc Natl Acad Sci U S A,* 108, 804-9.

Terasaki, K., Won, S. & Makino, S. 2013. The C-terminal region of Rift Valley fever virus NSm protein targets the protein to the mitochondrial outer membrane and exerts antiapoptotic function. *J Virol,* 87, 676-82.

Tian, H., Ji, X., Yang, X., Xie, W., Yang, K., Chen, C., Wu, C., Chi, H., Mu, Z., Wang, Z. & Yang, H. 2016. The crystal structure of Zika virus helicase: basis for antiviral drug design. *Protein Cell,* 7**,** 450-4.

Tong, Y., Lin, Y., Zhang, Y., Yang, J., Liu, H. & Zhang, B. 2009. Association between TCF7L2 gene polymorphisms and susceptibility to type 2 diabetes mellitus: a large Human Genome Epidemiology (HuGE) review and meta-analysis. *BMC Med Genet,* 10**,** 15.

Topisirovic, I., Svitkin, Y. V., Sonenberg, N. & Shatkin, A. J. 2011. Cap and cap-binding proteins in the control of gene expression. *Wiley Interdiscip Rev RNA,* 2**,** 277-98.

Torres, M. A., Yang-Snyder, J. A., Purcell, S. M., Demarais, A. A., Mcgrew, L. L. & Moon, R. T. 1996. Activities of the Wnt-1 class of secreted signaling factors are antagonized by the Wnt-5A class and by a dominant negative cadherin in early Xenopus development. *J Cell Biol,* 133**,** 1123-37.

Turell, M. J., Presley, S. M., Gad, A. M., Cope, S. E., Dohm, D. J., Morrill, J. C. & Arthur, R. R. 1996. Vector competence of Egyptian mosquitoes for Rift Valley fever virus. *Am J Trop Med Hyg,* 54**,** 136-9.

Valassina, M., Meacci, F., Valensin, P. E. & Cusi, M. G. 2000. Detection of neurotropic viruses circulating in Tuscany: the incisive role of Toscana virus. *J Med Virol,* 60**,** 86-90.

Van Knippenberg, I. & Elliott, R. M. 2015. Flexibility of bunyavirus genomes: creation of an orthobunyavirus with an ambisense S segment. *J Virol,* 89**,** 5525-35.

Vargason, J. M., Szittya, G., Burgyán, J. & Hall, T. M. 2003. Size selective recognition of siRNA by an RNA silencing suppressor. *Cell,* 115**,** 799-811.

Varjak, M., Donald, C. L., Mottram, T. J., Sreenu, V. B., Merits, A., Maringer, K., Schnettler, E. & Kohl, A. 2017a. Characterization of the Zika virus induced small RNA response in Aedes aegypti cells. *PLoS Negl Trop Dis,* 11**,** e0006010.

Varjak, M., Maringer, K., Watson, M., Sreenu, V. B., Fredericks, A. C., Pondeville, E., Donald, C. L., Sterk, J., Kean, J., Vazeille, M., Failloux, A. B., Kohl, A. & Schnettler, E. 2017b. Piwi4 Is a Noncanonical PIWI Protein Involved in Antiviral Responses. *mSphere,* 2.

Veeman, M. T., Slusarski, D. C., Kaykas, A., Louie, S. H. & Moon, R. T. 2003. Zebrafish prickle, a modulator of noncanonical Wnt/Fz signaling, regulates gastrulation movements. *Curr Biol,* 13**,** 680-5.

Vizcaíno, J. A., Csordas, A., Del-Toro, N., Dianes, J. A., Griss, J., Lavidas, I., Mayer, G., Perez-Riverol, Y., Reisinger, F., Ternent, T., Xu, Q. W., Wang, R. & Hermjakob, H. 2016. 2016 update of the PRIDE database and its related tools. *Nucleic Acids Res,* 44**,** D447-56.

Walter, C. T. & Barr, J. N. 2010. Bunyamwera virus can repair both insertions and deletions during RNA replication. *RNA,* 16**,** 1138-45.

Wang, A., Thurmond, S., Islas, L., Hui, K. & Hai, R. 2017. Zika virus genome biology and molecular pathogenesis. *Emerg Microbes Infect,* 6**,** e13.

Wang, H., Garcia, C. A., Rehani, K., Cekic, C., Alard, P., Kinane, D. F., Mitchell, T. & Martin, M. 2008. IFN-beta production by TLR4-stimulated innate immune cells is negatively regulated by GSK3-beta. *J Immunol,* 181**,** 6797-802.

Wang, L., Zhang, L., Zhao, X., Zhang, M., Zhao, W. & Gao, C. 2013. Lithium attenuates IFN-β production and antiviral response via inhibition of TANK-binding kinase 1 kinase activity. *J Immunol,* 191**,** 4392-8.

Wang, Y. K., Spörle, R., Paperna, T., Schughart, K. & Francke, U. 1999. Characterization and expression pattern of the frizzled gene Fzd9, the mouse homolog of FZD9 which is deleted in Williams-Beuren syndrome. *Genomics,* 57**,** 235-48.

Wasmoen, T. L., Kakach, L. T. & Collett, M. S. 1988. Rift Valley fever virus M segment: cellular localization of M segment-encoded proteins. *Virology,* 166**,** 275-80.

Watson, D. C., Sargianou, M., Papa, A., Chra, P., Starakis, I. & Panos, G. 2014. Epidemiology of Hantavirus infections in humans: a comprehensive, global overview. *Crit Rev Microbiol,* 40**,** 261-72.

Watts, D. M., Pantuwatana, S., Defoliart, G. R., Yuill, T. M. & Thompson, W. H. 1973. Transovarial transmission of LaCrosse virus (California encephalitis group) in the mosquito, Aedes triseriatus. *Science,* 182**,** 1140-1.

Weber, F., Bridgen, A., Fazakerley, J. K., Streitenfeld, H., Kessler, N., Randall, R. E. & Elliott, R. M. 2002. Bunyamwera bunyavirus nonstructural protein NSs counteracts the induction of alpha/beta interferon. *J Virol,* 76**,** 7949-55.

Webster, M. T., Rozycka, M., Sara, E., Davis, E., Smalley, M., Young, N., Dale, T. C. & Wooster, R. 2000. Sequence variants of the axin gene in breast, colon, and other cancers: an analysis of mutations that interfere with GSK3 binding. *Genes Chromosomes Cancer,* 28**,** 443-53.

Weingartl, H. M., Zhang, S., Marszal, P., Mcgreevy, A., Burton, L. & Wilson, W. C. 2014. Rift Valley fever virus incorporates the 78 kDa glycoprotein into virions matured in mosquito C6/36 cells. *PLoS One,* 9**,** e87385.

Wichgers Schreur, P. J. & Kortekaas, J. 2016. Single-Molecule FISH Reveals Non-selective Packaging of Rift Valley Fever Virus Genome Segments. *PLoS Pathog,* 12**,** e1005800.

Wilson, W. C., Bawa, B., Drolet, B. S., Lehiy, C., Faburay, B., Jasperson, D. C., Reister, L., Gaudreault, N. N., Carlson, J., Ma, W., Morozov, I., Mcvey, D. S. & Richt, J. A. 2014. Evaluation of lamb and calf responses to Rift Valley fever MP-12 vaccination. *Vet Microbiol,* 172**,** 44-50.

Won, S., Ikegami, T., Peters, C. J. & Makino, S. 2006. NSm and 78-kilodalton proteins of Rift Valley fever virus are nonessential for viral replication in cell culture. *J Virol,* 80**,** 8274-8.

Won, S., Ikegami, T., Peters, C. J. & Makino, S. 2007. NSm protein of Rift Valley fever virus suppresses virus-induced apoptosis. *J Virol,* 81**,** 13335-45.

Woodham, A. W., Sanna, A. M., Taylor, J. R., Skeate, J. G., Da Silva, D. M., Dekker, L. V. & Kast, W. M. 2016. Annexin A2 antibodies but not inhibitors of the annexin A2 heterotetramer impair productive HIV-1 infection of macrophages in vitro. *Virol J,* 13**,** 187.

Woodham, A. W., Taylor, J. R., Jimenez, A. I., Skeate, J. G., Schmidt, T., Brand, H. E., Da Silva, D. M. & Kast, W. M. 2015. Small molecule inhibitors of the annexin A2 heterotetramer prevent human papillomavirus type 16 infection. *J Antimicrob Chemother,* 70**,** 1686-90.

Wu, Q., Wang, X. & Ding, S. W. 2010. Viral suppressors of RNA-based viral immunity: host targets. *Cell Host Microbe,* 8**,** 12-5.

Xie, Q., Chen, L., Shan, X., Tang, J., Zhou, F., Chen, Q., Quan, H., Nie, D., Zhang, W., Huang, A. L. & Tang, N. 2014. Epigenetic silencing of SFRP1 and SFRP5 by hepatitis B virus X protein enhances hepatoma cell tumorigenicity through Wnt signaling pathway. *Int J Cancer,* 135**,** 635-46.

Xu, F., Chen, H., Travassos Da Rosa, A. P., Tesh, R. B. & Xiao, S. Y. 2007. Phylogenetic relationships among sandfly fever group viruses (Phlebovirus: Bunyaviridae) based on the small genome segment. *J Gen Virol,* 88**,** 2312-9.

Yadani, F. Z., Kohl, A., Préhaud, C., Billecocq, A. & Bouloy, M. 1999. The carboxy-terminal acidic domain of Rift Valley Fever virus NSs protein is essential for the formation of filamentous structures but not for the nuclear localization of the protein. *J Virol,* 73**,** 5018-25.

Yang, Z., Shi, Z., Guo, H., Qu, H., Zhang, Y. & Tu, C. 2015. Annexin 2 is a host protein binding to classical swine fever virus E2 glycoprotein and promoting viral growth in PK-15 cells. *Virus Res,* 201**,** 16-23.

Ye, K., Malinina, L. & Patel, D. J. 2003. Recognition of small interfering RNA by a viral suppressor of RNA silencing. *Nature,* 426**,** 874-8.

Zhu, X., Wen, L., Sheng, S., Wang, W., Xiao, Q., Qu, M., Hu, Y., Liu, C. & He, K. 2018. Porcine Circovirus-Like Virus P1 Inhibits Wnt Signaling Pathway. *Front Microbiol,* 9**,** 390.

Zhu, Z., Chan, J. F., Tee, K. M., Choi, G. K., Lau, S. K., Woo, P. C., Tse, H. & Yuen, K. Y. 2016. Comparative genomic analysis of pre-epidemic and epidemic Zika virus strains for virological factors potentially associated with the rapidly expanding epidemic. *Emerg Microbes Infect*, 5**,** e22.

Zhuang, L., Sun, Y., Cui, X. M., Tang, F., Hu, J. G., Wang, L. Y., Cui, N., Yang, Z. D., Huang, D. D., Zhang, X. A., Liu, W. & Cao, W. C. 2018. Transmission of Severe Fever with Thrombocytopenia Syndrome Virus by Haemaphysalis longicornis Ticks, China. *Emerg Infect Dis,* 24.